Controlling Inflammation: The Neurotrophic Anti-inflammatory Pathway in Chagas Heart Disease

A thesis

submitted by

Ryan Santiago Salvador

In partial fulfillment of the requirements

for the degree of

Doctor of Philosophy

in

Immunology

TUFTS UNIVERSITY

Sackler School of Graduate Biomedical Sciences

February, 2015

Advisor: Mercio PereiraPerrin, MD, PhD

Abstract

Trypanosoma cruzi is an obligate intracellular parasite that causes incurable Chagas disease that affects millions of people worldwide. In acute infection, *T cruzi* grows abundantly throughout the body, triggering severe inflammatory responses in most organs, including the nervous system and heart. Infected hearts display focal inflammatory infiltrates and fibrosis that lead to histological and functional alterations, such as cardiomyocytolysis, cardiac murmur, pleural effusion, and conduction abnormalities. Yet, acute myocarditis subsides in most patients without sequelae. This raises the possibility that *T cruzi* expresses agents that stimulate host repair mechanisms to help heal infected tissues. These putative agents cannot help in chronic Chagasic cardiomyopathy (CCC), characterized by relentless excessive inflammation and fibrosis that result in cardiac insufficiency and death in approximately 30% of patients, because tissue parasitism and, consequently, *T cruzi*-enabled tissue repair agents in CCC is extremely scarce. Therefore, administration of beneficial *T cruzi*-derived repair agents in CCC could prevent or revert tissue destruction. We have discovered one such agent, *T cruzi*'s parasite derived neurotrophic factor (PDNF), which, by binding neurotrophin receptors TrkA and TrkC, triggers parasite entry into cardiac host cells while promoting host cell survival, induces secretion of chemokines that facilitate migration of resident cardiac progenitor/stem cells (CPCs) in the myocardium, and further expand, induce cell survival, and stimulate the production of the anti-inflammatory protein TSG-6 (tumor necrosis factor-α

stimulated gene-6) by CPCs. Equally important, intravenous administration of recombinant PDNF dramatically ameliorates inflammation and fibrosis, and reduces pro-inflammatory cytokine expression in the hearts of mice with CCC. Therefore, our results validate the novel concept of a microbial pathogen stimulating mutually beneficial repair of infected tissues, and suggest a novel therapeutic opportunity for CCC.

Acknowledgements

Moving from Hawaii to Boston in the pursuit of science was a major milestone in my life. Entering the Immunology program at Tufts was a daunting endeavor, as I had never taken a course in Immunology, but I strongly believe it was through the opportunities, experiences, and crossing of paths with those I've met throughout my graduate career that brought me to where I am today. With that, I want to document my sincerest thanks to those who inspire me:

First and foremost, I owe a lot of gratitude to my mentor and PI Mercio PereiraPerrin. Mercio has been like a father to me during my time at Tufts. Our relationship has evolved so much from the beginning, as now our usual meetings are fluid and natural. Even through the toughest of times, he knew how to encourage me, whether it was imposing a needed deadline or a simple pat on the back, his timing was impeccable. I regarded him for his enthusiasm for science and the pursuit of the unknown, and his philosophy to constantly question things and sporadically think outside of the box without losing sight of the big picture.

My laboratory colleagues and rotation students have been like siblings to me. Kacey Caradonna took me under her wing and helped build my confidence during that tough first year. Craig Weinkauf further built my confidence as I helped him finish his projects. Daniel Aridgides and I went through a lot during a transition period in the lab; we both picked up the slack of the lab, we worked

endlessly and effectively as our projects shifted, he gave great feedback for my many, sometimes painful, practice talks, and I always knew I could rely on him for anything. Marina Chuenkova, Bo Lu, and Milena de Melo-Jorge did a lot of the work that our projects were based off of.

One truly learns when they are called upon to teach. It was an honor to teach masters and rotation students in the lab: Michelle Paczosa, Guy Supris, Nora Sherry, Matthew Brudner, Jessica Elman, Megan McPhillips, and Tamar Sarig.

I want to thank my committee members, Honorine Ward, Erik Selsing, and Henry Wortis, for their feedback during my meetings and keeping me on track. They provided a lot of moral support to get through the years. Special thanks go to Marc-Jan Gubbels for accepting my invitation for serving as my outside examiner.

I first started off in the PREP, the post-baccalaureate program at Tufts. Henry Wortis, Diana Pierce, Dan Jay, Maribel Rios, and Jerry Faust have put in so much work and effort into the program, which helped prepare me and solidify my desire to pursue a graduate education. Henry was actually the one who got me to apply to graduate school; I was glad to eventually have a familiar face on my thesis committee. Di is not only a program coordinator, but she is a therapist and truly the heart of the PREP and Immunology programs, and I am glad I can call her a true friend. Jennifer Coburn accepted me in her lab during my PREP

year, where I was exposed to new techniques and introduced to the crosstalk between Immunology and Microbiology.

The Immunology program was home for me, as I spent the majority of my time in and around lab. The old and new program staff, including Diana Pierce, Libby Jensen, Alfonse Borj, Cindy Welch, Anne, Cecelia, Gretchen, Karen, and Ed are always helpful and pleasant to be around. I made many friends in the Immunology program, as well as other programs, that I can now call colleagues.

Being 5,000 miles away from home has been difficult, but this time away from family and friends made me realize how much more they mean to me. My parents, Jorge and Marcelina Salvador, emigrated from the Philippines to Hawai'i to give my siblings and me a better life. They instilled in me the importance of education, on account of their own absence of educational opportunities. Their love and tireless work ethic taught me to persevere, to use what I learn to better myself as a person, and to always help those around me. My older sisters, Marjorie, Arlene, and Leilani, have always encouraged me to do the best I can, and more, but always kept me grounded whenever I get too full of myself. I embarked on my educational journey along with a few of my good friends, Coty Gonzales, Joel Sabugo, Mark DeBlois, and Monette Galario, who also went on their own journeys. We supported each other from a long-distance through the wonders of the Internet, and I can't wait till the day we can all call each other doctor.

During my time at Tufts, I made friends that filled the void of not having family around. These friends became my Boston family. Dennise de Jesus was my Microbiology counterpart coming into Sackler. We've been through thick and thin and supported each other while in grad school. Jesus Bernardy, Marcos Salazar, Eydith Commenencia, Angela Tanudra, Carla Cugini, Julianna Lewis, Seblewongel Asrat, and Laurice Jackson, all, in some way or form, got me through school and tough times, whether it was a quick pep-talk or a general hangout session; they all helped with mixing work and play. I wish them all luck with their scientific endeavors. Countless others not mentioned here made my time spent in Boston memorable; they know who they are.

TABLE OF CONTENTS

List of Tables

List of Figures

List of Abbreviations

AIDS – Acquired Immunodeficiency Syndrome

BDNF – Brain Derived Neurotrophic Factor

BMC – Bone Marrow-derived Cell

BZA – Border Zone Area

CCC – Chronic Chagasic Cardiomyopathy

CCR2 – C-C Chemokine Receptor 2

CD[#] – cluster of differentiation molecule [#]

CDC – Center for Disease Control

c-Kit (CD117, SCFR) – tyrosine-protein kinase Kit

CX3CR1 – CX3C Chemokine Receptor 1

CM – Cardiomyocyte

CNS – Central Nervous System

CPC – Cardiac Progenitor Cell

CF – Cardiac Fibroblast

HF – Heart Failure

CTGF – Connective Tissue Growth Factor

DAPI – 4'6-diamidino-2-phenylindole

DMEM – Dulbecco's Modified Eagle's Medium

ECG – Electrocardiogram

ECM – Extracellular Matrix

ELISA – Enzyme-linked Immunosorbent Assay

FCS – Fetal Calf Serum

FDA – Food and Drug Administration

FKN (CX3CL1) – Fractalkine (CX3C Chemokine Ligand 1)

GP[#] – Glycoprotein #

GPI - Glycosylphosphatidylinositol

HA - Hyaluronan

HIV – Human Immunodeficiency Virus

I/R – Ischemia/Reperfusion

IαI – Inter-α-trypsin Inhibitor

IFA – Immunoflurescent-antibody assay

IL[#] – Interleukin #

LV – Left Ventricular

Ly6C – Lymphocyte Antigen 6C

MAPK/ERK – Mitogen Activated Protein Kinase/Extracellular signal-regulated Kinase

MCP-1 (CCL2) – Monocyte Chemotactic Protein-1 (C-C Chemokine Ligand 2)

MI – Myocardial Infarction

microPET – Small animal Positron Emission Tomography

MIP2-α (CXCL2) – macrophage inflammatory protein 2-alpha

MMP – Matrix Metalloproteinase

MOI – Multiplicity of Infection

MSC – Mesenchymal Stem Cell

Msh-1 – Musashi-1

NF-κB – Nuclear Factor κB

NGF – Nerve Growth Factor

NIH – National Institutes of Health

NT-3 – Neurotrophin-3

$P75^{NTR}$ – Pan-neurotrophin Receptor of 75 kDa

PBS(T) – Phosphate Buffered Saline (Tween) solution

PI – Propidium Iodide

PI3K/AKT – Phosphoinositide 3-kinase/protein kinase B

PLCγ – Phospholipase Cγ

PNS – Peripheral Nervous System

RV – Right Ventricular

Sca-1 – Stem Cell Antigen-1

SDF-1 – Stromal cell-derived Factor 1

(s)PDNF – (short) Parasite Derived Neurotrophic Factor

TGFβ – Transforming Growth Factor β

TNFα – Tumor Necrosis Factor α

Trk – Tropomyosin-Related Kinase

TS – *Trans*-sialidase

TSG-6 – TNF Stimulated Gene 6

vWf – von-Willebrand factor

Controlling Inflammation: The Neurotrophic Anti-inflammatory Pathway in Chagas Heart Disease

CHAPTER 1. INTRODUCTION

1.1 History of *Trypanosoma cruzi* and Chagas disease

Phylogenetic analysis of 18S rRNA sequences indicates that salivarian trypanosomes (the *Trypanosoma brucei* clade transmitted by insect bites, associated with African sleeping sickness) diverged from the stercorarian trypanosomes (the *T cruzi* clade transmitted by insect fecal contamination) approximately 100 million years ago (Stevens et al., 1999). Though it was postulated that continental divide contributed to this divergence, the lack of high diversity of the *T cruzi* clade in South American terrestrial mammals suggests no co-evolution generating host-species-specific genotypes have occurred (Hamilton et al., 2012). Recent molecular evidence indicates that *T cruzi* may have evolved from a bat trypanosome, a scenario known as the 'bat seeding' hypothesis (Hamilton et al., 2012).

Based on paintings dating back approximately 26,000 years in cave/rock shelters that represented a prime habitat for the *T cruzi* insect vector *Triatoma brasiliensis*, it was postulated that Chagas disease existed for as long as humans have inhabited the Americas (Araújo et al., 2009). Recently, mummified remains dating back 9,000 years, found in pre-Colombian Andean countries, were observed to display lesions typical of Chagas disease and tested positive for *T cruzi* as assessed by PCR (Araújo et al., 2009). However, *T cruzi* was identified

and characterized as the etiological agent of Chagas disease just over a hundred years ago.

On April 15, 1909, Carlos Chagas (1878-1934, Figure 1.1a), a young researcher from the Instituto Oswaldo Cruz (Oswaldo Cruz Institute), proclaimed to the scientific world of a new tropical disease caused by the protozoan *T cruzi* that was transmitted by a hematophagous bug, known locally as ‘barbeiro’ or kissing bug, that proliferated in the mud walls typically found in houses of poor, rural areas now known as the Brazilian municipality of Lassance, located north of the state of Minas Gerais (Kropf and Sá, 2009). Chagas was the first, and to this day remains the only, scientist in the history of medicine to completely describe an infectious disease by identifying the insect vector, causative pathogen, and characterizing the human disease epidemiology and manifestations and phase of the disease that afflicts millions of people worldwide, indeed a great breakthrough for which many say Carlos Chagas should have been awarded the Nobel Prize (Kropf and Sá, 2009).

Carlos Chagas’ discovery started when he was dispatched by his mentor, Oswaldo Cruz, to Minas Gerais in 1907 with the purpose of combating malaria, which was impeding the construction of a new railroad (Kropf and Sá, 2009). Once there, Carlos Chagas learned of a common hematophagous beetle that fed on locals during their sleep. Aware that blood-sucking insects could serve as vectors for infectious diseases, he examined the bug and found trypanosomes in their feces and sent the insects back to Cruz for further analysis. The insects

were allowed to feed on a marmoset monkey, which became ill, while trypanosomes were detected in their blood. Carlos Chagas christened this new species of infectious protozoan, *T cruzi*, in honor of his mentor (Chagas, 1909a). Carlos Chagas then returned to Lassance, where he had initially found the insect vector. There, he isolated trypomastigotes from a febrile and anemic two year-old girl, Berenice (Figure 1.1c), the first documented human case of Chagas disease (Chagas, 1909b). Carlos Chagas continued to characterize the different developmental stages of *T cruzi* in both the insect and mammalian host (Chagas, 1909c). Shortly thereafter, Carlos Chagas published an early characterization of the clinical stages of the disease in humans (Chagas, 1910). Carlos Chagas was nominated for a Nobel Prize in Physiology or Medicine in 1920, but unscrupulous political bureaucracy denied him the award, which was left unawarded in 1921 (Bestetti et al., 2013, 2009).

Treatment options for Chagas disease have proven to be elusive and remain inadequate more than a century after discovery of the disease. Thus, Chagas disease still remains a menace to the Americas, where the disease is endemic, and to other parts of the world due to easy travel and migration of populations out of endemic regions.

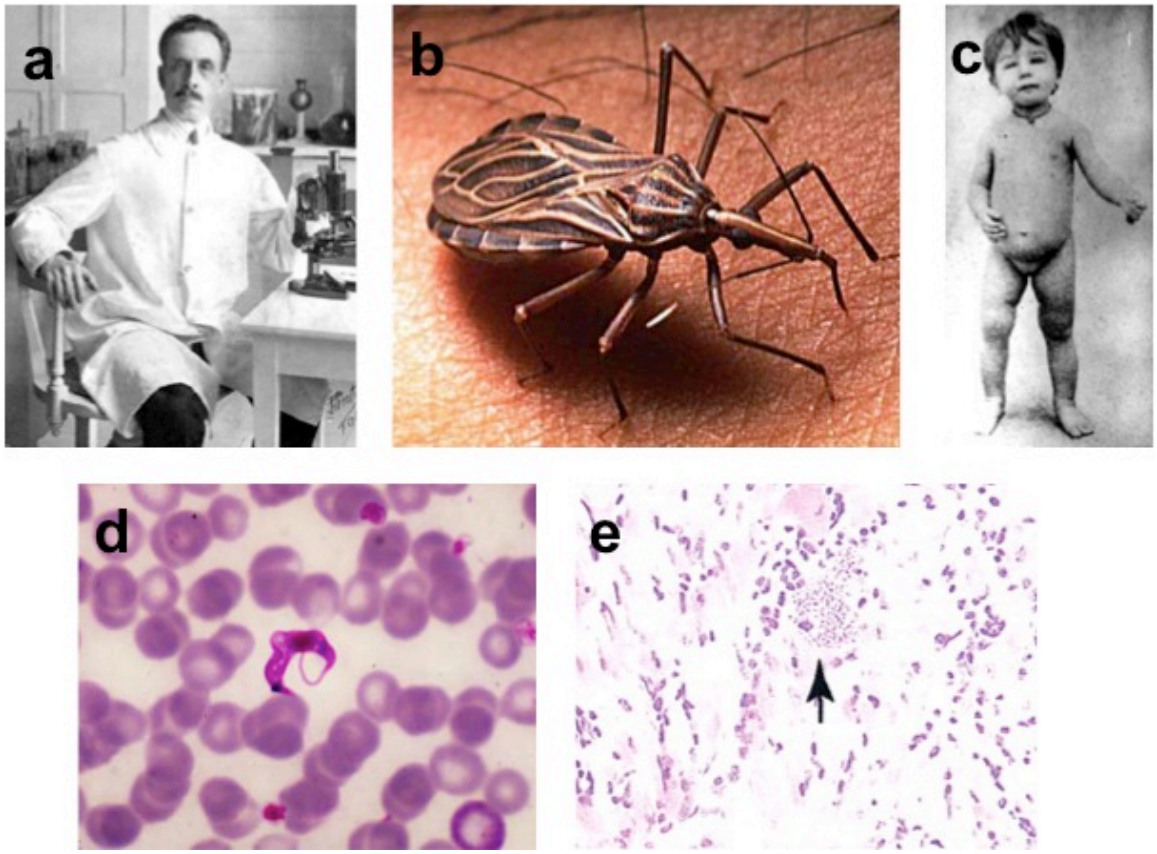

Figure 1.1. Discovery of *Trypanosoma cruzi* and the origins of Chagas disease.

(**a**) Carlos Chagas, discoverer of Chagas' disease (credit: Wikipedia). (**b**) *Rhodnium prolixus*, an example of a 'kissing bug' insect vector, capable of transmitting *T cruzi* (credit: WHO). (**c**) Berenice, the first recorded live patient of Chagas disease (credit: Tuoto, 2010). (**d**) Trypomastigote form of *T cruzi* in a blood smear (credit: CDC, Dr. Mae Melvin). (**e**) *T cruzi* cardiac parasitism of a mouse 30 days post-infection (Hardison et al., 2006).

1.2 *T cruzi* life cycle

Scientific classification: domain - Eukarya; kingdom - Excavata; phylum - Euglenozoa; class - Kinetoplastida; order - Trypanosomatida; genus - Trypanosoma; and species - T. cruzi.

Chagas disease is caused by *T cruzi*, a protozoan member of the Trypanosomatidae family, and has a high incidence and negative economic impact in developing countries in Central and South America (de Souza et al., 2010). One specific feature of trypanosomatids is that they change their general shape during their life cycle (de Souza et al., 2010). *T cruzi* presents a complex life cycle (Figure 1.2) involving several developmental stages found in its invertebrate host, as well as in the bloodstream of its vertebrate host (de Souza et al., 2010; Rassi Jr et al., 2010).

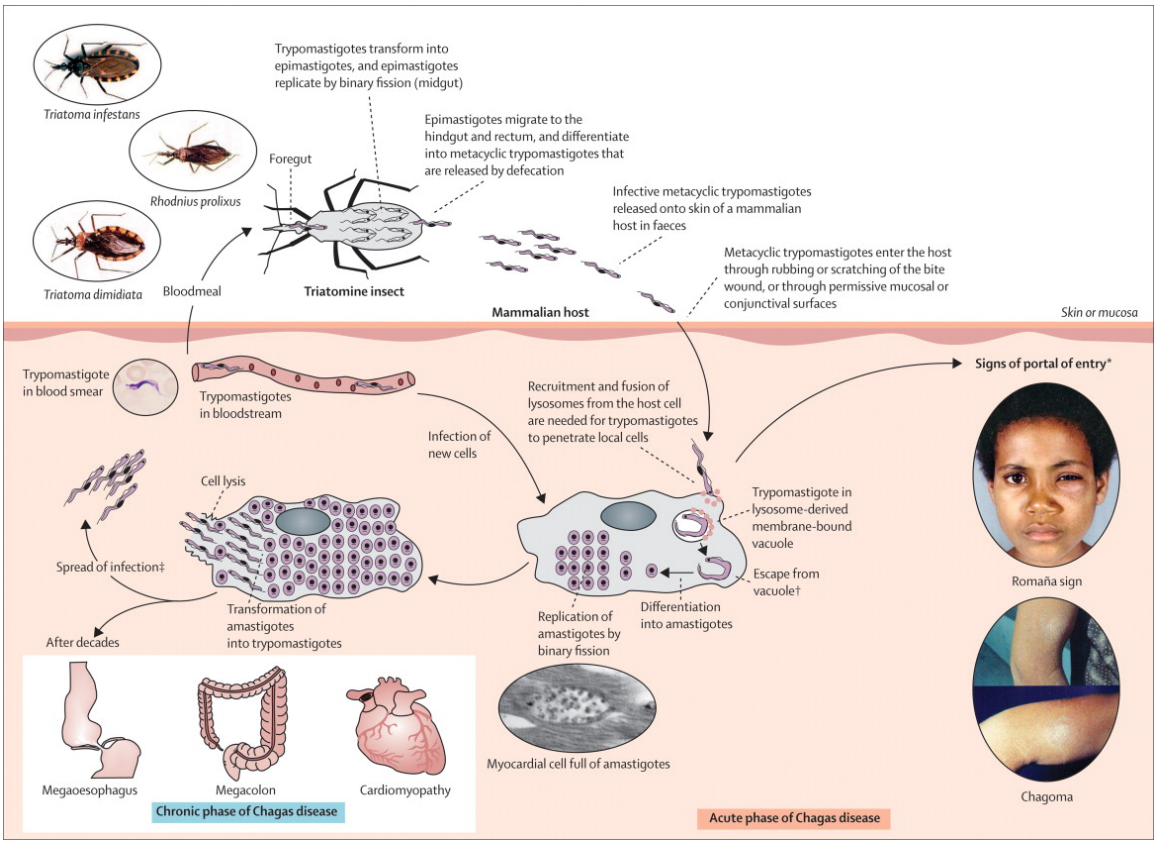

Figure 1.2. Vector-borne transmission and life cycle of *Trypanosoma cruzi*.

Reprinted from The Lancet, Vol. 375, Rassi Jr, A., Rassi, A., Marin-Net, J.A., Chagas disease, pg. 1388-1402, (2010), with permission from Elsevier. (Figure 1 from Rassi Jr et al., 2010)

1.2.1 Invertebrate host

The life cycle of *T cruzi* begins when an insect of the Reduviidae family sucks the blood of a *T cruzi* infected vertebrate host (de Souza et al., 2010). Once ingested, most of the trypomastigotes are lysed in the insect's stomach and the surviving trypomastigotes transform into spheromastigotes or epimastigotes (de Souza et al., 2010). Epimastigotes migrate to the insect's intestine where they divide intensely and attach to the perimicrovillar membranes of intestinal cells in the posterior midgut (Andrade and Andrews, 2005; Brener, 1973; de Souza et al., 2010). This adhesion step is important to trigger the process of transformation of the noninfective epimastigotes into highly infective metacyclic trypomastigotes, a process that involes the participation of surface-exposed glycoconjugates (Andrade and Andrews, 2005). At the most posterior regions of the intestine and at the rectum, many epimastigotes detach, transform into metacyclic trypomastigotes, and are then released, together with feces and urine, when the insect takes another blood meal of a vertebrate host (de Souza et al., 2010).

1.2.2 Vertebrate host

Usually, infection of mammalian hosts takes place through direct inoculation of metacyclic trypomastigotes through the ocular mucosa or the lesioned skin during the insect blood meal (de Souza et al., 2010). Newer forms of transmission are mediated digestively, congenitally, or through blood transfusion or organ transplant (Bern et al., 2011; Coura, 2009; Dias et al., 2002; Hotez et

al., 2012; Ventura-Garcia et al., 2013). Once in the mammalian host, metacyclic trypomastigotes invade cells at the inoculation site, including fibroblasts, macrophages, and epithelial cells, through the recognition of parasite and host-cell molecules (de Souza et al., 2010).

These host-pathogen interactions contribute to the adherence, signaling, and invasion of the parasite into vertebrate host cells. The parasite is engulfed by an endocytic vacuole known as the parasitophorous vacuole (Rassi Jr et al., 2010). Phagolysosome fusion is essential for parasite retention inside host cells and development. The long and thin trypomastigote forms differentiate into rounded amastigote forms with a short flagellum, while at the same time, parasite enzymes lyse the parasitophorous vacuole membrane so that the amastigote forms become in direct contact with host cell organelles in the cytoplasm (de Souza et al., 2010).

In the cytoplasm, amastigotes replicate by binary fission with a doubling time of about 12 h over a period of 4-5 days (Bern et al., 2011). At the end of this period, the amastigotes transform into trypomastigotes, the host cell ruptures, and the trypomastigotes are released into the circulation. The circulating parasites can then invade new cells and initiate new replicative cycles, or are taken up by naïve insect vectors that feed on the host. In the absence of successful antitrypanosomal treatment, the infection can last for the lifetime of the mammalian host (Bern et al., 2011).

1.3 Chagas disease epidemiology

Before widespread vector control was instituted in the early 1990s, it was common to find that >60% of adults infected with *T cruzi* in communities that are endemic for Chagas disease (Bern et al., 2011). In cross-sectional community surveys, most infected individuals are asymptomatic; an estimated 70 to 80% will remain asymptomatic throughout their lives (Rassi Jr et al., 2010). Since 1991, the estimated global prevalence of *T cruzi* infection has fallen from 18 million to 8 million, due to intensive vector control and blood bank screening initiatives previously set in place (Dias et al., 2002). The Pan American Health organization estimates that approximately 60,000 new *T cruzi* infections occur each year. Based on the reported number of immigrants from countries in Latin America where Chagas disease is endemic, there are an estimated 300,000 persons with *T cruzi* infection currently living in the United States (Bern and Montgomery, 2009). Patients with clinical manifestations of Chagas disease, especially cardiomyopathy, are assumed to be present, but go unrecognized in hospitals and health care facilities in the United States. Because cardiac and gastrointestinal manifestations usually begin in early adulthood and progress over a period of years to decades, the prevalence of clinical disease increases with increasing age (Bern et al., 2011). Factors that contribute to clinical manifestations of Chagas disease are the insect vector, *T cruzi* strain, and mammalian hosts.

1.3.1 Triatomine vector biology

Triatomines of both sexes must take blood meals to develop through their nymphal stages to adults, and females require a blood meal to reproduce (Bern et al., 2011). Sylvatic triatomine species colonize nests of rodent or marsupial reservoir hosts, but are also capable of adapting to colonize human dwellings, partly due to pressures of deforestation and human immigration from the Amazon and Panama. More than 130 triatomine species in the Americas can transmit *T cruzi* (Bern et al., 2011; Dias et al., 2002; A. R. Teixeira et al., 2006). These genotypes are classified based on size polymorphism or sequence analysis of several gene loci. Eleven species of triatomine bugs have been reported in the continental United States: *Triatoma gerstaeckeri*, *T incrassata*, *T indictiva*, *T lecticularia*, *T neotomae*, *T protracta*, *T recurva*, *T rubida*, *T rubrofasciata*, *T sanguisuga*, and *Paratriatoma hirsuta* (Bern et al., 2011). One species, *T rubrofasciata*, is found in Hawaii. *T gerstaeckeri* is one of the most frequently collected and tested species in the US, and in one study out of 1,800 collected specimens, 1,038 (57.7%) were shown to be infected with *T cruzi* (Bern et al., 2011).

Triatomine feeding and defecation behaviors are important risk factors for vector-borne transmission (Bern et al., 2011). North American vector species in general exhibit greater post-feeding defecation delays than important Latin American vector species, and thus, delayed defecation may contribute to lower vector-

borne transmission efficiency in the US (Bern et al., 2011; Coura, 2009; Dias et al., 2002).

1.3.2 *T cruzi* genetic diversity

T cruzi is a genetically heterogenous species that has a wide variability in biological and biochemical characteristics. Historically, two major groups, TcI and TcII, existed, wherein TcII was later subdivided to TcIIa-e (Bern et al., 2011). Recently, consensus was reached to rename them to the six major lineages, TcI to TcVI. TcI and historic TcII (TcII-V) represent ancestral groups, whereas TcV and TcVI lineages are products of at least two hybridization events (Zingales et al., 2009).

TcII, TcV, and TcVI are the lineages most commonly reported in human Chagas disease in southern South America. These lineages are closely associated with the domestic transmission cycle and the domestic vector *Triatoma infestans* (Bern et al., 2011; Rassi Jr et al., 2010; A. R. Teixeira et al., 2006). TcV and TcVI have been reported in cardiomyopathy and intestinal megasyndromes in the Southern Cone (Argentina, Chile, Bolivia, and Brazil) (Coura, 2009; Dias et al., 2002). In contrast, intestinal Chagas disease is rare in northern South America, Central America, and Mexico, where TcI is the predominant lineage. In the US, two genotypes, TcI and TcIV, have been reported (Bern et al., 2011; Dias et al., 2002).

1.3.3 Mammalian reservoirs and hosts

All mammals are considered to be susceptible to infection; to date, over 100 mammalian species have been reported as natural hosts for *T cruzi* (Bern et al., 2011). As in humans, the majority of infected animals are in the chronic phase of infection. Primary reservoirs and transmission dynamics of *T cruzi* differ between the eastern and western regions of the US; the western US has the greatest reservoir diversity, where woodrats are most commonly infected. In the eastern US, raccoons, opossums, armadillos, and skunks are infected (Bern and Montgomery, 2009; Montgomery et al., 2014). In addition, domesticated animals such as felines and canines can be infected, with canines developing similar disease characteristics to humans (Pereira and Navarro, 2013). Older dogs were more likely to be infected, as studies in both the US and Latin America have reported increasing seropositivity with increasing age (Bern et al., 2011). Recently, cases of dogs suddenly dying, likely due to cardiac dysfunction, in kennels in Texas highlight a growing crisis of canine Chagas in the US (Tompkins, 2014).

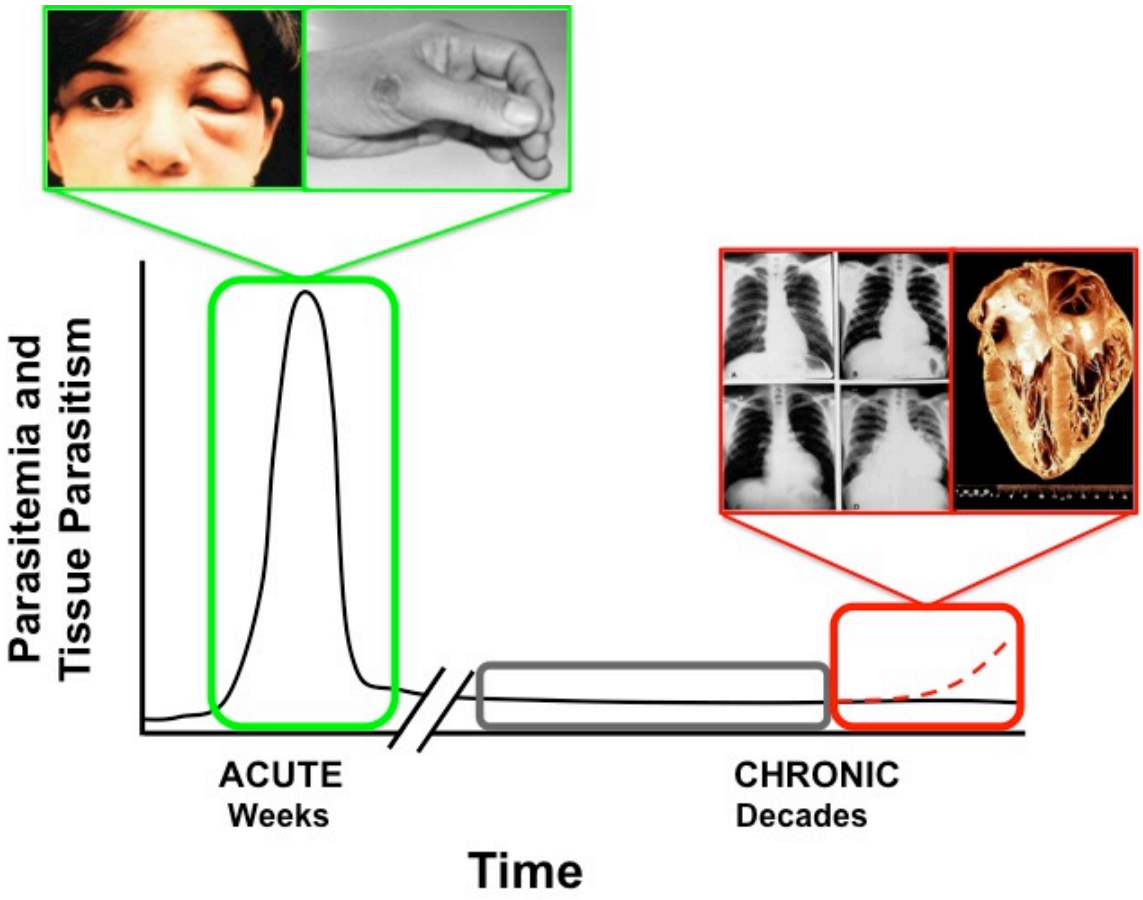

Figure 1.3. Chagas disease progression.

The acute phase (green box, images from WHO) of Chagas disease is marked by parasitemia and tissue parasitism which peaks weeks after initial infection, characterized by strong inflammatory responses and fever-like symptoms. The indeterminate phase (gray box) follows with undetectable/low parasitemia and parasitism, and 60-70% of those infected remain in this phase for the remainder of theirs lives without sequelae. 30-40% of infected individuals eventually develop the chronic clinical forms of Chagas disease (the most common forms affect the heart; cardiomegaly and cardiac fibrosis are depicted), with parasite levels increasing, decades after initial infection (red box, images from CDC).

1.4 Chagas disease manifestations

1.4.1 Acute phase

The incubation period following vector-borne *T cruzi* exposure is 1 to 2 weeks, which subsequently gives rise to the acute phase (Bern et al., 2011). The acute phase lasts 8 – 12 weeks and is characterized by circulating trypomastigotes detectable by microscopy of fresh blood smears. Most patients remain asymptomatic or have mild, nonspecific symptoms, such as fever, and do not need clinical attention. In some patients (Figure 1.3, green), severe inflammation and swelling at the site of cutaneous inoculation, known as a chagoma, occurs (de Souza et al., 2010; Rassi Jr et al., 2010). Inoculation via the conjunctiva leads to the characteristic unilateral swelling of the upper and lower eyelids known as the Romaña's sign.

Severe acute disease occurs in less that 1% of patients, which manifests as acute myocarditis, pericardial effusion, and/or meningoencephalitis (Boscardin et al., 2010). Children under the age of 2 years are at higher risk of severe manifestations than older individuals (Hoff et al., 1978). Orally transmitted *T cruzi* infection appears to be associated with more severe acute morbidity and higher mortality than vector-borne infections; recent findings suggest parasite contact with host gastric acid renders trypomatigotes more invasive through changes in parasite surface glycoproteins (Bern et al., 2011).

1.4.2 Chronic phase

Eight to 12 weeks after infection, parasitemia levels become undetectable by microscopy, and the infected individual passes into the chronic phase of Chagas disease (Bern et al., 2011). Persons chronically infected with *T cruzi* maintain the potential to transmit the parasite to the vector or directly to other humans through blood components, organ donation, or congenitally. Diagnosis of chronic infection relies on serological methods to detect IgG antibodies that recognize *T cruzi* antigens, via enzyme-linked immunosorbent assay (ELISA) and immunofluorescent-antibody assay (IFA). No single assay has sufficient sensitivity and specificity; thus, two or more different assays are used to increase accuracy of the diagnosis (Bern et al., 2011).

1.4.3 Indeterminate form

Those chronically infected with *T cruzi* without signs or symptoms are considered to have the indeterminate form (Figure 1.3, gray), defined by testing positive for anti-*T cruzi* serology, no physical abnormalities, normal 12-lead electrocardiogram (ECG), and normal radiological examination of the chest, esophagus, and colon (Bern et al., 2011). However, an estimated 20-30% of those with chronic Chagas disease progress, after a period of years to decades, to clinically evident cardiac and/or gastrointestinal disease (Bern et al., 2011).

1.4.4 Gastrointestinal manifestations

Gastrointestinal involvement is less common than Chagas heart disease, and is predominantly seen in patients infected in the countries of the Southern Cone (Argentina, Bolivia, Chile, Paraguay, Southern Peru, Uruguay, and parts of Brazil), and rare in northern South America, Central America, and Mexico (Bern et al., 2011; Dias et al., 2002; Rassi Jr et al., 2010). Gastrointestinal Chagas disease usually affects the esophagus and/or colon, resultant of damage to intramural neurons. The effects on the esophagus or colon span a spectrum from asymptomatic motility disorders to severe megasyndromes (Bern et al., 2011).

1.4.5 Chronic Chagasic Cardiomyopathy (CCC)

CCC is the most common chronic form of Chagas disease and is also the leading cause of heart failure in Latin America, where Chagas disease is endemic (Rosenbaum, 1964; Soares et al., 2010). CCC develops decades after initial infection (Figure 1.3, red) and is characterized by a chronic inflammatory process that involves all heart chambers, damage to the conduction system, and often an apical aneurysm (Bern et al., 2011). Pathogenesis is hypothesized to involve parasite persistence in cardiac tissue and immune-mediated myocardial injury. The earliest manifestations are conduction system abnormalities, most frequently right-bundle branch block or left anterior fascicular block, and segmental left ventricular wall motion abnormalities (Bern et al., 2011). Later manifestations include complex ventricular extrasystoles and nonsustained and sustained

ventricular tachycardia, sinus node dysfunction that may lead to severe bradycardia, high-degree heart block, apical aneurysm usually in the left ventricle, thromboembolic phenomena due to thrombus formation in the dilated left ventricle, and progressive dilated cardiomyopathy with congestive heart failure (Bern et al., 2011). These abnormalities lead to palpitations, presyncope, syncope, and a high risk of sudden death (Bern et al., 2011).

Due to a wide spectrum of CCC severities, there are likely multiple mechanisms that constitute the development of CCC. Factors that contribute to CCC are inflammation, oxidative stress, and cardiac fibrosis (Gupta et al., 2009; Lefer and Granger, 2000; Soares et al., 2010). Acute *T cruzi* infection triggers myocarditis in humans and animal models and eventually resolves, for the most part, as parasitism is controlled, but focal myocarditis persists, even in the absence of visible parasites (Kroll-Palhares et al., 2008; Marino et al., 2004; Michailowsky et al., 2001; Paiva et al., 2009). Cardiomyocytes are vulnerable to oxidative stress due to their high metabolic rates and low stores of reducing agents, such as NAD(P)H (Gottlieb, R.A., 2011; Lefer and Granger, 2000). Overtime, CCC slowly destroys viable cardiomyocytes, leading to fibrotic replacement, giving rise to fibrosis and impaired cardiac function (Gupta et al., 2009; Jacoby et al., 2003; Soares et al., 2010).

1.4.6 Progression of Chagas disease pathogenesis

The progression of chronic Chagas disease cannot be explained by one single mechanism, but rather it may be explained by multiple interacting factors. Several theories have been proposed, but they remain hotly debated.

The most accepted view is that the progression of chronic Chagas disease is directly related with the persistence of *T cruzi* in affected tissue, particularly the heart (Tarleton, 2003; Tarleton and Zhang, 1999; Vianna, 1911). Some immunological theories implicate sensitivity of $CD4^+$ and $CD8^+$ lymphocytes to *T cruzi* and, inadvertently, to anti-myocardial cells, which contribute to the migration and activation of macrophages and the release of platelet aggregation factors, thereby respectively inducing chronic Chagas myocarditis and myocardial ischemic lesions (Higuchi, 1999; Santos-Buch and Teixeira, 1974; Teixeira et al., 1975; A. R. L. Teixeira et al., 2006). The autoimmune theory suggests *T cruzi* infection contributes to the production of autoantibodies directed against host proteins, such as adrenergic, muscarinic (Borda and Sterin-Borda, 1996; Labovsky et al., 2007) , and neurotrophin receptors (Lu et al., 2008), but they have yet to be directly implicated to pathology. The neurogenic theory suggests megaesophagus, megacolon, and cardiac conduction disturbances in Chagas disease are a consequence of the denervation of the parasympathetic autonomous system (Koberle, 1968). Neuron destruction in innervated organs may be explained by both direct inflammatory phenomena and by immunological

mechanisms (Prata, 2001; A. R. Teixeira et al., 2006), suggesting relatedness between the different theories.

1.5 Treatment of Chagas disease

Nifurtimox and benznidazole are the only drugs with proven efficacy against Chagas disease. Nifurtimox (Lampit, Bayer 2502), a nitrofuran, interferes with *T cruzi* carbohydrate metabolism by inhibiting pyruvic acid synthesis (Bern et al., 2011; Coura and Castro, 2002). Benznidazole (Rochagon, Roche 7-1051) is a nitroimidazole derivative, considered more trypanocidal than nifurtimox (Bern et al., 2011; Coura and Castro, 2002). Neurological toxicity and side effects are fairly common for both drugs, with side effects more common in adults than in children. Despite not being FDA approved, both drugs can be obtained from the CDC and used under investigational protocols.

In acute Chagas disease, both drugs reduce the severity of symptoms, shorten the clinical course, and reduce the duration of detectable parasitemia. Treatment initiated during the acute phase of disease is thought to be most effective as an anti-parasitic therapy (Bern et al., 2011; Coura and Borges-Pereira, 2011; Garcia et al., 2005). In one study, serological cure was documented at the 12-month follow-up in 81% of those treated during the acute phase of disease (Wegner and Rohwedder, 1972). Other trials of benznidazole treatment in children with chronic *T cruzi* infection demonstrated approximately 60% cure, as measured by

conversion to negative serology 3-4 years after the end of treatment (Estani et al., 1998; Sgambatti de Andrade et al., 1996). Several follow-up studies suggest that the earlier patients are treated for Chagas disease, the higher the rate of reversion to negative serology (Andrade et al., 2004; Streiger et al., 2004). The average cure rate among treated acute cases is 80%, whereas it is less than 20% among treated chronic cases (Coura, 2009; Coura and Borges-Pereira, 2011; Coura and Castro, 2002).

1.5.1 Chagas disease in immuno-suppressed patients

Reactivation of *T cruzi* infection in HIV/AIDS patients can cause severe clinical disease with a high risk of mortality (Bern et al., 2011). The level of parasitemia is higher among HIV-coinfected than among HIV-negative patients. Symptomatic *T cruzi* reactivation in AIDS patients is most commonly reported to cause meningoencephalitis and/or *T cruzi* brain abscesses; the presentation may be confused with CNS toxoplasmosis and should be considered in the differential diagnosis of mass lesions on imaging of CNS syndromes in AIDS patients (Coura and Borges-Pereira, 2012; Coura and Dias, 2009; Hotez et al., 2012; Rassi Jr et al., 2010). The second most commonly reported sign of reactivation is acute myocarditis, sometimes superimposed on preexisting chronic Chagas cardiomyopathy. Reactivation in an HIV-coinfected patient should be treated with standard courses of antitrypanosomal treatment and antiretroviral therapy, which should be optimized (Bern et al., 2011).

1.5.2 Cardiac management

Patients with chronic *T cruzi* infection can be candidates for organ transplants (Bern et al., 2011). In a large cohort of heart transplant patients, survival of those who received the transplant because of chronic Chagas cardiomyopathy was longer than survival among those with idiopathic or ischemic cardiomyopathy, and *T cruzi* reactivation was a rare cause of death (Bern et al., 2011). Immunosuppressed CCC patients must be carefully monitored for signs of parasite reemergence.

1.5.3 Stem cell therapy

The discovery of the pluripotency of adult bone marrow stem cells has opened new perspectives for the treatment of patients with chronic regenerative diseases for which there are no effective treatments available (Krause, 2002). Heart transplantation for chagasic patients, in addition to its high financial costs and failure rate, brings about the additional complication of relapse of *T cruzi* infection, especially with transplantation-related immunosuppressive treatment (Soares et al., 2004). Several studies have shown great promise of adult bone marrow transplants in models of dilated cardiomyopathy of *T cruzi* origin, with results showing the efficacy of bone marrow cell (BMC) therapy in chagasic myocarditis contributing to repairing heart tissue, reducing cardiac inflammation, and reversing inflammatory gene expression in CCC mouse hearts, suggesting it may be utilized for treating CCC and similar dilated cardiomyopathies in humans

(Soares et al., 2011, 2010, 2004). However, BMC therapy has failed in a clinical trial (Santos et al., 2012), leaving the door open for new ideas on regenerative therapy in CCC. Such sorely needed regenerative treatment options for chronic Chagas disease may well be the major contribution of my thesis research project, as detailed in Chapter 6.

1.6 Host-pathogen interactions leading to cellular invasion

The first steps of the *T cruzi*-host cell interaction process can be divided into three stages: adhesion/recognition, signaling, and invasion (de Souza et al., 2010). The adhesion stage involves recognition of molecules present on the surface of both parasite and host cells, but may also include molecules secreted by the parasite (de Souza et al., 2010). For example, gp90, a glycosidase, has antiphagocytic activity, mediated by the removal of sugar residues necessary for parasite internalization in macrophages (Nogueira, 1983). Another example is TC85, an 85 KDa glycoprotein which was identified as a ligand of fibronectin in different cell types, such as monocytes, neutrophils, and fibroblasts (Alves et al., 1986; Ouaissi et al., 1986). The Tc85 molecule is part of the gp85/*trans*-sialidase family, composed of multi-adhesive glycoproteins, and is capable of binding to different host receptor molecules either located on the cell surface, like host cell cytokeratin 18 (Magdesian et al., 2007), or components of the extracellular

matrix, such as fibronectin (Ouaissi et al., 1986) and laminin (Giordano et al., 1999).

1.7 The *trans*-sialidase gene family of *T cruzi*

Sialic acids and sialidases play important roles in cellular interactions and modulate the interplay of pathogenic microbes by mammalian host cells (Faillard, 1989; Schenkman et al., 1994). In vertebrates, sialic acids are implicated in a variety of biological events, including embryogenesis (Fenderson et al., 1990), cell differentiation (Feizi, 1991), endothelial cell-leukocyte adhesion (Bevilacqua and Nelson, 1993), and tumor cell invasiveness (Fukuda, 1991). In the context of host-pathogen interactions, sialic acids have been implicated as important mediators that contribute to viral entry of host cells (Crowell, 1986) and evasion of pathogenic bacteria from its host immune system (Troy, 1992). Although *T cruzi* lacks the ability to synthesize sialic acid, it harbors a unique mechanism to incorporate negatively charged sialic acids to its surface.

1.7.1 The *trans*-sialidase gene family

Trans-sialidase (TS), a unique enzyme expressed by *T cruzi*, is a surface-bound protein that can be shed by the parasite into the external milieu. TS, and TS-like proteins, which lack enzymatic activity due to mutations in the conserved tyrosine residue, constitute a gene family of over 1,400 members, underscoring their

importance in parasite evolution and biology (Najib M. El-Sayed et al., 2005; N. M. El-Sayed et al., 2005). TSs expressed by trypomastigotes are anchored by glycosylphosphatidylinositol (GPI) anchors on the parasite plasma membrane (de Souza et al., 2010). They consist of N-terminal catalytic β-barrel region, a lectin-like domain, and a C-terminal immunodominant long-tandem repeat (LTR) extension, which consist of 12-amino acids repeated in tandem (referred to as shed-acute phase antigen (SAPA)) (Chuenkova et al., 1999; Pereira, 1983) (Figure 1.4).

TS was initially identified as a neuraminidase (Pereira, 1983), but later found to be a modified sialidase (Schenkman et al., 1991). Instead of only releasing sialic acid, TSs can reversibly transfer α-2,3-linked sialic acid from external β-galactose on host cell surface sialoglycoconjugates to a terminal β-galactose of an appropriate sialoglycoconjugate acceptor on the parasite surface (Buschiazzo et al., 2002; Colli, 1993; Previato et al., 1985; Schenkman et al., 1994, 1991).

Within the catalytic portion of TS are four copies of an Asp-box motif (Chuenkova et al., 1999), previously identified ubiquitously in bacterial neuraminidases (Copley et al., 2001). These Asp-box motifs are located distally from the catalytic site and are thought to not be involved in the catalysis of neuraminidase activity (Buschiazzo et al., 2002). Asp-box motifs form β-turn hairpins on the surface of TSs (Buschiazzo et al., 2002; Copley et al., 2001), and their variability in non-conserved positions makes them prime candidate motifs for interaction with other

molecules. However, the function of Asp-boxes in neuraminidases remains largely unknown.

TSs have various roles in the pathogenicity of *T cruzi* that can promote adherence to host cells, as well as help the parasite evade host immune responses. The C-terminal LTR domain of TS has been characterized as a T cell-independent B cell mitogen that polyclonally induces B cells to produce and secrete non-specific immunoglobulin (Gao et al., 2002). Sialylation of the parasite surface catalyzed by TS is necessary for successful invasion of the host cell (Colli, 1993). Using trypomastigotes expressing TS (TS+) and trypomastigotes that did not (TS-), it was found that the TS+ population was highly invasive, whereas TS- was extremely inefficient to infect nonphagocytic cells (Pereira et al., 1996). Another function for TS activity is protection from lysis by the alternative pathway of complement while the parasite is circulating in the acute phase of the disease (Colli, 1993). Sialylated mucins on the parasite surface are implicated in attachment to host cells as well as evasion of the immune response by masking parasite epitopes (Pereira-Chioccola et al., 2000).

1.7.2 Parasite Derived Neurotrophin Factor (PDNF), recombinant short-PDNF (sPDNF)

Our lab studies a particular *trans*-sialidase of *T cruzi* we named PDNF (Figure 1.4), for its neurotrophic activity. Work from our lab has characterized several biological roles of PDNF in *T cruzi* pathogenesis, host cell adherence/invasion,

and neurotrophic activities (see section 1.9). TSs and PDNF can function independently of their enzymatic activity via direct protein-protein interactions (Chuenkova et al., 1999; Chuenkova and PereiraPerrin, 2005). De Souza et al. (2010) recently summarized a multitude of surface exposed molecules involved in *T cruzi*-host cell interactions, of which TS is mentioned to bind sialic acids as well as several members of the Trk family of receptors, TrkA and TrkC.

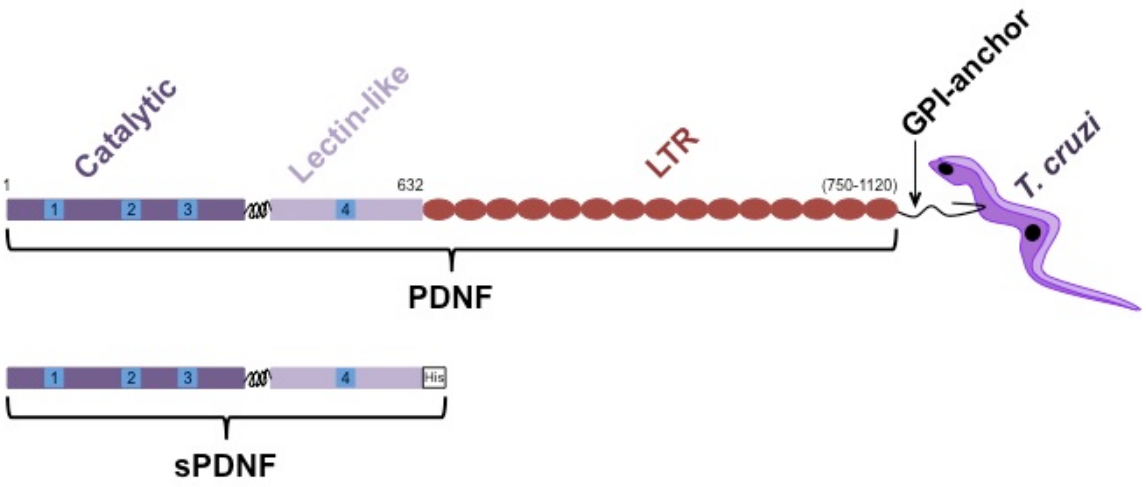

Figure 1.4. Diagram of PDNF and sPDNF.

TS/PDNF consists of catalytic and lectin-like domains (632 amino acids), an immunogenic long-tandem repeat (LTR) domain, and is GPI-anchored to the surface membrane of *T cruzi*. The four Asp-box motifs are represented by blue boxes. The 68 kDa recombinant sPDNF lacks the immunodominant LTR, which is replaced with a histidine-tag (His).

1.8 Trk receptors and neurotrophins

Several aspects of the neurogenic theory that drives Chagas disease may coincidently implicate important roles of *T cruzi*'s interaction with neurotrophic Trk receptors. *T cruzi* is known to infect nervous tissue and highly innervated organs (Koberle, 1968), though a correlation between neuronal loss and severity of Chagas disease has yet to be determined (Higuchi et al., 2003). Trk receptors and their neurotrophin ligands have important roles in developmental neurobiology, essential for cellular interactions in controlling cell survival and differentiation (Reichardt, 2006). *T cruzi* invasion of the brain coincides with a lack of damage despite heavy inflammation (Caradonna and Pereiraperrin, 2009), supporting the concept that *T cruzi* expresses beneficial factors enabling a mutually beneficial environment for host and parasite cell survival.

1.8.1 Nerve growth factor (NGF) and TrkA

NGF was first discovered by Rita Levi-Montalcini, who observed nerve sprouting around a mouse tumor transplanted into a developing chick embryo (Levi-Montalcini, 1952; Levi-Montalcini and Hamburger, 1951). With the invitation from her friend Dr. Carlos Chagas Filho (son of the *T cruzi* discoverer) to do tissue culture work in Rio de Janeiro, Dr. Levi-Montalcini was able to purify NGF (Cohen et al., 1954; Levi-Montalcini et al., 1954). Levi-Montalcini was awarded the Nobel Prize in Physiology or Medicine in 1986 for her seminal work. The receptors of NGF were identified to be the low affinity (K_d ~10^{-9} M) $p75^{NTR}$ and

high affinity (K^d ~10^{-11} M) TrkA, which, when stimulated, could synergize to enhance responsiveness (Hempstead et al., 1991, 1989; Ross, 1991).

1.8.2 Brain derived neurotrophic factor (BDNF), neurotrophin-3 (NT-3), TrkB, and TrkC

Based on sequence homology to TrkA, two more Trk family members, TrkB and TrkC, were cloned and identified, with BDNF and NT-3 identified as their preferred ligands, respectively (Klein et al., 1989; Lamballe et al., 1991). NT-3 is a more promiscuous neurotrophin, as it can activate TrkA and TrkB, albeit with lower affinity. $P75^{NTR}$ can also be activated by any of the neurotrophins, but has greater affinity for their pro-forms (Huang and Reichardt, 2003).

Ligation of neurotrophins to Trk receptors induces the dimerization and autophosphorylation of intracellular tyrosine residues, which in turn activates three downstream signaling pathways: MAPK/ERK, PI3 kinase/Akt, and PLCγ (Huang and Reichardt, 2003). Trk receptor activation induces pro-survival and differentiation signals in the peripheral and central nervous systems (Reichardt, 2006). Though the Trk family of receptors was classically thought to be neuronal-specific, TrkA has been found to regulate functions in immune cells such as mast (Levi-Montalcini, 1987) and B cells (Coppola et al., 2004). Endothelial cells have also been shown to express all three Trk receptors and function in part to promote angiogenesis (Caporali and Emanueli, 2009).

1.8.3 Cardiac involvement of Trk receptors and neurotrophins

Trk receptor expression is important for embryonic development. Mutations of TrkA can lead to insensitivity to pain (Indo, 2001), TrkB mutations in humans lead to cognitive defects (Yeo et al., 2004), and TrkC mutants have not yet been identified, likely because they are not viable. In mice and chickens, TrkC-knockouts result in gross developmental abnormalities in the heart, including defective cardiomyocyte proliferation (Lin et al., 2000), as well as septal and arterial defects that lead to embryonic or peri-natal lethality (Donovan et al., 1996; Tessarollo et al., 1997).

NGF has been shown to protect hearts in a mouse model of diabetic cardiomyopathy, presumed to be mediated via rescue of sympathetic innervation (Ieda et al., 2006). Furthermore, activation of TrkA on adult mouse cardiomyocytes has been shown to promote anti-apoptotic signals (Caporali et al., 2007), and to rescue mice from experimental myocardial infarction (Meloni et al., 2010) and diabetic cardiomyopathy (Meloni et al., 2012). Such work brings focus to the importance of Trk receptor and neurotrophin expression in the heart, which so happens to be the organ most associated with the major clinical manifestation of Chagas disease.

1.9 Trk receptors and Chagas disease

T cruzi has been noted to have a propensity to infect nervous tissue and highly innervated organs (Koberle, 1968), although such observations have yet to be proven causative. In the brain, TrkA expression predominates in younger animals, and switches, in older animals, to a situation in which $p75^{NTR}$, a pro-apoptotic receptor, expression predominates, and constitutes a mechanism for degenerative neurological disorders, such as Alzheimer's disease (Costantini et al., 2006; Fortress et al., 2011; Parikh et al., 2013; Reichardt, 2006). Although expression of Trk receptors has not been characterized in other organs or systems, changes in Trk receptor expression as infected individuals age may in part be related to why only a small percentage of those infected with *T cruzi* manifest the clinical forms of Chagas disease, arising years or decades after initial infection.

1.9.1 Parasite adherence/invasion of host cells

Neuraminidase/TS expression in *T cruzi* is developmentally regulated; TS/PDNF is highly expressed in the infective trypomastigote, but not amastigote, form of the parasite (Pereira, 1983). A short recombinant TS, sPDNF (Figure 1.4), that lacks the immunodominant C-terminal extension, has been cloned (Chuenkova et al., 1999) and characterized, and continues to be studied in our laboratory.

sPDNF has been characterized to bind TrkA (Chuenkova and PereiraPerrin, 2004) and TrkC (Weinkauf and Pereiraperrin, 2009). In relation to *T cruzi*

pathogenesis, both TrkA (de Melo-Jorge and PereiraPerrin, 2007) and TrkC (Weinkauf et al., 2011) were shown to act as invasion receptors, as chemical inhibition, or blockade of either Trk receptor, inhibited *T cruzi* infection of neuronal and glial cells. In cardiac cells, *T cruzi* has a preference for invading cardiac cells through TrkC than TrkA (Aridgides et al., 2013a).

1.9.2 Host cell survival/differentiation

In line with neurotrophins, sPDNF was shown to trigger downstream signaling pathways, such as MAPK/ERK and PI3K/Akt, through TrkA (Chuenkova and PereiraPerrin, 2004) and TrkC (Weinkauf and Pereiraperrin, 2009). Activation of Trk receptors by sPDNF enhanced neuron and glial cell survival in response to oxidative stress, serum deprivation, and exposure to neurotoxins (Chuenkova and Pereira, 2000; Chuenkova and PereiraPerrin, 2004; Weinkauf and Pereiraperrin, 2009). sPDNF modulates cholinergic (Akpan et al., 2008) and dopaminergic (Chuenkova and PereiraPerrin, 2006) gene expression in neuronal PC12 cells. As amastigotes differentiate to intracellular trypomastigotes in the host cell cytoplasm, study of intracellular PDNF shows that PDNF is phosphorylated by Akt and, in turn, can enhance Akt phosphorylation as a mode of inducing pro-survival signals (Chuenkova and PereiraPerrin, 2009). The diverse impacts of PDNF on pro-survival host kinase signaling demonstrate a mechanism for *T cruzi* to cause little damage to moderately parasitized brains (Caradonna and Pereiraperrin, 2009).

sPDNF was also shown to activate TrkC on cardiac fibroblasts to produce NGF, which contributed to an anti-apoptotic paracrine effect on cardiomyocytes that were exposed to oxidative stress (Aridgides et al., 2013a, 2013b). Furthermore, manipulation of paracrine survival signals by *T cruzi* PDNF may represent a feature that promotes a balance between invasion and host cell survival actions that favors chronic infection of mammalian hosts, which befits both the parasite and host.

1.10 Induction of chemokines monocyte chemotactic protein-1 (MCP-1) and fractalkine (FKN)

The persistence of *T cruzi* infection remains a biological quandary; despite the parasite stimulating a strong host inflammatory response, it is still able to evade innate immune responses and chronically persist in hosts without causing major symptoms. MCP-1 (CCL2) has emerged as a critical factor in infectious and autoimmune myocarditis (Paiva et al., 2009). This chemokine is produced in great amounts in the hearts of *T cruzi*-infected mice and is known to enhance parasite uptake and destruction by macrophages (Paiva et al., 2009). Thus chemokines may serve as mediators that contribute to strong inflammatory responses and partake in orchestrating some facets of *T cruzi* pathogenesis.

1.10.1 Recruitment of immune cells by chemokines

Upon infection, auxiliary innate host defenses, such as neutrophils, macrophages, and dendritic cells (DCs) are induced to combat the pathogen (Serbina et al., 2008). Circulating monocytes are increasingly implicated as essential players in the defense against a wide range of microbial pathogens. In humans, circulating monocytes are divided into two subsets that either specifically traffic into inflamed tissues or, in the absence of overt inflammation, constitutively maintain tissue macrophage/DC populations, and are based on the expression of the CD14 and CD16 cell surface markers (Serbina et al., 2008). In mice, monocytes that express CCR2 ($Ly6C^{hi}$) are most similar to human $CD14^{+}$ monocytes, while those that express CX3CR1 ($Ly6C^{lo}$) are most similar to human $CD16^{+}$ monocytes (Serbina et al., 2008). MCP-1/CCR2 signaling also stimulates surface expression of CX3CL1, facilitating leukocyte adhesion to sites of inflammation (Green et al., 2006). Thus, the chemokines MCP-1 and fractalkine (FKN, CX3CL1), whose receptors are CCR2 and CX3CR1, respectively, should represent important mediators for modulating monocytes and other immune cells in response to *T cruzi* infection.

Chemokines, or chemoattractant cytokines, consist of ~50 related proteins that induce leukocyte chemotaxis *in vitro* and recruitment *in vivo*. They possess other activities, such as integrin activation during leukocyte-endothelium interactions, activation of leukocyte function (e.g. degranulation and lipid mediator release), angiogenesis, and angiostasis (Teixeira et al., 2002). Chemokines are low

molecular weight proteins that contain four cysteine residues subdivided into four families based on the arrangement of the first two N-terminal cysteine residues: CC, CXC, CX3C, and C families (Teixeira et al., 2002). MCP-1 and FKN represent chemokines that are temporally expressed in a healing myocardium after an inflammatory stress caused by a myocardial infarction; MCP-1 being induced initially, followed by FKN (Nahrendorf et al., 2007). Regulation of these chemokines in relation to *T cruzi* infection would thus provide insight into the orchestrating inflammatory events during the acute phase of Chagas disease.

1.10.2 Trk receptors as a link between *T cruzi*/PDNF and chemokines

Inflammation at the site of *T cruzi* inoculation, Romaña's sign or chagoma, is characterized histologically by intense mononuclear infiltration in a local inflammatory response, which can last up to 40 days (Teixeira et al., 2002). In *in vitro* infections of cardiomyocytes and macrophages, *T cruzi* stimulates iNOS activation, the secretion of pro-inflammatory cytokines and chemokines perceived to control parasite growth, and immune cell influx, contributing to the pathogenesis of chagasic cardiomyopathy (Machado et al., 2000). *In vivo* infection of MCP-$1^{-/-}$ mice resulted in higher parasitemia, exhibited more frequent amastigote nests in the heart, and died earlier than WT mice (Paiva et al., 2009), suggesting the importance of MCP-1/CCR2 signaling for controlling *T cruzi* infection. The impact of *T cruzi* infection on the expression of FKN has not yet been described. Thus, continued study on factors that contribute to chemokine induction should be fruitful for understanding *T cruzi* pathogenesis.

TrkA has been identified as a receptor for the matricellular protein connective tissue growth factor (CTGF, CCN2) that has been implicated as a factor that promotes tissue fibrosis (Wahab et al., 2005). In cardiomyocytes, activation of TrkA by CTGF induced extracellular matrix (ECM) formation and degradation genes, and also induced pro-inflammatory cytokines and chemokines, including MCP-1 (Wang et al., 2010). Specifically, cardiomyocyte stimulation with NGF led to the induction of MCP-1, but not TNF-α or IL-6, suggesting specificity for TrkA activation to induce MCP-1 (Wang et al., 2010). Prolonged exposure to *T cruzi* in chronically infected hearts is thought to contribute to cardiac dysfunction and fibrosis. Thus, it is feasible that *T cruzi* PDNF induces chemokine expression via activation of Trk receptors.

1.10.3 Cardioprotective functions of MCP-1

MCP-1 mRNA and protein have been detected at high levels in the lesions of several non-infectious cardiovascular diseases, such as atherosclerosis (Boring et al., 1998), ischemic heart disease (Matsumori et al., 1997), dilated cardiomyopathy (Lehmann et al., 1998), congestive heart failure (Aukrust et al., 1998), autoimmune myocarditis (Fuse et al., 2001), and myocardial infarction (MI). In addition to promoting migration of immune cells, MCP-1 has beneficial effects in settings of cardiac inflammation. Cardiac overexpression of MCP-1 causes chronic infiltration and activation of leukocytes, which in turn elevate TNF-α secretion and SAPK/JNK1/2 activation, and contribute to a preconditioning effect that serves as an endogenous mechanism by which the

myocardium protects itself against infarction (Martire et al., 2003), thus linking innate immunity to ischemic preconditioning. Cardiac overexpression of MCP-1 induces macrophage infiltration, neovascularization, myocardial IL-6 secretion, and accumulation of cardiac myofibroblasts, resulting in the prevention of left ventricular (LV) dysfunction and remodeling after MI (Morimoto et al., 2006). In ischemia/reperfusion (I/R), cardiac MCP-1 overexpression prevents LV dysfunction through ROS-dependent and K_{ATP} channel-independent pathways (Morimoto et al., 2008). Thus, it is feasible that *T cruzi*-PDNF may activate TrkA and/or TrkC in cardiac cells to induce MCP-1 secretion, which can recruit immune cells to fight off infection and condition the heart to protect itself. *T cruzi*-PDNF may directly or indirectly, via chemokine induction, activate other cell types, such as stem cells, in the heart to facilitate wound healing and/or tissue repair.

1.11 Involvement of cardiac progenitor cells (CPCs) in *T cruzi* infection

Advances in medicine have dramatically increased the lifespan of individuals. With increasing numbers of ageing patients suffering from heart failure (HF) coupled with the lack of heart donors, initiatives for alternatives to heart transplant are of utmost importance (Behfar et al., 2014; Bernstein and Srivastava, 2012). Regeneration trials in patients with cardiovascular disease have utilized stem cell-based therapy in the period immediately following

myocardial injury in an attempt to halt progression towards ischemic cardiomyopathy, or, in the setting of congestive heart failure, to target the disease process and prevent organ decompensation (Behfar et al., 2014). ‘First generation’ cell-based therapies comprised of unselected cell mixtures exemplified by unfractionated bone-marrow-derived mononuclear stem cells. However, poor definition of cell types used, diversity in cell-handling procedures, and functional variability intrinsic to autologously-derived cells have been identified as main factors limiting adoption of cell-based therapies. ‘Next-generation’ cell therapy ushers a new era in regenerative medicine by targeting organ or disease before implantation (Behfar et al., 2014). The main goal of both therapies are to limit the extent of damage sustained in the myocardium, and prevent organ failure by altering the innate myocardial injury response (Behfar et al., 2014). Fortunately, several studies have utilized bone marrow cell (BMC) therapy to treat CCC, with promising results.

1.11.1 Stem cells as therapeutics for CCC

Intravenous injection of BMCs into CCC mice were shown to migrate to the heart and significantly reduce the degree of inflammatory infiltrates and interstitial fibrosis characteristic of CCC (Soares et al., 2004). By using magnetic resonance imaging to assess changes in cardiac morphology of CCC hearts, serial imaging revealed BMC therapy contributed to the regression of the right ventricular dilatation typically observed in the chagasic mouse model (Goldenberg et al., 2008). Microarray analysis of hearts from CCC mice identified significant

alterations in the expression of immune-inflammatory and fibrotic genes (Soares et al., 2010), most of which were restored to normal after BMC therapy (Soares et al., 2011). Using small animal positron emission tomography (microPET) to monitor BMC biodistribution and heart morphology, the beneficial effects of BMC therapy in chagasic mice was shown to arise from an indirect interaction of the cells in the heart, rather than a direct action due to incorporation of large numbers of transplanted BMCs into the myocardium (Jelicks et al., 2012).

Recent studies showing cell division, telomerase activity, telomere shortening, and cardiomyocyte apoptosis in normal hearts have provided evidence of cardiomyocyte turnover in adult human hearts, which challenged previous beliefs that the adult heart was a terminally differentiated, post-mitotic organ without the capacity for cellular regeneration (Bernstein and Srivastava, 2012; Urbanek et al., 2003). This led to the study of resident cardiac progenitor cells (CPCs) possibly contributing to tissue healing effects in the heart. CPCs are characterized by the expression of several stem cell markers, the two main markers being stem cell antigen-1 (Sca-1) (Chen et al., 2003; Matsuura et al., 2004; Oh et al., 2003) and c-Kit (CD117) (Saravanakumar and Devaraj, 2013; Urbanek et al., 2003), which can be further subdivided by Isl-1 (Ye et al., 2012), CD31 (Pfister et al., 2005), CD34, nestin and/or musashi-1 (Tamura et al., 2011; Tomita et al., 2005) markers, to name a few. Cardiac side population (Pfister et al., 2005) and epicardial (Chong et al., 2011) cells have been described to harbor stem cell-like properties as well. There is a significant reduction in the number of CPCs in hearts as neonates develop and age to adults (Saravanakumar and

Devaraj, 2013). CPC distribution varies in different areas of the heart, as there are more CPCs in the atrium than in the ventricle (Saravanakumar and Devaraj, 2013).

1.11.2 CPCs as immunomodulators

During MI, MCP-1 is expressed at the ischemic border zone area (BZA) of the infarct, which in turn recruits stem cells (Tamura et al., 2011). Inflammatory stress caused by endogenous or exogenous mechanisms activate progenitor/stem cells in tissues, which participate in a negative feedback loop to attenuate the inflammatory cascade before inflammatory factors accumulate and exert unwanted adverse systemic effects (Choi et al., 2011; Lee et al., 2009). Similar to cells used in BMC therapy, resident CPCs may also harbor beneficial effects in the myocardium.

CPCs are capable of producing substantial quantities of paracrine molecules; stromal-cell derived factor-1α (SDF-1) was identified as one of many dominant paracrine factors secreted, which activates CXCR4, mediating acute cardioprotection through the signal transducer and activator of transcription 3 (Jak2/STAT3) signaling, observed to improve cell growth and inhibit apoptosis (Huang et al., 2011).

1.11.3 CPCs secrete anti-inflammatory TNF stimulated gene-6 (TSG-6)

Continued efforts to study factors that CPCs produce to exert immunomodulatory and tissue repairing mechanisms have identified a novel anti-inflammatory factor, TSG-6. TSG-6 is a link protein that binds hyaluronan (HA), a glycosaminoglycan that has a central role in the formation and stability of extracellular matrix (Milner and Day, 2003; Yoshioka et al., 2000). Distribution of HA in ovarian follicles has also been studied to play an especially significant role in the expansion of the cumulus cell-oocyte complex (COC), linking TSG-6 to the ovulation process, in which it was initially described (Yoshioka et al., 2000). Treatment of leukocytes with soluble HA-TSG-6 complex inhibits the CD44-mediated adhesion to immobilized HA in vitro (Lesley et al., 2004). Various cell types secrete TSG-6 in response to proinflammatory stimuli, and have been detected in large quantities in the synovial fluids and tissues of inflamed joints of rheumatoid arthritis patients (Nagyeri et al., 2011; Wisniewski et al., 1994). It was postulated that TSG-6 exerts its anti-inflammatory and chondroprotective effects through inhibition of the plasmin protease network, a key activator of matrix metalloproteinases (MMPs), by virtue of binding and enhancing the inter-α-trypsin inhibitor (IαI), a major serine protease inhibitor in serum (Glant et al., 2002; Nagyeri et al., 2011). Conjunctivochalasis, defined as a loose, redundant, and nonedematous bulbar conjunctiva interposed between the globe and the eyelid resultant of excessive proteolytic degradation by MMPs is inhibited by TSG-6, which inhibits MMP-1 and MMP-3 expression and MMP-1 activation (Guo et al., 2012).

Stem cells have been implicated as a major source of TSG-6. In cell-based therapies, upon intravenous injection of mesenchymal stem cells (MSCs), cells would become embolized in the lungs, where they become activated to express TSG-6, which is systemically delivered via blood circulation (Lee et al., 2009; Wang et al., 2012). MSCs intraperitoneally injected are unable to secrete TSG-6, as they accumulate in the spleen and are phagocytosed by macrophages (Wang et al., 2012), highlighting the importance of cell delivery in promoting anti-inflammatory effects. After MI induction, intravenous MSC infusion which embolized in the lung and secreted an exuberant amount of TSG-6, or treatment with recombinant TSG-6 alone, decreased infarct size (Lee et al., 2009). MSCs with a knockdown of TSG-6 had no effect on echocardiography or heart function 3 weeks after infusion, whereas scrambled TSG-6 siRNA treated MSCs produced significant improvements in percent left ventricular fractional shortening and left ventricular ejection fraction in hearts (Lee et al., 2009), suggesting the long-term beneficial tissue/organ repair effects of MSCs is dependent on TSG-6 expression.

This is in line with the genetic reversion of the inflammatory state in CCC mice after treatment with BMC therapy (Goldenberg et al., 2008; Soares et al., 2011), and likely suggests a link between *T cruzi* PDNF, resident CPCs, and the induction of TSG-6 activity contributing to long lasting beneficial effects in this chronic inflammatory state.

1.12 Summary and goals

To paraphrase the wise words of Friedrich Nietzsche, “that which does not kill us makes us stronger.” The complex life cycle of *T cruzi*, reflected by the acute inflammatory response and subsequent indeterminate chronic phase of Chagas disease in its mammalian host, implicates *T cruzi* as a worthy foe to learn from. Some of the most successful pathogens utilize protective host mechanisms as a means of immune response evasion, exemplified by *Mycobacterium tuberculosis*, which evades host immunity and establishes a persistent infection by recruiting MCSs to the site of infection and suppressing T-lymphocyte responses (Raghuvanshi et al., 2010).

It is important to keep in mind that 70% of those infected do not develop the clinical manifestations of Chagas disease. This is reflective of the need for *T cruzi* to continue and perpetuate its life cycle, to chronically infect mammalian hosts, without sequelae, so that it can retransmit infection to new insect vectors. *T cruzi* factors, like PDNF, are thought to preserve host tissues to minimize damage, best exemplified by the lack of sequelae in highly parasitized brains (Caradonna and Pereiraperrin, 2009). Patients that do progress to the clinical forms of Chagas disease tend to develop them decades after initial infection, suggesting some sort of breakdown in protective host responses over time.

Our central hypothesis is that *T cruzi* expresses factors that are beneficial for the host. We sought to determine the role of *T cruzi* PDNF-Trk interaction in the

heart, in relation to the acute and chronic phase of Chagas disease. Trk receptors are expressed by cells in the heart, which include cardiomyocytes, cardiac fibroblasts, and CPCs. PDNF is known to be implicated in *T cruzi* invasion of host cells, promoting host cell survival, and promoting paracrine crosstalk between cardiac fibroblast and cardiomyocytes, all of which are mediated, at least in part, by Trk receptor activation (chapter 3). In this thesis, we investigate the contribution of PDNF-Trk activation that leads to the induction of the MCP-1 and FKN chemokine response that reflect aspects of the acute phase of infection (chapter 4), which may contribute to setting up anti-inflammatory and tissue repairing mechanisms by activating CPCs (chapter 5), subsequently progressing to the indeterminate chronic phase of infection. To further validate PDNF as a beneficial factor, and as a proof of concept, we investigated the effect of recombinant PDNF in the context of CCC, to supplement PDNF levels in the heart during a stage where *T cruzi*/PDNF levels are low (chapter 6).

CHAPTER 2. MATERIALS AND METHODS

2.1 Mouse strains

C57BL/6 (stock number: 000664), Balb/c (stock number: 000651), CCR2$^{-/-}$ (stock number: 004999), and CX3CR1$^{-/-}$ (stock number: 008451) mice aged 6-8 weeks, were purchased from Jackson Laboratories (Bar Harbor, ME). Female mice were used for all *in vivo* experiments and males were kept for breeding purposes. All mouse work was approved by the Institutional Animal Care and Use Committee (IACUC) and Department of Laboratory Animal Medicine (DLAM) of Tufts University School of Medicine (protocols B2010-32, B2013-28). MyD88$^{-/-}$ mice were a generous gift from Dr. Thereza Imanishi-Kari (Tufts Medical School).

2.2 Cell lines

2.2.1 PC12, Schwann, Vero, HL-1, H9c2

PC12 (a rat pheochromocytoma neuronal cell line from Dr. Lloyd Green, Columbia University), Schwann (a glial cell line), H9c2 (ATCC® CRL-1446, a rat cardiomyocyte cell line) and HEK 293 (used generate lentiviral particles) cells were maintained in DMEM/10% FCS. Vero cells (used to maintain *T cruzi*, *in*

vitro) were grown in DMEM/1% FCS. Cells were incubated at 37°C in a humidified atmosphere containing 5% CO_2.

2.3 Primary cell isolations

2.3.1 Astrocytes

Primary cortical astrocytes were isolated from newborn C57BL6 mouse pups, as described before (Hertz et al., 1998; Weinkauf et al., 2011). In short, pups were sacrificed by decapitation, and the whole brain was removed from the skull. Cortices were minced and a dissociated cell suspension was created by prolonged vortexing in complete astrocyte medium (DMEM supplemented with 20% horse serum (PAA) and 1x penicillin-streptomycin (Gibco)). The cell suspension was sequentially filtered through 70- and 10-mm meshes and cells plated on Falcon Primeria dishes in complete astrocyte medium. Cultures were washed 3 days after isolation, and medium changed every 3 to 4 days thereafter. Astrocytes were used after at least 2, and at most 6, weeks in culture.

2.3.2 Cardiac fibroblasts (CF) and cardiomyocytes (CM)

Primary cardiac cells were isolated using a modified version of a previously described procedure (Sreejit et al., 2008). In short, neonatal C57BL/6 mouse pups (1-3 days old) were sacrificed by decapitation, their hearts excised and washed twice in PBS, then kept in 20 mM HEPES, 130 mM NaCl, 1mM

NaH_2PO_4, 4 mM glucose, 3 mM KCl, pH 7.6 for 10 minutes on ice. Hearts were minced and digested in 0.25% Trypsin-EDTA (Gibco) 3-4 times at 37°C with periodic mixing. Dissociated cells were pooled and digestion stopped with the addition of DMEM/10% FCS to the cell suspension, which is filtered through a 100 μm cell strainer, centrifuged at 500 x g, and plated for 3 h on 1% gelatin-coated plates in cardiomyocyte medium (50:50 ratio of DMEM (Gibco)/F12 Ham's (Sigma), 20% FCS (PAA), 5% horse serum (PAA), 2 mM L-glutamine (Gibco), 0.1 mM nonessential amino acids (Gibco), 3 mM sodium pyruvate (Gibco), and 1 μg/ml bovine insulin (Sigma) with 1x penicillin-streptomycin (Gibco)). Non-adherent cells (cardiomyocytes) were removed and plated onto new gelatin-coated plates while adherent cells (cardiac fibroblasts) remained in the initial plate in DMEM/10% FCS until needed. Cardiomyocytes contained <5% cardiac fibroblasts and vice versa for cardiac fibroblasts, as determined by immunofluorescence using antibodies against the cardiomyocyte marker myosin heavy chain (MHC) and cardiac fibroblast marker vimentin, as described earlier.

2.3.3 Cardiac progenitor cells (CPCs)

Primary CPCs were isolated by positive selection based on the expression of the stem cell antigen-1 (Sca-1) marker. Subsets of Sca-1^+ cells have been designated as progenitor/stem cells in mouse heart (Oh et al., 2003; Pfister et al., 2005). Single-cell suspensions of mouse hearts were obtained with the use of the gentleMACS™ Dissociator (Miltenyi Biotec), which allowed for automated tissue dissociation in a closed system, enabling sterile sample handling. An anti-Sca-1

microbead kit (#130-092-529, Miltenyi Biotec) was used to isolate murine stem cells from single-cell cardiac suspensions by positive selection. In short, cells are immunolabeled with Anti-Sca-1-FITC, after which magnetic labeling of Sca-1^+ cells are achieved using Anti-FITC MicroBeads. The labeled cell suspension is applied to a MACS® Column placed in a magnetic field of a MACS® Separator, where Sca-1^+ cells remain retained within the column. After removal of the column from the magnetic field, the retained Sca-1^+ CPCs are eluted. CPCs were maintained in CPC medium containing DMEM (66.2%), IMDM (8.1%), Ham's F12 (16.2%), FCS (5.9%), horse serum (1.25%), B27 supplement (0.5%), 1.75 mM Glutamax, penicillin/streptomycin (1X), 0.025 mM NEAA, 2.25 mM sodium pyruvate, basic fibroblast growth factor (FGF, R&D 3139-FB/CF, 20 ng/ml), epidermal growth factor (EGF, R&D, 2028-EG, 6.25 ng/ml), thrombin (R&D, 2196-SE, 0.25 U/ml), cardiotrophin-1 (R&D, 438-CT/CF, 1 ng/ml), insulin (Sigma, 0.25 μg/ml), and 0.025 mM β-mercaptoethanol.

2.4 *T cruzi* strains

2.4.1 Silvio, Tulahuén, Colombian

Experiments were performed with *T cruzi* Silvio, Tulahuén and Colombian strains, which were all propagated in Vero cells. The Silvio and Tulahuén strains have been used in *in vitro* studies of adhesion and cell invasion. The Tulahuén

and Colombian strains have been used in *in vivo* studies, for they infect mice that proceed to develop acute and chronic phase characteristics of Chagas disease.

Free-swimming infective trypomastigotes were harvested from Vero cell supernatants (3-5 d (Silvio) or 5-7 d (Tulahuén and Colombian) after infection) by initial low speed centrifugation (500 x g, 5 min) to remove host cells and debris. Parasites are pelleted by high-speed centrifugation (1,200 x g, 10 min), and resuspended in DMEM/0.1% FCS to be used in *in vitro* experiments. For *in vivo* experiments, parasites were resuspended in PBS prior to injection into mice.

2.5 sPDNF purification

PDNF was cloned from the *T cruzi* Silvio X-10/4 strain (GenBank accession number AJ002174), and a N-terminal short-form of PDNF (sPDNF) that contains Trk-binding sites and a 6-His-tag was expressed in BL21(DE3) bacteria by IPTG (isopropyl β-D-1-thiogalactopyranoside) induction, and purified by Ni-affinity chromatography, as described previously. Buffers were prepared in sterile endotoxin-free water, and sPDNF preparations screened with the *Limulus* amebocyte assay to have undetectable levels of endotoxin. sPDNF migrates as a 68 kDa protein on a SDS-PAGE gel. sPDNF protein was buffer exchanged into PBS (0.01 M phosphate buffered saline, pH 7.2), filter-sterilized (0.22 μm), and kept at 4°C. sPDNF was quantified by scanning densitometry (Bio-Rad, GS-800) of SDS-PAGE gels stained with Coomassie brilliant blue.

2.6 *In vitro* and *ex vivo*

2.6.1 Cell stimulation

(i) *T cruzi* infection: Primary cardiomyocytes and cardiac fibroblasts were seeded at 6-8 x 10^4 cells per well in DMEM/10% FCS and allowed to adhere overnight. Medium was changed to DMEM/5% FCS and cells were infected with *T cruzi* at an MOI (multiplicity of infection) of 10 for at most 24 h, at which time parasites were rinsed away. At 3, 24, and 72 h post-infection, cell monolayers were collected in Trizol reagent (Invitrogen) to isolate RNA to generate cDNA for qPCR later discussed in section 2.8.

(ii) sPDNF stimulation: Primary cardiomyocytes and cardiac fibroblasts, and H9c2 cardiomyocytes were seeded at 6-8 x 10^4 cells per well in DMEM/10% FCS and allowed to adhere overnight, serum starved (DMEM/0.1% FCS overnight), and treated with sPDNF (0.5 ng/ml - 8 μg/ml, 0-16 h). In some cases, cells were starved in serum-free DMEM for at least 2 h prior to stimulation. Cell supernatants were collected and stored at -80°C and cell monolayers rinsed with PBS and collected in Trizol for qPCR analysis.

2.6.2 Inhibition by α-Trk blocking antibodies

H9c2 cardiomyocytes were pre-treated with 1 μg/ml neutralizing antibodies against TrkA (α-TrkA, Santa Cruz SC-118), TrkB (α-TrkB, Santa Cruz SC-8316),

and TrkC (α-TrkC, Santa Cruz SC-14025) for 30 min, and then stimulated with 1 μg/ml sPDNF for 3 h. In some cases, a mixture of α-TrkA and α-TrkC antibodies was used in combination. Supernatants and/or cell monolayers were collected and processed as in section 2.6.1.

2.6.3 Inhibition by chemical inhibitors

H9c2 cells were pre-treated with 0.1% DMSO vehicle control or 200 nM K252a for 1 h prior to addition of sPDNF (1 μg/ml for 3 h). Supernatants and/or cell monolayers were collected and processed as in section 2.6.1.

2.6.4 Hydrogen peroxide oxidative stress protection assay

CPCs (4,000 cells/well) were plated in 96-well plates overnight in CPC medium. Cells were washed with PBS and replaced with 0.1% FCS/DMEM (50 μl). Cells were pre-treated with 50 μl of a 2X stock of sPDNF (600 ng/ml) for 30 minutes (final concentration of 300 ng/ml). 50 μl of a 3X stock of H_2O_2 (3.75 mM) were added to respective wells for a final concentration of 1.25 mM for 3 h. 10 μl of a 16X stock of propidium iodide (PI, 80 μg/ml) and Hoechst (160 μg/ml) were added per well [final concentrations: 5 μg/ml (PI) and 10 μg/ml (Hoechst)] for 5 minutes, 3 wells at a time. The Hoechst dye stains all cell nuclei blue. Propidium iodide, a vital stain, stains dead cells red, for they are unable to exclude the dye. Pictures were taken and dead (red) and total (red and blue) cells were counted.

At least 200 cells/well were counted. % Cell Death was expressed as (dead cells) ÷ (total cells) × 100%.

2.7 *In vivo*

2.7.1 *T cruzi* infection

Female C57BL/6 mice (6-8 weeks old) were infected subcutaneously in the left hind footpad with 5,000 trypomastigotes (Tulahuén strain) in 30 μl PBS under isofluorine anesthesia. Mice were sacrificed at various days post-infection (DPI) by CO_2 asphyxiation and cervical dislocation. For in vivo inhibition experiments, parasites were mixed with bovine serum albumin (BSA) or α-Trk antibodies prior to subcutaneous injection and mice sacrificed 3 days later. Organs were perfused by intracardiac injection of 5 ml ice-cold PBS, and the heart (sometimes, atria and ventricle were collected separately) and other organs were collected and flash frozen in liquid nitrogen and stored at -80°C. Tissues were processed for gene expression as described in section 2.8. Tissue parasitism was quantified using a qPCR method utilizing genomic tissue DNA, previously described (Cummings and Tarleton, 2003).

2.7.2 Single intravenous (IV) sPDNF injections

sPDNF was diluted in sterile endotoxin-free PBS in 200 μl and injected via the tail vein into 6-8 week old female C57BL/6 mice. Mice receiving single IV injections of 150 μg sPDNF per mouse were sacrificed at 3, 6, 9, and 12 h post-injection, or

various doses of sPDNF (100 ng-150 μg) and sacrificed 3-h post-injection. After sacrifice, mice were perfused with PBS and organs harvested and processed as described in section 2.7.1.

2.7.3 Multiple IV sPDNF injections

Mice receiving multiple injections of sPDNF or PBS vehicle control (0, 3, and 24 h, 50-100 μg per injection) were sacrificed 24 h after the last injection (i.e., 48 h after the first injection). Mice were perfused with PBS and organs harvested and processed as described above in section 2.7.1.

2.7.4 IV sPDNF treatment

Female C57BL/6 and Balb/c mice (6-8 weeks old) were intraperitoneally infected with 800 or 80 trypomastigotes (Colombian strain), respectively, in a volume of 200 μl PBS. Mice were allowed to progress through the acute phase, when parasites can be detected in the blood, into the chronic phase of disease, when parasitemia is low to undetectable. At approximately 4 months post-infection, mice received placebo (IV PBS) or IV sPDNF treatment. The IV sPDNF treatment consisted of 25 μg sPDNF IV injections at 0, 3, and 24 h intervals, weekly for 3 weeks. In some cases, mice were tail bled at various days post-infection or post-treatment, from which serum samples were isolated and kept frozen and -80°C until used. Approximately 2 months after the initiation of the IV sPDNF treatment, mice were sacrificed and their organs harvested and processed as in section 2.7.1.

2.7.5 Tissue histology

In addition, heart samples were fixed in 4% paraformaldehyde for 48 h and sent to DLAM for tissue sectioning and staining. In short, tissue samples were embedded in paraffin wax, sectioned (5 μm thick), and placed on slides for staining. Tissue sections were subjected to hematoxylin and eosin (H&E) stain to visualize inflammatory infiltrates/foci and the degree of inflammation. Tissue sections were subjected to Masson's trichrome stain, which distinguishes cells (visually red) from connective tissue or fibrotic areas (visually blue), to visualize fibrosis. A hallmark of cardiac fibrosis is the deposition of collagen in heart tissue, where collagen is usually limited. Multiple bright field images (Nikon camera, SPOT imaging system software) were taken and subjected to analysis by a custom script using ImageJ (NIH) software. For each image, every pixel was determined to represent either red (tissue) or blue (collagen); white pixels are ignored. Percent fibrosis was quantified as fibrotic area (blue pixels) ÷ total area (red + blue pixels) × 100%.

2.8 qPCR analysis

RNA was isolated from Trizol lysates of cell monolayers or liquid nitrogen snap frozen tissue samples dissociated by a Tissue-Tearor mechanical homogenizer (Biospec Products, Inc.). cDNA was synthesized using the Quantitect Reverse Transcription kit (Qiagen) according to manufacturer's instructions. Gene

transcripts were amplified using specific primers and normalized to the housekeeping gene, hypoxanthine-guanine phosphoribosyltransferase (HPRT), using SYBR Green (Qiagen), and, if needed, expressed relative to control/unstimulated samples (Livak and Schmittgen, 2001). The primers used are summarized in Table 1.

Table 1. qPCR primer list.

Gene	Forward (5'→3')	Reverse (5'→3')
INFLAMMATORY		
MCP-1/CCL2	TCTCTTCCTCCACCACTATGCA	GGCTGAGACAGCACGTGGAT
FKN/CX3CL1	GCCCGCCGAATTCCTGCACT	CAATGGCACGCTTGCCGCAG
TNF-α	TGGGAGTAGACAAGGTACAACC	CATCTTCTCAAAATTCGAGTGACA
IFN-γ	ACAGCAAGGCGAAAAAGGATG	TGGTGGACCACTCGGATGA
IL-6	CTGCAAGAGACTTCCATCCAG	AGTGGTATAGACAGGTCTGTTGG
IL-1β	TGGAGAGTGTGGATCCCAAGCAAT	TGTCCTGACCACTGTTGTTTCCCA
FIBROTIC		
TGF-β	AAGGACCTGGGTTGGAAGTG	TGGTTGTAGAGGGCAAGGAC
CTGF	GAGGAAAACATTAAGAAGGGCAAA	CGGCACAGGTCTTGATGA
ANTI-INFLAMMATORY		
TSG-6	CGTCTCGCAACCTACAAGCA	GGTATCCGACTCTACCCTTGG
IL-1RA	GCTCATTGCTGGGTACTTACAA	CCAGACTTGGCACAAGACAGG
IL-10	GCTCTTACTGACTGGCATGAG	CGCAGCTCTAGGAGCATGTG
CELL MARKERS		
CD4	CTTCGCAGTTTGATCGTTTTGAT	CCGGACTGAAGGTCACTTTGA
CD8	AAGAAAATGGACGCCGAACTT	AAGCCATATAGACAACGAAGGTG
CD11b	GGCTCCGGTAGCATCAACAA	ATCTTGGGCTAGGGTTTCTCT
CCR2	AATGAGAAGAAGAGGCACAGGGCT	ATGGCCTGGTCTAAGTGCTTGTCA
CX3CR1	CGACATTGTGGCCTTTGGAACCAT	AGATGTCAGTGATGCTCTTGGGCT
STEM CELL MARKERS		
Sca-1	TCCTGGGTACTAAGGTCAACG	CTCCATTGGGAACTGCTACATT
c-kit	GGCCTCACGAGTTCTATTTACG	GGGGAGAGATTTCCCATCACAC
CD34	ATCCCCATCAGTTCCTACCAAT	TGGTGTGGTCTTACTGCTGTC
Msh1	TAAAGTGCTGGCGCAATCG	TCTTCGTCCGAGTGACCATCT
NESTIN	CCCCTTGCCTAATACCCTTGA	GCCTCAGACATAGGTGGGATG
***T CRUZI* QUANTIFICATION**		
TCZ	GCTCTTGCCCACA(A/C)GGGTGC	CCAAGCAGCGGATAGTTCAGG
TNF	TCCCTCTCATCAGTTCTATGGCCCA	CAGCAAGCATCTATGCACTTAGACCCC
HOUSEKEEPING GENE		
HPRT	CAGCGTCGTGATTAGCGATGATG	CGAGCAAGTCTTTCAGTCCTGTC

2.9 ELISA

2.9.1 MCP-1

96-well Maxisorp plates (Nunc) were coated overnight with relevant supernatants or MCP-1 standards (R&D Systems, 479-JE/CF) in carbonate-bicarbinate coating buffer (50 mM $NaHCO_3/Na_2CO_3$, pH 9.6, 0.02% NaN_3), blocked in 5% BSA/PBST, reacted with a MCP-1 detection antibody (Santa Cruz, SC-28879; 1:200; 2 h), and then alkaline-phosphatase (AP) conjugated secondary antibody (Sigma A3687; 1:1000; 1 h). Between each step, plates were washed 2-4 times with PBST. Wells were then incubated with colorigenic AP substrate (Sigma N9389; 1 mg/ml in 100 mM glycine, 1 mM $MgCl_2$, 1 mM $ZnCl_2$, pH 10.4) and absorbance read at 405 nm on an Emax precision microplate reader (Molecular Devices). MCP-1 concentrations were calculated relative to a 4-parametric standard curve using the SOFTmax Pro program. In some cases, to test supernatants from neutralizing α-Trk antibody experiments, a MCP-1 ELISA kit (R&D Systems, DY479) was used according to manufacturer's protocol.

2.9.2 TSG-6

96-well Maxisorp plates (Nunc) were coated with anti-MsTSG-6 antibody (Millipore MAPT108; 1:300) overnight in carbonate-bicarbinate coating buffer. Wells were washed, blocked with PBST/5% BSA (1-2 h), incubated with standards and supernatants (2 h), followed by biotinylated TSG-6 detection antibody (R&D Systems, BAF2326, 1:300, 2h) and then streptavidin-conjugated

alkaline-phosphatase protein (Invitrogen, SA1008, 1:1000, 30 min). All incubations were at room temperature and wells washed 2-4 times with PBST in between each step. Wells were incubated with colorigenic AP substrate, absorbance read, and TSG-6 concentrations calculated in a similar manner to the MCP-1 ELISA, above.

For serum TSG-6 levels, a TSG-6 (TNFAIP6) ELISA kit (MyBioSource, MBS919938) was used according to manufacturer's protocol.

2.9.3 MIP-2α and IL-6

MIP-2α (R&D Systems, DY452) and IL-6 (R&D Systems, DY406) ELISAs were done according to manufacturer's protocols.

2.10 shRNA knockdown of Trk receptors

Lentiviral vectors encoding shRNA constructs targeting TrkA (clones 1-4), TrkC (clones 1-5) or GFP mRNA (Open Biosystems) were generated from transfected HEK 293 cells following manufacturer's instructions, and aliquots were kept frozen at -80°C until use. Lentiviral transduction of H9c2 cells was performed after pretreatment with 8 μg/ml polybrene (Sigma-Aldrich) in DMEM/10% FCS, with a dose of 200 μl vector-containing supernatant/2 ml medium in 6-well plates. Lentiviral particles were removed 24 h after infection and, 7-8 d later, cells were

serum starved in serum-free DMEM for 2 h and stimulated without or with sPDNF (4 μg/ml, 3 h).

2.11 Immunofluorescence

2.11.1 Primary cultures

Primary cultured cells or differentiated CPCs were fixed in 4% paraformaldehyde, permeabilized with 0.1% Triton X-100 for 5 minutes, then blocked overnight in PBST/10% FCS at 4°C. After washing with PBST, cells were incubated with primary antibody in PBST/5% FCS overnight at 4°C, washed, and secondary antibodies were added for two hours at room temperature. Table 2 summarizes antibodies used for immunofluorescence. Cells were washed three times with PBST for 20 minutes and counter-stained with 4'6-diamidino-2-phenylindole (DAPI) to visualize nuclei. Images were acquired with the SPOT imaging system. All image exposures and preparations were identical within a single experiment.

2.12 Statistical Analyses

Statistics were performed using GraphPad Prism software (version 5.0) using Student's *t*-test (for comparing two samples) or one-way ANOVA with Tukey's post-test (for comparing three or more samples).

Table 2. Antibodies used for Trk blocking, immunofluorescence and ELISA.

Antibody Antigen	Method	Source
TrkA	Trk inhibition	Santa Cruz SC-118, 1 μg/ml
TrkB	Trk inhibition	Santa Cruz SC-8316, 1 μg/ml
TrkC	Trk inhibition	Santa Cruz SC-14025, 1 μg/ml
TrkA	Immunofluorescence	Millipore 06-574, 1:100
TrkC	Immunofluorescence	R&D Systems MAB1404, 1:100
vWf (von Willebrand factor)	Immunofluorescence	DAKO, A0082, 1:100
MHC (myosin heavy chain)	Immunofluorescence	Upstate 05-716, 1:100
Vimentin	Immunofluorescence	Sigma V4630, 1:100
Alexa fluor 488 GtαRb-IgG	Immunofluorescence	Molecular probes A11008, 1:500
Alexa fluor 594 GtαRt-IgG	Immunofluorescence	Molecular probes A11007, 1:500
Alexa fluor 350 DkαGt-IgG	Immunofluorescence	Molecular probes A21081, 1:500
Alexa fluor 350 DkαMs-IgG	Immunofluorescence	Molecular probes A11035, 1:500
Alexa fluor 568 GtαMs-IgG	Immunofluorescence	Molecular probes A11004, 1:500
Alexa fluor 568 DkαSh-IgG	Immunofluorescence	Molecular probes A21099, 1:500
MCP-1 (detecting)	ELISA	Santa Cruz SC-28879, 1:200
TSG-6 (capture)	ELISA	Millipore MAPT108, 1:300
TSG-6 (detecting)	ELISA	R&D systems BAF2326, 1:300
GtαRb-IgG-AP	ELISA	Sigma A3687, 1:1000
Streptavidin-AP	ELISA	Invitrogen SA1008, 1:1000

CHAPTER 3. *T CRUZI* INTERACTION WITH TRK RECEPTORS VIA PDNF

This chapter includes excerpts of work from the following publications:

Aridgides, D., Salvador, R., PereiraPerrin, M., 2013a. Trypanosoma cruzi highjacks TrkC to enter cardiomyocytes and cardiac fibroblasts while exploiting TrkA for cardioprotection against oxidative stress. Cell. Microbiol. 15, 1357–1366.

Aridgides, D., Salvador, R., PereiraPerrin, M., 2013b. Trypanosoma cruzi Coaxes Cardiac Fibroblasts into Preventing Cardiomyocyte Death by Activating Nerve Growth Factor Receptor TrkA. PLoS ONE 8, e57450.

Weinkauf, C., Salvador, R., PereiraPerrin, M., 2011. Neurotrophin Receptor TrkC Is an Entry Receptor for Trypanosoma cruzi in Neural, Glial, and Epithelial Cells. Infect. Immun. 79, 4081–4087.

3.1 Introduction

The interaction of *T cruzi* with its host can be studied at the molecular level. Studying the interaction of specific *T cruzi* proteins with host cell receptors may very well highlight important pathways involved in Chagas disease progression. Studies focused on the *T cruzi* protein PDNF have identified the Trk family receptors as an important pathway that implicates a variety of biological outcomes most likely important in *T cruzi*-host interaction. Results presented in this chapter introduce aspects of *T cruzi*-PDNF and host Trk receptor interaction that results in parasite invasion of cells and the promotion of survival of neural and cardiac cells.

3.2 TrkC mediates *T cruzi* invasion of primary astrocytes

T cruzi is an obligate intracellular parasite that can invade a wide range of nucleated cell types, such as muscle cells, epithelial cells, and macrophages. Work in our lab has identified TrkA, a member of the Trk receptor family, as an invasion receptor for *T cruzi*, mediated through PDNF in neuronal cells (de Melo-Jorge and PereiraPerrin, 2007). With this finding in mind, we set out to identify other potential Trk receptors involved in host cell invasion. Within the central nervous system (CNS), *T cruzi* preferentially invades astrocytes. Thus, we utilized this cell type in *T cruzi* infection inhibition experiments.

Primary astrocytes were isolated from neonatal mouse pups and pre-treated with various ligands against TrkA (NGF, sPDNF), TrkB (BDNF), and TrkC (NT-3, sPDNF). Our results show that NT-3, but not the other neurotrophins NGF and BDNF, dose-dependently inhibited invasion of *T cruzi* into primary astrocytes. sPDNF was as effective as NT-3 in inhibiting invasion of astrocytes, in agreement with the notion that sPDNF binds to the same sites on TrkC as native TrkC ligand NT-3 (Figure 3.1). Thus, these competitive inhibition experiments suggest TrkC as an invasion receptor for astrocytes. Though astrocytes express all three Trk receptors (Wang et al., 1998), the results highlight a preferential use of Trk receptors in the *T cruzi* invasion of various cell types; for example, in neuronal cells, invasion occurs through TrkA, whereas in astrocytes, it is mediated through TrkC (Weinkauf et al., 2011).

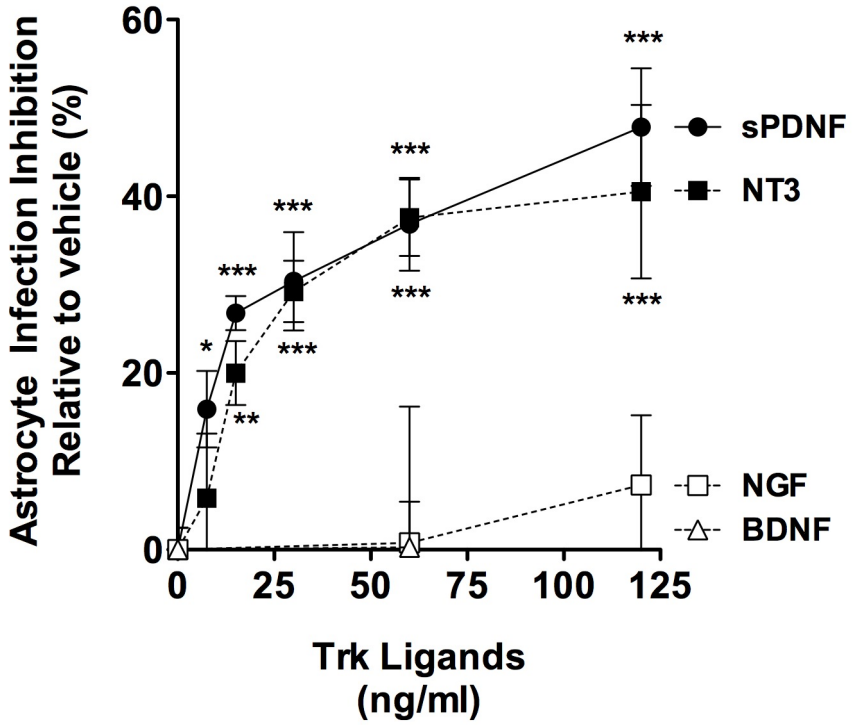

Figure 3.1. TrkC blockers inhibit *T cruzi* infection of primary astrocytes in a dose-dependent manner.

Various concentrations of TrkC blockers (sPDNF and NT3) and non-blockers (NGF and BDNF) were added to cells (in triplicate) 1 hour before infection with *T cruzi* (3.5 h), washed (to remove uninvaded parasites), and the infection allowed to proceed for 3 days. Infection inhibition of pre-treated cells were made relative to vehicle-controls. Data are representative of two experiments; points represent mean ± SEM. **P* ≤ 0.05, ***P* ≤ 0.01, and ****P* ≤ 0.005. Reprinted with permission from Copyright © American Society for Microbiology, Infection and Immunity, Vol. 79, 2011, p. 4081-4087, doi:10.1128/IAI.05403-11.

3.3 TrkC and TrkA, but not TrkB, antibodies block *T cruzi* infection *in vivo*

As previous *in vitro* and *ex vivo* experiments have identified TrkA and TrkC as important invasion receptors for distinct cell types, we wanted to determine the *in vivo* relevance of the *in vitro T cruzi* infection results.

T cruzi can be transmitted after an insect vector takes a bloodmeal from a mammalian host. When the insect vector defecates onto its host, infective trypomastigotes can invade through the insect bite, cuts or abrasions of the skin, resulting in the initial cutaneous infection, from which parasites disseminate. We mimicked the natural transmission of *T cruzi* with subcutaneous injections into the hind footpads of mice. To determine the role of Trk receptors *in vivo*, we subcutaneously injected mice with *T cruzi* in combination with blocking antibodies directed against the different Trk receptors to compete for receptor access. *T cruzi* is an obligate intracellular pathogen; it not only invades cells to replicate, it does so to also evade its host's immune response. Therefore, if Trk-specific antibodies block *T cruzi* access/invasion, the parasites become more susceptible to host immune responses and are cleared.

We found that antibodies directed against TrkA and TrkC, but not TrkB, are able to inhibit footpad parasitism (Figure 3.2), thus supporting the concept that *T cruzi* uses TrkA and TrkC receptors to invade various cell types in the mammalian host (Weinkauf et al., 2011).

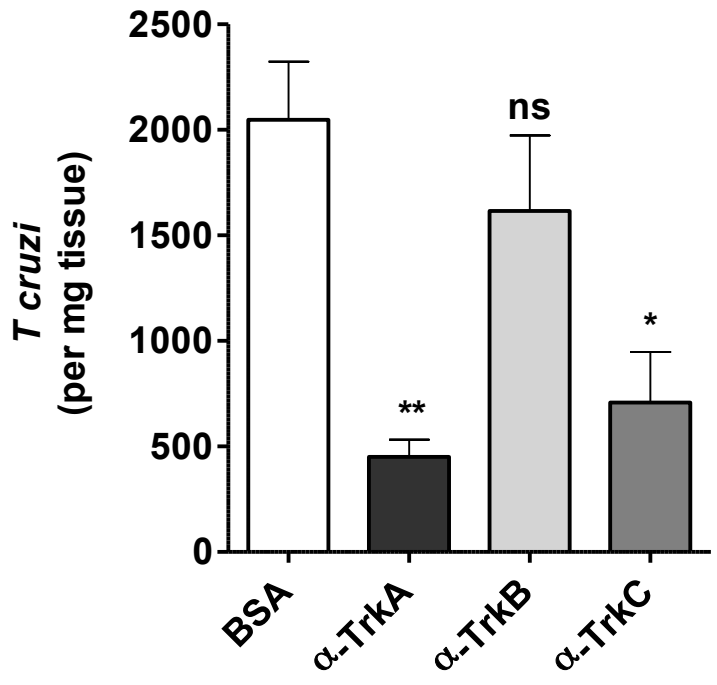

Figure 3.2. TrkC and TrkA, but not TrkB, antibodies block *T cruzi* infection *in vivo*.

Mice (5/group) were infected subcutaneously in the footpad with 5×10^3 *T cruzi* trypomastigotes (Tulahuén strain) mixed with 2 μg BSA or antibodies specific for TrkA (α-TrkA), TrkB (α-TrkB), TrkC (α-TrkC), and footpad parasitism was quantified 3 days later by qPCR. Bars represent mean ± SEM footpad parasitism of three independent experiments (15 mice per group). * and **, $P = 0.011$ and 0.009, respectively, compared to BSA controls. Reprinted with permission from Copyright © American Society for Microbiology, Infection and Immunity, Vol. 79, 2011, p. 4081-4087, doi:10.1128/IAI.05403-11.

3.4 *T cruzi* hijacks TrkC to enter cardiac cells, and exploits TrkA for cardioprotection against oxidative stress

For unknown reasons, approximately 30% of Chagas disease patients suffer or will suffer from chronic chagasic cardiomyopathy (CCC). Continued work delineating the interaction between *T cruzi* PDNF with TrkA and TrkC was studied in the context of the heart. TrkA and TrkC have been identified in cardiac cells, including cardiomyocytes and cardiac fibroblasts (Aridgides et al., 2013b; Kawaguchi-Manabe et al., 2007; Meloni et al., 2010). We discovered that *T cruzi* preferentially invaded cardiomyocytes and cardiac fibroblasts through TrkC, compared to TrkA (Aridgides et al., 2013a). Furthermore, activation of TrkA on cardiac fibroblasts stimulates the expression/secretion of an exuberant amount of NGF, which, in a paracrine fashion, promotes the cell survival of cardiomyocytes (Aridgides et al., 2013b).

3.5 Summary

The results summarized above support the concept that *T cruzi* recognition of Trk receptors facilitates parasite entry into cells of the nervous system in culture and *in vivo*. Given that Trk receptors are expressed by many cell types of non-neural origin, the results suggest that *T cruzi* uses Trk receptors to invade non-neural cells, such as those found in the heart.

CHAPTER 4. INDUCTION OF CHEMOKINES BY *T CRUZI* AND PDNF

This chapter is representative of the following accepted publication (in press):

Salvador, R., Aridgides, D., PereiraPerrin, M., 2014. Parasite-Derived Neurotrophic Factor/trans-Sialidase of Trypanosoma cruzi Links Neurotrophic Signaling to Cardiac Innate Immune Response. Infect. Immun. 82, 3687–3696.

4.1 Introduction

T cruzi elicits a potent inflammatory response in acutely infected hearts. The inflammatory response keeps tissue parasitism in check, and at the same time, may contribute to cardiac abnormalities due to several factors, including oxidative stress. The inflammatory response wanes in most (>95%) infected patients with acute Chagas disease, who progress to symptomless and pathology-free indeterminate phase that can last years or a lifetime. However, less than 5% of patients progress and succumb to widespread and fulminating myocarditis.

Here, we show that *T cruzi* strongly upregulates the chemokines monocyte chemoattractant protein-1 (MCP-1)/CCL2 and fractalkine (FKN)/CX3CL1 in the context of cellular and mouse models of heart inflammation (Salvador et al., 2014). Given that MCP-1 and FKN are innate immunity mediators, they are essential for the recruitment of immune cells to combat inflammation triggers and enhance tissue repair (Green et al., 2006; Morimoto et al., 2008; Paiva et al., 2009; Serbina et al., 2008), our findings uncover a new mechanism in innate

immunity of *T cruzi* infection mediated by Trk signaling. Thus, PDNF may serve as a link between *T cruzi* and Trk receptors on the host for the parasite to actively modulate acute inflammatory and subsequent wound healing responses.

4.2 *T cruzi* and sPDNF augment MCP-1 and FKN expression in primary cultures of cardiomyocytes and cardiac fibroblasts

In line with an earlier study (Machado et al., 2000), we found that *T cruzi* infection of primary cardiomyocytes and cardiac fibroblasts upregulates MCP-1 and FKN transcripts in a time-dependent manner (Figure 4.1). In addition, the stimulatory activity of *T cruzi* is mimicked by sPDNF, as it stimulates an increase in MCP-1 and FKN transcripts in both primary cardiomyocytes and cardiac fibroblasts in a dose-dependent manner (Figure 4.2). Differences in the responses of cardiac cells to *T cruzi* or sPDNF may be attributed to the conditions in which cells are stimulated (serum-containing or serum-starved, respectively), timing, or the plethora of molecules present on the surface of live parasites.

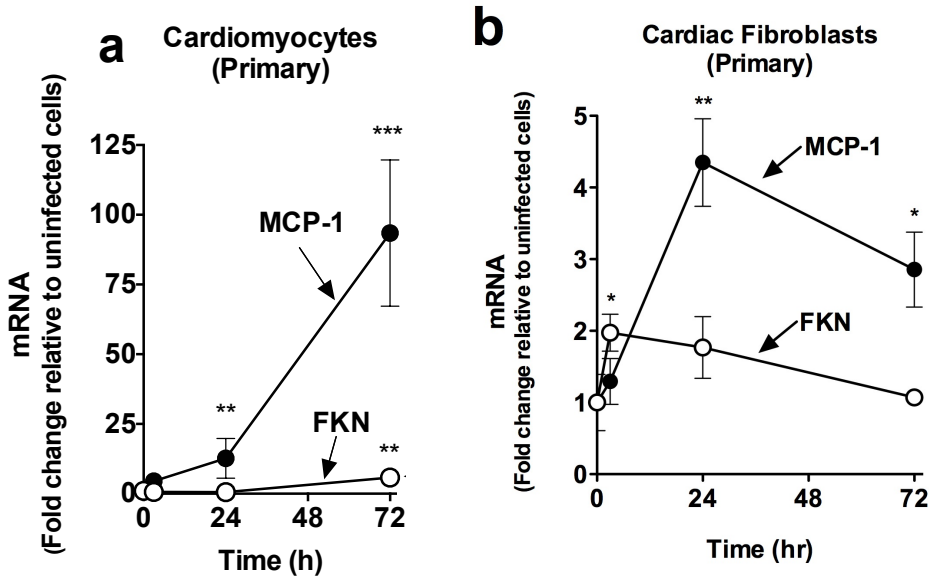

Figure 4.1. *T cruzi* infection stimulates monocyte chemotactic protein-1 (MCP-1) and fractalkine (FKN) in primary cultures of cardiomyocytes and cardiac fibroblasts over time.

Primary cultures of mouse (**a**) cardiomyocytes and (**b**) cardiac fibroblasts were plated in 6-well plates, infected with *T cruzi* (Tulahuen strain; MOI = 10) for 3, 24, and 72 h, and MCP-1 and FKN transcripts were quantified by qPCR. Chemokine gene expression was normalized to HPRT and fold change calculated relative to uninfected cells. Points represent mean ± SD fold change expression of triplicate samples. **P* < 0.05, ***P* < 0.01, and ****P* < 0.005, compared to uninfected cells. Graph is representative of two experiments, with similar results.

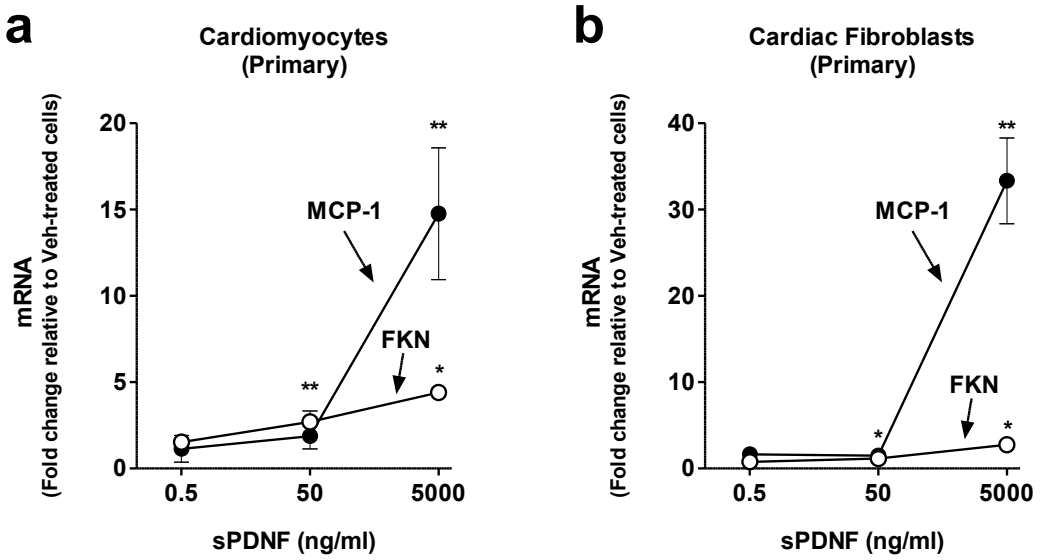

Figure 4.2. sPDNF stimulates MCP-1 and FKN expression in primary cultures of cardiomyocytes and cardiac fibroblasts in a dose-dependent manner.

Primary (**a**) cardiomyocytes and (**b**) cardiac fibroblasts were plated in 6-well plates, serum starved overnight, then stimulated with indicated concentrations of sPDNF (3 h), and MCP-1 and FKN transcripts were quantified by qPCR. Chemokine gene expression was normalized to HPRT and fold change calculated relative to vehicle (Veh)-treated cells. Points represent mean ± SEM fold change expression of triplicate samples from two independent experiments; **P* < 0.05, ***P* < 0.01, and ****P* < 0.005, compared to Veh-treated cells.

4.3 sPDNF upregulates MCP-1 and FKN expression in H9c2 cardiomyocytes dose-dependently, in a pulse-like manner

In the cardiomyocyte cell line H9c2, TrkA activation by CTGF and NGF leads to the induction of MCP-1 (Wahab et al., 2005). Therefore, we set out to determine whether *T cruzi* PDNF recognition of TrkA would also stimulate MCP-1 expression.

Here, we show that sPDNF dramatically increased secretion of MCP-1 dose-dependently and specifically, as sPDNF does not alter secretion of another chemokine, macrophage inflammatory protein-2α/MIP-2α/CXCL2, or the cytokine IL-6 (Figure 4.3a). Similar to results obtained from sPDNF stimulated primary cardiomyocytes, the increase of MCP-1 and FKN mRNA in H9c2 cardiomyocytes is dose-dependent (Figure 4.3b). Furthermore, time-course analysis reveals that MCP-1 transcript induction peaks 3 h after sPDNF stimulation, in a typical pulse-like manner, whereas FKN continues to be induced 5 h after stimulation (Figure 4.3c). It is interesting to note that, though similar, FKN expression is induced at higher sPDNF concentrations and lasts longer than MCP-1 (Figure 4.3b and c), suggesting they are differentially regulated in response to sPDNF.

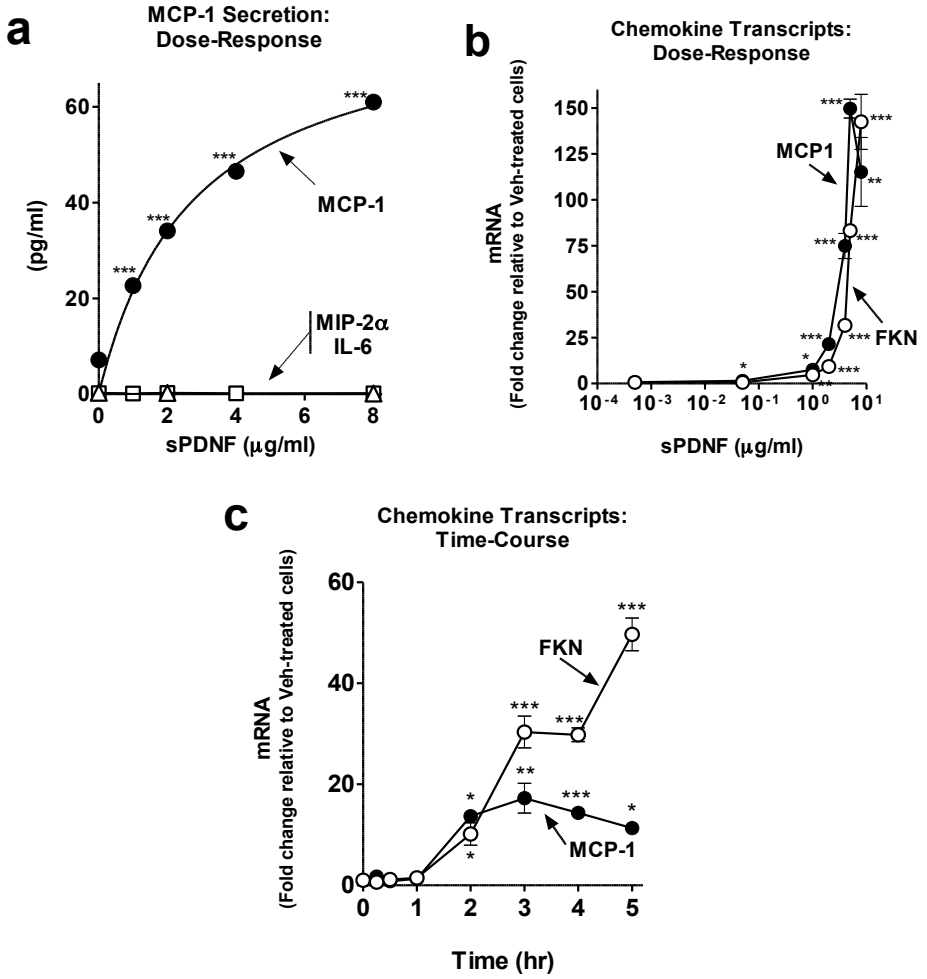

Figure 4.3. sPDNF upregulates MCP-1 and FKN expression in H9c2 cardiomyocytes in a dose- and time-dependent manner.

(**a**) H9c2 cardiomyocytes were plated in 6-well plates grown in low serum (0.1% FCS) overnight, and stimulated with the indicated doses of sPDNF for 3 h. Supernatants were collected and secretion of MCP-1, MIP-2α and IL-6 was determined by ELISA (samples run in triplicate). Points represent mean ± SEM protein secretion of triplicate samples.
(**b**) H9c2 cardiomyocytes were prepared as in Figure 4.3a and chemokine transcripts quantified by qPCR. Chemokine expression was normalized to HPRT and fold change calculated relative to vehicle-treated cells. Points represent mean ± SEM fold change expression of triplicate samples from 3 independent experiments.
(**c**) H9c2 cardiomyocytes were plated in 6-well plates, grown in low serum (0.1% FCS) overnight, stimulated with sPDNF (1 μg/ml) for the indicated times, and chemokine expression quantified by qPCR. Points represent mean ± SEM fold change expression of triplicate samples from 2 independent experiments. For all graphs, **P* < 0.05, ***P* < 0.01, and ****P* < 0.005, compared to vehicle-treated cells.

4.4 Neurotrophic receptors TrkA and TrkC are targeted by sPDNF for upregulation of MCP-1 and FKN in cardiomyocytes

We used three distinct criteria to determine whether *T cruzi* PDNF exploits TrkA or TrkC to increase MCP-1 and FKN production in cardiac cells.

First, we pre-incubated H9c2 cardiomyocytes with control DMSO or the Trk antagonist K252a, which blocks Trk signaling by inhibiting Trk autophosphorylation, followed by stimulation with sPDNF or vehicle, and quantified MCP-1 and FKN transcripts by qPCR. We found that K252a completely abrogates the stimulatory effect of sPDNF (Figure 4.4), indicating that the agonistic induction of MCP-1 and FKN by sPDNF requires Trk signaling.

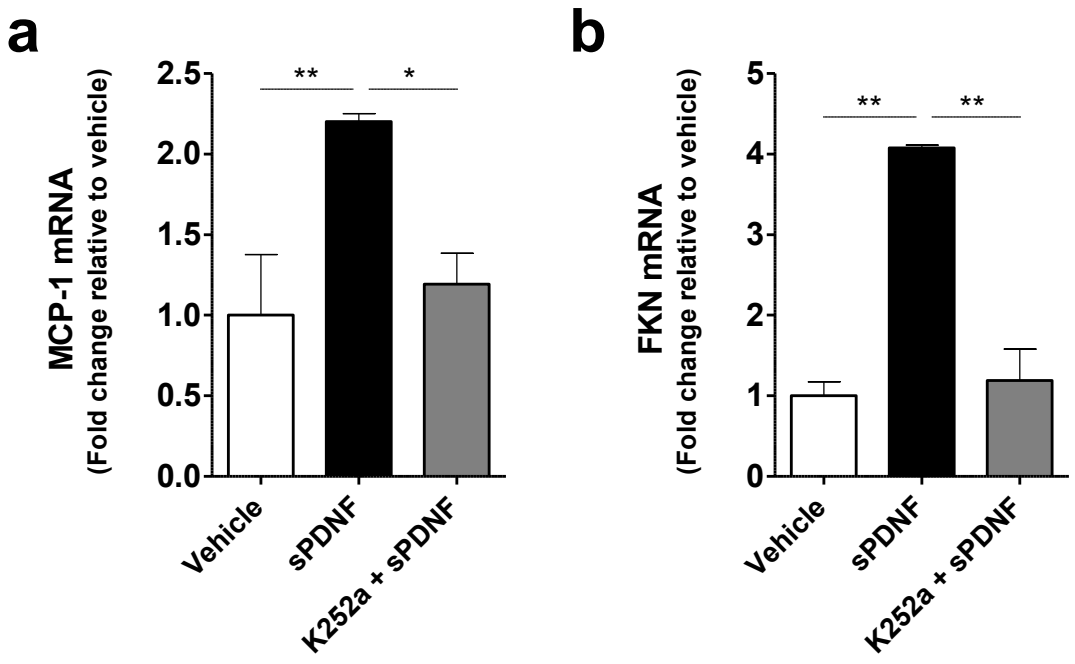

Figure 4.4. Trk-signaling inhibition by K252a abrogates sPDNF-mediated induction of MCP-1 and FKN mRNA in H9c2 cardiomyocytes.

H9c2 cardiomyocytes were stimulated with sPDNF (1 μg/ml, 3 h) without pre-treatment (sPDNF) or after pre-treatment with K252a (200 nM, 1 h) (K252a + sPDNF), and transcripts of (**a**) MCP-1 and (**b**) FKN were quantified by qPCR. Chemokine gene expression was normalized to HPRT and fold change calculated relative to vehicle-treated cells. Bars represent mean ± SD fold change expression of duplicate samples. Graphs are representative of three experiments, with similar trends; *$P < 0.05$ and **$P < 0.01$, compared to Vehicle-treated cells.

Second, we pre-incubated cardiomyocytes with neutralizing antibodies against neurotrophin receptors prior to stimulation with sPDNF. If sPDNF utilizes Trk receptors to augment chemokine expression, then neutralizing these receptors with non-stimulatory antibodies against their extracellular domain would prevent receptor access and block sPDNF-mediated induction of MCP-1 and FKN expression. We found that antibodies against TrkA significantly inhibited sPDNF-induced upregulation of MCP-1 (20.0% inhibition) and FKN (32.8% inhibition), as do antibodies against TrkC (MCP-1 inhibition, 44.5%; FKN inhibition, 55.0%) (Figure 4.5). In contrast, neutralizing antibodies against TrkB are ineffective in preventing sPDNF upregulation of both MCP-1 and FKN (Figure 4.5), consistent with findings that TrkB is not recognized by sPDNF (Weinkauf et al., 2011), thus serving as a negative control in this neutralizing Trk-antibody experiment/assay. A combination of α-TrkA and α-TrkC neutralizing antibodies inhibited sPDNF-induced secretion of MCP-1 in H9c2 cells, whereas the individual antibodies alone did not (Figure 4.5c).

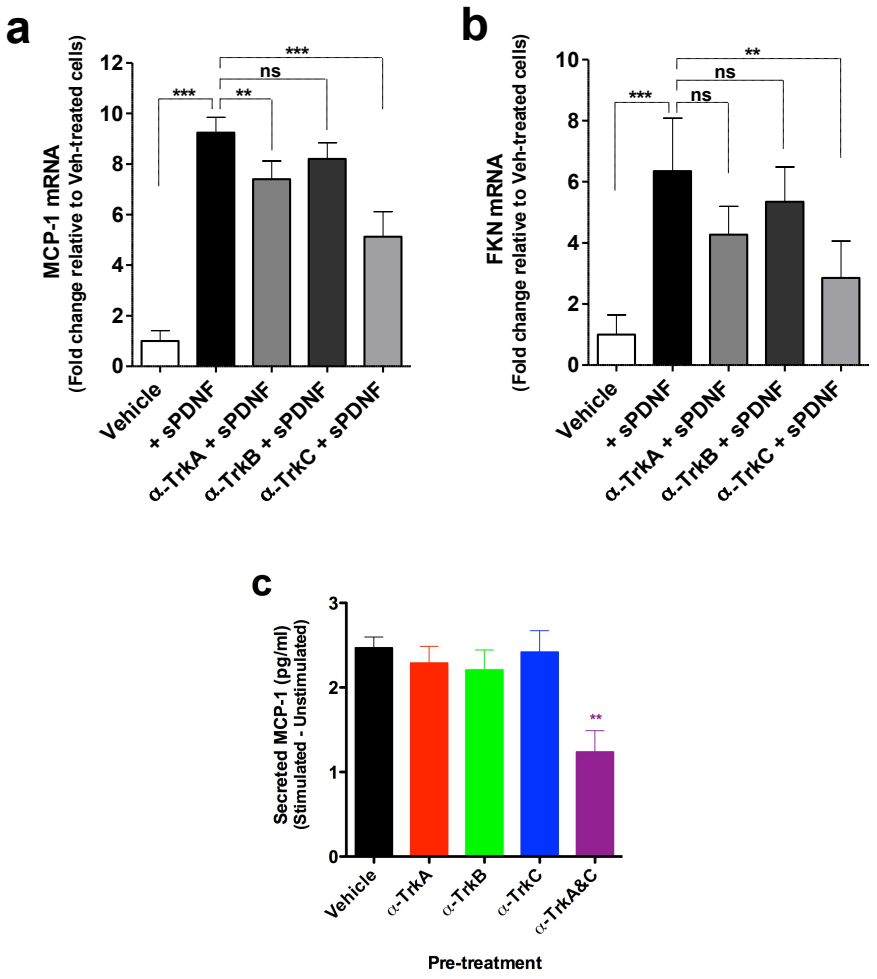

Figure 4.5. Blockade, by neutralizing antibodies, of TrkA and TrkC, but not TrkB, dampens induction of (**a**) MCP-1 and (**b**) FKN mRNA in H9c2 cells.

H9c2 cardiomyocytes were stimulated with sPDNF (1 μg/ml, 3 h) without pre-treatment (+ sPDNF) or after pre-treatment with neutralizing antibodies (1 μg/ml, 30 min) against TrkA (α-TrkA + sPDNF), TrkB (α-TrkB + sPDNF), and TrkC (α-TrkC + sPDNF). Bars represent mean ± SD fold change expression of triplicate samples. Graphs are representative of two experiments, with similar trends; **P* < 0.05 and ***P* < 0.01, ns = not significant. (**c**) For α-TrkA and α-TrkC combination pre-treatment (α-TrkA&C), 2 μg/ml of each antibody were used. Secreted MCP-1 was measured from cell supernatants by ELISA (R&D systems), and expressed as the difference of stimulated cells normalized to unstimulated. ***P* < 0.01 compared to vehicle pre-treatment, by one-way ANOVA; representative of two experiments.

Third, we designed experiments to reduce Trk expression with short hairpin mRNA (shRNA) to further validate that enhanced expression of MCP-1 and FKN results from the binding of sPDNF to TrkA and TrkC. For this purpose, we transfected H9c2 cardiomyocytes with lentivirus encoding shRNA for control green fluorescence protein (shGFP), TrkA (four distinct vectors), or TrkC (five distinct vectors). After 7 days post-transduction, we stimulated untransfected and transfected cardiomyocytes with sPDNF, and assessed the inhibitory effect of gene silencing by comparing secreted MCP-1 levels in sPDNF-stimulated cells normalized to their unstimulated/vehicle-treated counterparts. Compared to shGFP-transfected and/or untransfected cardiomyocytes, cardiomyocytes transfected with shTrkA- or shTrkC-containing lentiviral particles significantly reduced MCP-1 secretion in response to sPDNF stimulation (Figure 4.6).

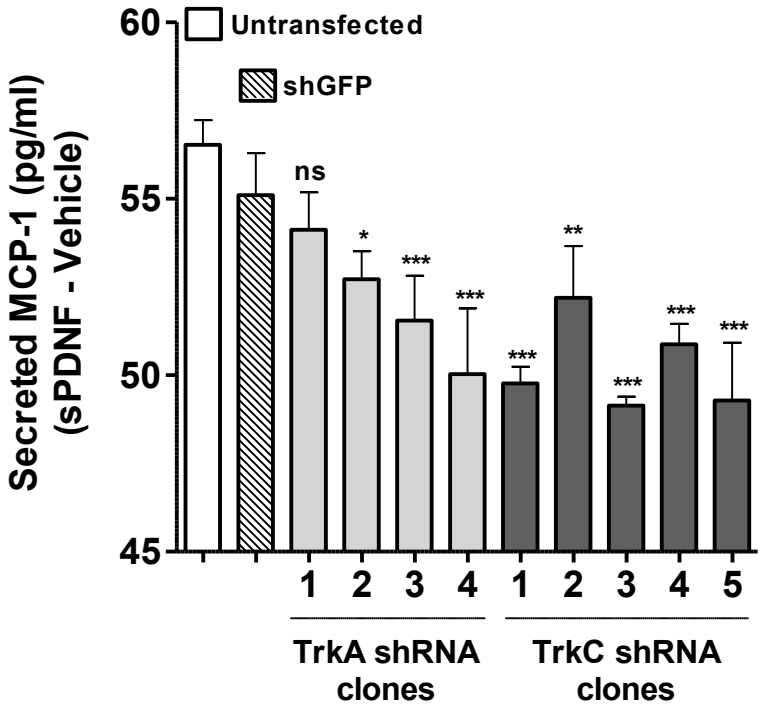

Figure 4.6. Knockdown of TrkA and TrkC, by lentiviral shRNA gene silencing, abrogates secretion of MCP-1 by sPDNF-stimulated H9c2 cells.

H9c2 cardiomyocytes were transfected with lentiviral particles containing shRNAs targeting GFP (control), TrkA (clones 1-4) and TrkC (clones 1-5). After 7 d, cells were serum starved (2 h) and stimulated with vehicle or sPDNF (1 μg/ml, 3 h), and cell supernatants analyzed for secreted MCP-1 by ELISA (samples ran in duplicate). Bars represent mean ± SD secreted MCP-1 (normalized to vehicle-treated cells) of triplicate samples. Graph is representative of three experiments, with similar trends; ns = not significant, $*P < 0.05$, $**P < 0.01$, and $***P < 0.005$, compared to shGFP transfected cells.

Therefore, on the basis of these three distinct criteria, we conclude that sPDNF uses both TrkA and TrkC to upregulate MCP-1 and FKN expression, akin to the utilization of TrkA by the matricellular protein CTGF/CCN2 to induce MCP-1 in cardiomyocytes (Wahab et al., 2005; Wang et al., 2010).

Dual usage of TrkA and TrkC to upregulate MCP-1 and FKN is analogous to *T cruzi* invasion of neuronal cells, which depend on both TrkA (de Melo-Jorge and PereiraPerrin, 2007) and TrkC (Weinkauf et al., 2011). However, preferential utilization of TrkC for parasite entry into cardiac fibroblasts or cardiomyocytes (Aridgides et al., 2013a) and selective usage of TrkA for NGF secretion by cardiac fibroblasts (Aridgides et al., 2013b) suggest specialized roles for Trk receptors within a chagasic heart that may contribute to a complex autocrine and paracrine signaling network.

4.5 MCP-1 and FKN expression correlate with parasite burden in acute chagasic hearts

Mice were infected with *T cruzi* (Tulahuen strain), sacrificed at various days post-infection, and cardiac MCP-1 and FKN expression and parasite burden levels were determined by qPCR. In line with a previous study (Paiva et al., 2009), our results show that MCP-1 expression parallels the degree of heart parasite burden (Figure 4.7a). However, unlike MCP-1, expression of FKN remains elevated for at least 20 days after cardiac parasitism becomes barely detectable (Figure

4.7b), in agreement with the view that FKN plays an important role in recruiting blood monocytes that promote cardiac healing after myocardial injury (Nahrendorf et al., 2007).

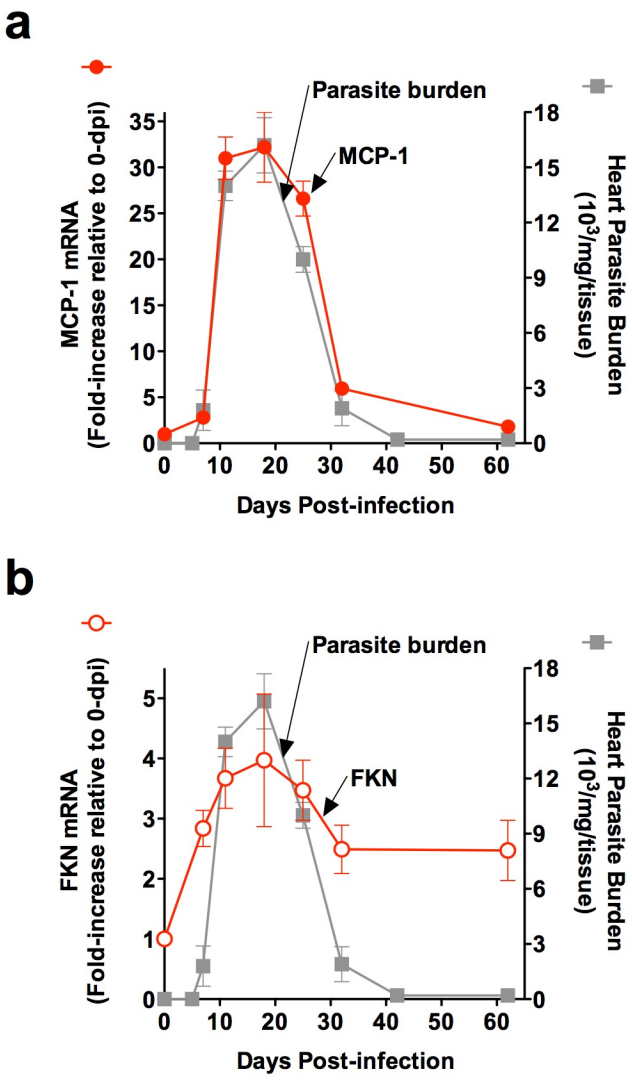

Figure 4.7. MCP-1 and FKN expression correlate with *T cruzi* heart parasitism, *in vivo*.

(**a**) and (**b**) show the expression of cardiac MCP-1 and FKN mRNAs, respectively, in relation to heart parasite burden over the course of acute *T cruzi* infection. C57BL/6 mice (3 per group) were subcutaneously infected with *T cruzi*, and sacrificed at indicated time points. Hearts were harvested and flash frozen until processed for total RNA and genomic DNA. Cardiac MCP-1 and FKN expression (RNA) and parasite burden (DNA) were quantified by qPCR methods. Points represent the mean ± SEM chemokine expression or parasite burden of 3-5 mice per group from two independent experiments.

4.6 Intravenous sPDNF upregulates MCP-1 and FKN in the heart and liver of C57BL/6 and MyD88$^{-/-}$ mice

The robust MCP-1 increase in acutely infected hearts (Figure 4.7) is likely due to the stimulation of TLRs and other canonical pro-inflammatory pathways by *T cruzi* molecules, exemplified by glycosylphosphatidylinositol-anchored mucin-like glycoproteins, which increase MCP-1 and mediate leukocyte recruitment in the pleural cavity of IFN-γ-primed mice (Coelho et al., 2002). If *T cruzi*-PDNF is also a mechanism responsible for triggering MCP-1 expression in *T cruzi*-infected hearts, then intravenous (IV) administration of sPDNF should upregulate chemokine expression in the heart of uninfected, naïve mice.

A previous pharmacokinetic study showed that IV sPDNF administered to naïve mice has a half-life of ~15 min in the blood and peaks in the myocardium ~15 min post-injection, triggering cardiac responses such as NGF upregulation hours after injection (Aridgides et al., 2013).

To determine the effect of sPDNF on the heart, we injected naïve C57BL/6 mice with vehicle (PBS) or a single dose of IV sPDNF, sacrificed the mice at various time points post-injection, and measured cardiac chemokine expression by qPCR. IV sPDNF significantly upregulates cardiac MCP-1 and FKN transcripts with transient-, pulse-like kinetics, as both chemokines peak shortly after administration (3 h post-injection) and return to baseline levels of vehicle-injected mice, thereafter (Figure 4.8). We then screened the agonistic effect of IV sPDNF

in various organs at the peak response time (3 h post-injection) using the same dose as in Figure 4.8. We found that sPDNF upregulated MCP-1 in the heart, liver (where the response was most robust) and spleen, but not in the bone marrow, aorta, esophagus, colon and skin (Figure 4.9). FKN induction in response to IV sPDNF in the same organs was also similar to that observed for MCP-1. Furthermore, IV sPDNF-triggered MCP-1 and FKN upregulation is dose-dependent in the heart and liver (Figure 4.10), akin to results obtained from sPDNF-stimulated cultured cardiac cells (Figures 4.2 & 4.3). FKN induction was more notable in the heart than the liver, which may be attributed to the capacity of the liver to regenerate via other mechanisms involving hepatocytes and Kupffer cells (Fujiyoshi and Ozaki, 2011). The selective increase of MCP-1 and FKN in various organs likely reflects the differential expression of TrkA and TrkC receptors in neural and non-neural tissues, as well as the amount of circulating sPDNF that reaches the organs.

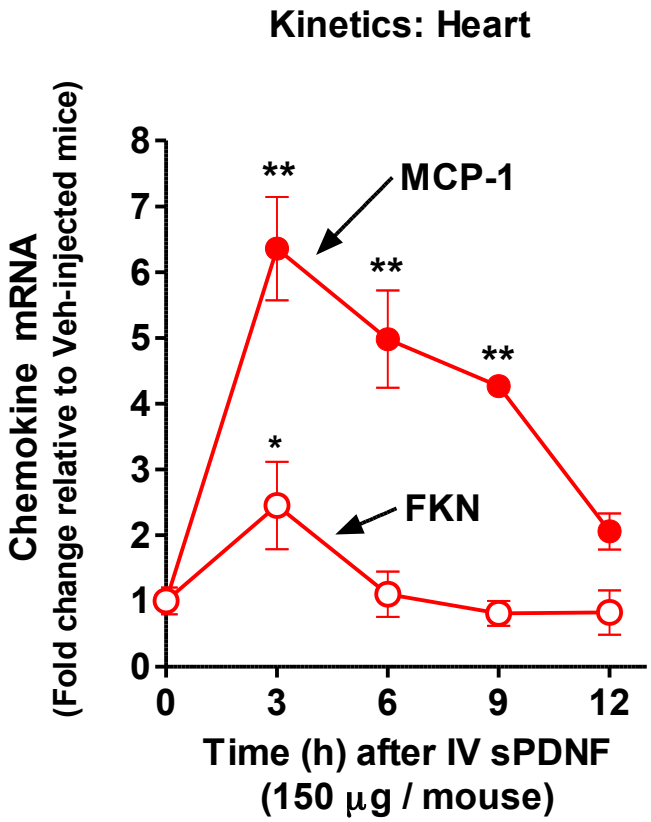

Figure 4.8. Single intravenous (IV) injection of sPDNF in C57BL/6 mice transiently induces MCP-1 and FKN expression in the heart, peaking at 3 h.

Groups of mice (3 per group) were injected with vehicle (Veh) or sPDNF (150 μg/mouse) and sacrificed at 3, 6, 9, and 12 h post-injection. Cardiac MCP-1 and FKN transcripts were quantified by qPCR. Points represent fold change of the mean ± SD expression, normalized to HPRT and made relative to vehicle-injected mice. *$P < 0.05$ and **$P < 0.01$ compared to vehicle-injected mice. Graph is representative of three experiments, with similar trends. Chemokine expression in the liver also responded with pulse-like kinetics (data not shown).

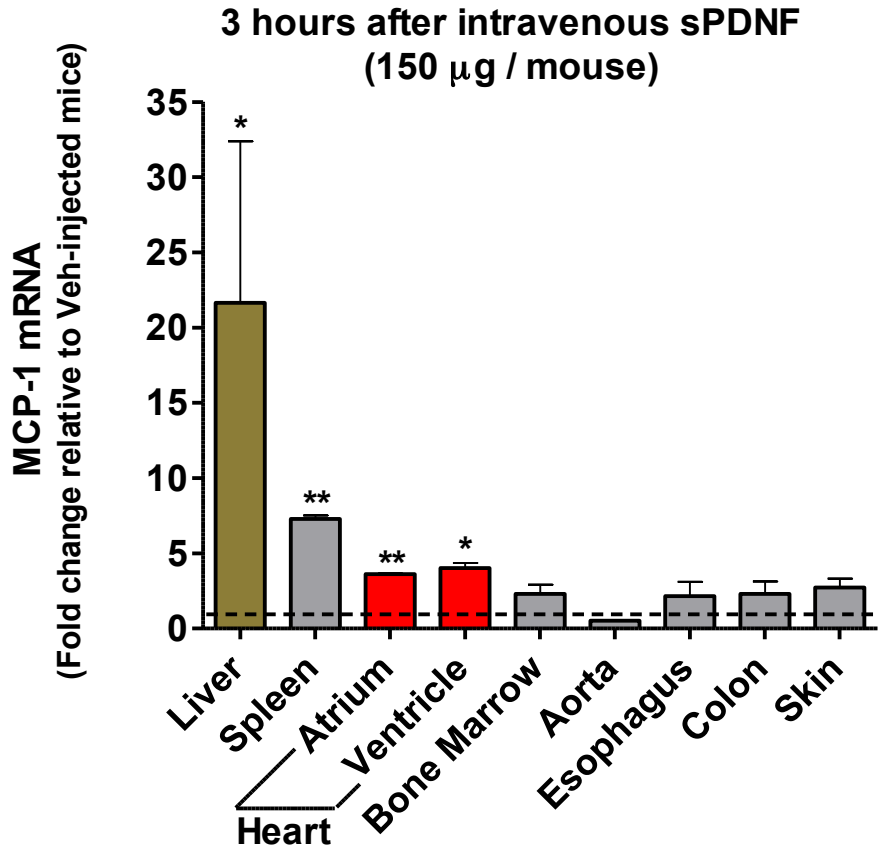

Figure 4.9. MCP-1 is differentially induced in the liver, spleen, and heart, but not the aorta, esophagus, colon, skin, or bone marrow, 3 h after single IV sPDNF in C57BL/6 mice.

Experimental design is analogous to that summarized in Figure 4.8. At 3 h post-injection, mice were sacrificed and the indicated organs were harvested and flash frozen until processed for qPCR. Organ-specific MCP-1 expression was normalized to HPRT and made relative to respective organs from vehicle-injected mice, depicted as the dotted line (1). Bars represent the mean ± SD MCP-1 expression of each organ. *P < 0.05 and **P < 0.01, compared to respective organs of vehicle-injected mice. Graph is representative of two experiments.

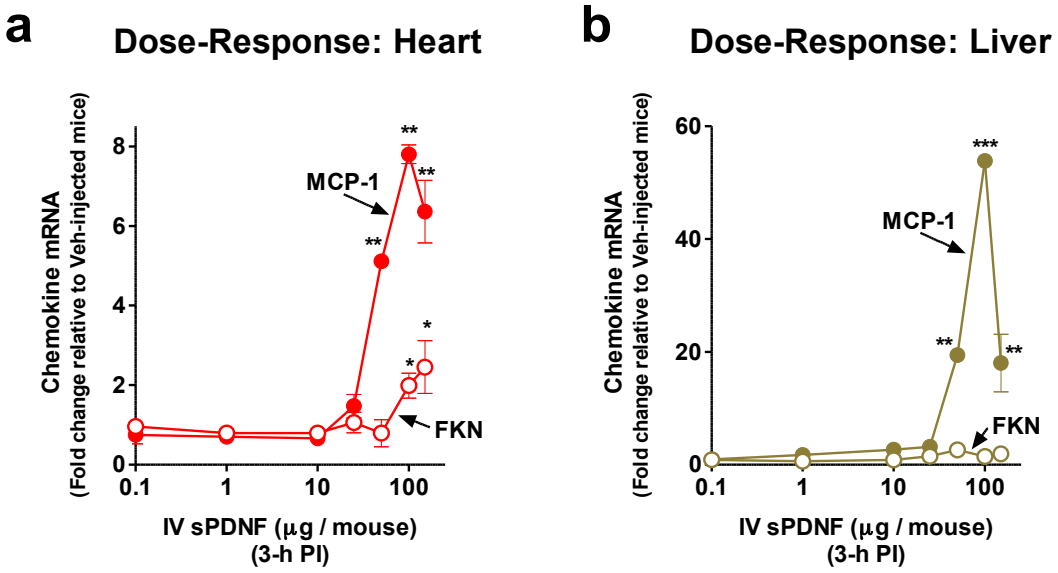

Figure 4.10. Single IV sPDNF induces MCP-1 and FKN expression in the heart and liver in a dose-dependent manner.

Groups of three mice were injected with vehicle or various doses of sPDNF, and (**a**) heart and (**b**) liver harvested 3 h post-injection to quantify MCP-1 and FKN by qPCR. The results are plotted as a composite of three distinct experiments. Points represent mean ± SEM chemokine expression; **P* < 0.05, ***P* < 0.01, and ****P* < 0.005, compared to vehicle-injected mice.

Although our sPDNF preparations do not have detectable levels of endotoxin (as assessed by Limulus amebocyte assay), and are non-toxic in recombinase-activating gene-2 ($RAG2^{-/-}$)-deficient mice, which are highly susceptible to endotoxin shock (Reid et al., 1997), we sought to further ensure the response observed in wild-type mice was not due to TLR activation by assessing MCP-1 and FKN response to IV sPDNF in $MyD88^{-/-}$ mice (Kawai and Akira, 2007). Accordingly, our results show that IV sPDNF gives rise to a sharp increase in the expression of both MCP-1 and FKN in the heart and liver of $MyD88^{-/-}$ mice (Figure 4.11a-d), further supporting the concept that sPDNF acts through Trk receptors, independent of MyD88 signaling.

Recombinant sPDNF mutants, in which several Asp-boxes are swapped, result in proteins that preferentially function in blocking invasion or promoting survival, compared to wild-type sPDNF. Also, preliminary data on synthetic peptides, modeled after the different PDNF Asp-boxes, mimic several aspects of sPDNF compared to scrambled control peptides, *in vitro*, supporting the idea that the effects of PDNF are mediated through binding Trk receptors.

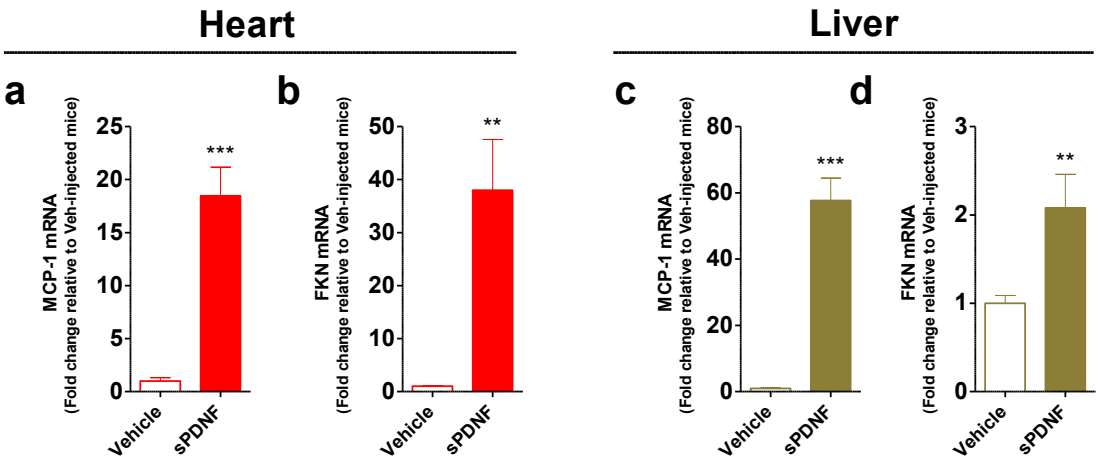

Figure 4.11. Single IV sPDNF induces MCP-1 and FKN in the heart and liver of MyD88$^{-/-}$ mice.

MyD88$^{-/-}$ mice (two per group) were IV injected with vehicle (PBS) or sPDNF (100 μg per mouse), sacrificed 3 h post-injection, and MCP-1 and FKN mRNA was quantified in the heart (**a** and **b**) and liver (**c** and **d**) by qPCR. Bars represent mean ± SEM expression from two independent experiments. $^{**}P < 0.01$ and $^{***}P < 0.005$, compared to vehicle-injected counterparts.

4.7 Multiple intravenous injections of sPDNF increase transcripts of respective MCP-1 and FKN receptors, CCR2 and CX3CR1, in the heart and liver

A major function for chemokines such as MCP-1 and FKN is to attract cells expressing their receptors (CCR2 and CX3CR1, respectively) to sites of tissue inflammation (Green et al., 2006; Serbina et al., 2008). Thus, if sPDNF induces chemokine expression in the heart and liver, CCR2 and CX3CR1 expressing cells would be recruited to these organs. Here, we used chemokine receptor transcript levels in the heart and liver as readout for recruitment of CCR2- and CX3CR1-expressing cells. We found that after a single IV sPDNF dose, CCR2 and CX3CR1 transcript levels did not increase in cardiac or hepatic tissues (Figure 4.12), contrary to the transient and pulse-like induction of MCP-1 and FKN (Figure 4.10).

We reasoned that 3 h was not sufficient time for the recruitment of CCR2 and CX3CR1 expressing cells into the heart or liver. Therefore, we implemented sustained tissue exposure of sPDNF by multiple, closely spaced IV sPDNF injections into naïve mice at times 0, 3 and 24 h, and measuring chemokine receptor transcripts 24 h after the last injection. Multiple IV sPDNF injections resulted in a significant increase in CCR2 and CX3CR1 transcript levels in the liver and heart (Figure 4.13). Thus, these findings support sPDNF-induced MCP-1 and FKN promotes migration of cells expressing CCR2 and CX3CR1 receptors to organs such as the heart and liver.

IV sPDNF Single Dose

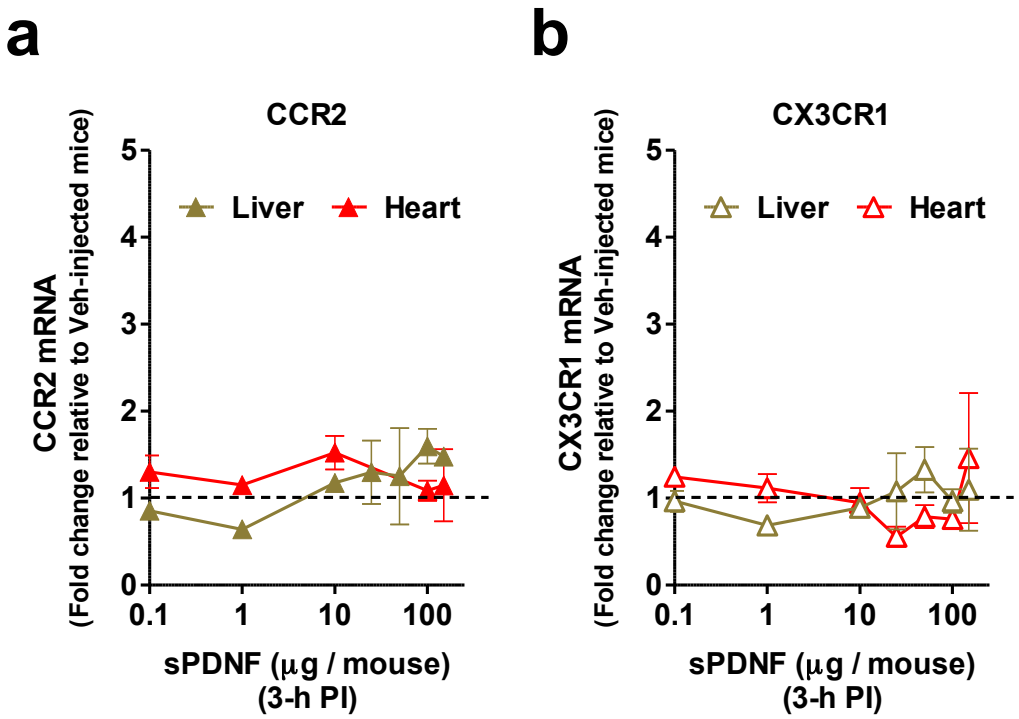

Figure 4.12. Single IV sPDNF does not increase MCP-1 and FKN receptor transcripts, CCR2 and CX3CR1, respectively, in the heart or liver.

Experimental design was the same as in Figure 4.10. Transcript levels of MCP-1 receptor, (**a**) CCR2, and FKN receptor, (**b**) CX3CR1, were quantified by qPCR in the heart and liver. Chemokine receptor transcripts did not increase following single doses of IV sPDNF, 3 h post-injection.

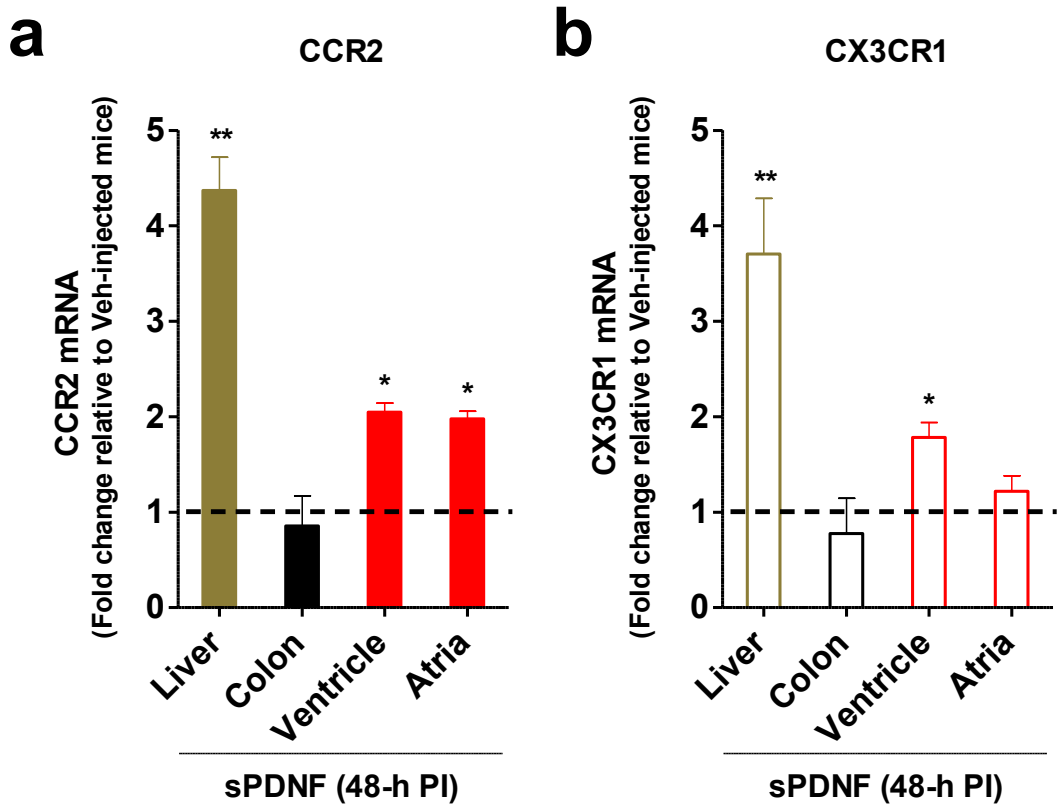

Figure 4.13. Multiple IV sPDNF injections (0, 3, and 24 h) increases CCR2 and CX3CR1 transcript levels in the liver and heart.

C57BL/6 mice (3 per group) were injected with vehicle (Veh) or IV sPDNF (25 μg per injection) at 0, 3, and 24 h, and sacrificed 24 h after the last injection (48-h). (**a**) CCR2 and (**b**) CX3CR1 mRNA transcript levels in the liver, colon and heart (ventricles and atria) were quantified by qPCR. Bars represent mean ± SEM receptor transcript levels from two independent experiments; **P* < 0.05 and ***P* < 0.01, compared to respective organ of vehicle-injected mice (dotted line).

4.8 Summary

We demonstrated that *T cruzi* infection stimulates MCP-1 and FKN expression in cardiac cells and the heart. Chemokine induction in cardiac cells or the heart was mimicked by *in vitro* stimulation or intravenous administration of sPDNF, which featured pulse-like kinetics. Sustained exposure to PDNF *in vivo* via multiple intravenous injections of sPDNF increased the levels of CCR2 and CX3CR1 transcripts over time in organs such as the heart and liver, suggesting recruitment of chemokine receptor expressing cells to these organs. The notion that MCP-1 is cardioprotective and FKN contributes to tissue repair following myocardial injury highlights a conceivable beneficial link between *T cruzi*, chemokines, and the heart. PDNF-mediated modulation of chemokines, over the course of *T cruzi* infection, may affect other resident cardiac cells, such as tissue resident stem cells, that also contribute to promoting reparative and anti-inflammatory responses.

CHAPTER 5. *T CRUZI* PDNF INTERACTS WITH CARDIAC PROGENITOR CELLS (CPCs)

5.1 Introduction

In chapter 4, we discovered that *T cruzi* PDNF modulates the expression of the chemokines MCP-1 and FKN in the heart, liver, and spleen. It has been established that MCP-1 plays an important role in models of acute Chagas disease by attracting immune cells to keep parasitism in check (Hardison et al., 2006; Paiva et al., 2009). On the other hand, FKN is an anti-inflammatory chemokine implicated in myocardial infarction (Green et al., 2006) and other conditions (Sheridan and Murphy, 2013) and, thus, may play a similar role in *T cruzi*-infected hearts. Although FKN has not been previously studied in Chagas heart disease, our results are consistent with the notion of FKN playing a role in tissue repair, as, contrary to MCP-1, it remains expressed in the heart despite low heart parasitism (Figure 4.7).

However, MCP-1 has biological activities additional to promoting recruitment of inflammatory cells, like, for example, inducing cardioprotection by directly interacting with cardiomyocytes (Morimoto et al., 2008; Niu and Kolattukudy, 2009; Wahab et al., 2005; Wang et al., 2010). Moreover, MCP-1/CCR2 signaling was shown to contribute to the activation and recruitment of neural crest-derived stem cells (NCSCs) to sites of inflammation (Tamura et al., 2011). In a model of

cardiac ischemia/reperfusion, NCSCs were found to accumulate at the ischemic border zone area (BZA), where MCP-1 is expressed (Tamura et al., 2011).

Thus, it is reasonable to hypothesize that *T cruzi* PDNF-mediated induction of MCP-1 promotes stem cell migration to sites of parasite-driven inflammatory response. If so, studying the mechanism of action of *T cruzi*/PDNF on cardiac stem cell expansion may not only start the understanding of a novel mechanism of *T cruzi*/host interaction in the heart, but also unveil a therapeutic opportunity in Chagas disease, in accordance with the emerging concept in regenerative medicine:

> *"Stem cell therapy represents the first realistic strategy for reversing the effects of what has until now been considered terminal heart damage."* (Bernstein and Srivastava, 2012)

In this chapter, we characterize several properties of a novel subset of host stem/progenitor cells that have not been previously associated with *T cruzi* infection.

5.2 Upregulation of stem cell marker expression in hearts infected with *T cruzi* is recapitulated by sPDNF

Stem cell antigen-1 (Sca-1) is a marker for stem/progenitor cells, and many studies have focused on tissue resident Sca-1^+ cell populations in the heart.

Here, we focus on a population of Sca-1$^+$ cells in the heart, and the effects that *T cruzi* and PDNF have on those cells. As shown in Figure 4.13, we used the transcript levels of chemokine receptors, CCR2 and CX3CR1, as an indication of monocyte or immune cell recruitment to the heart. Using the same strategy, we measured transcript levels of Sca-1 and other stem cell markers as an indication of cardiac expansion of progenitor cells. Upregulation of Sca-1 transcript by *T cruzi* or sPDNF would suggest that infection and recombinant PDNF expand cardiac stem cells. Given that Sca-1 is not the only marker of cardiac stem cells, we tested whether systemic administration of sPDNF upregulates other markers of cardiac stem/progenitor cells, such as c-kit and Musashi-1 (Msh-1) (Leri, 2009).

Thus, to determine whether *T cruzi* infection has an effect on stem cell populations, we looked at the levels of several stem cell transcripts in infected hearts over time. At peak heart parasitism, or 18 days post-infection, Sca-1, as opposed to c-kit or Msh-1, transcript levels are elevated in infected hearts (Figure 5.1). In cardiac tissue sections of acutely infected mice, the number of Sca-1$^+$ cells is elevated, compared to uninfected mice, shown by immunofluorescence (Figure 5.2). This suggests *T cruzi* is stimulating the Sca-1$^+$ cell population in the heart.

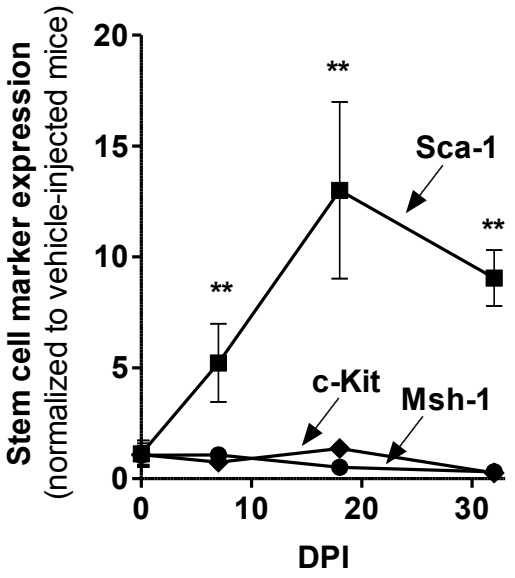

Figure 5.1. Sca-1 transcript is elevated in the heart during acute *T cruzi* infection.

C57BL/6 mice were subcutaneously infected with *T cruzi* (Tulahuén strain, 5×10^3 parasites per mouse) and sacrificed at indicated time points. Hearts were harvested and flash frozen until processed for total RNA. Stem cell marker transcript levels were measured by qPCR methods. Points represent the mean ± SEM stem cell marker expression of 3-5 mice from 2 independent experiments. $^{**}P < 0.01$, compared to uninfected mice (0 dpi).

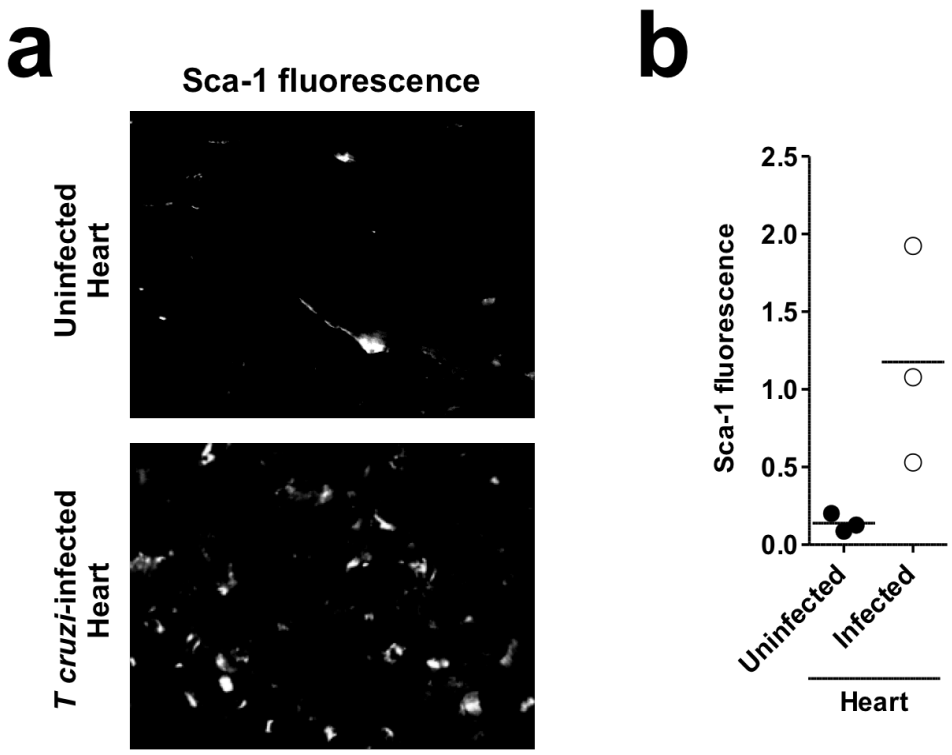

Figure 5.2. The number of Sca-1^{+} cells is elevated in the heart during acute *T cruzi* infection.

C57BL/6 mice were infected subcutaneously with *T cruzi* Tulahuén strain, sacrificed at 22-d post-infection, and atria tissue sections were stained with Sca-1 antibodies followed by fluorescence-labeled secondary antibodies. Fluorescently labeled cells were visualized by fluorescence microscopy (white spots, **a**) and quantified using NIH ImageJ software (**b**) in three distinct fields. Fluorescence in atria sections of infected mice was relative to the fluorescence of uninfected mice arbitrarily assigned 0.1. Similar results were seen in distinct tissue sections of ventricles and atria of two other mice.

In C57BL/6 mice injected with multiple doses of IV sPDNF, we observed an increase in Sca-1 transcript levels in the heart, suggesting recruitment and/or expansion of stem cells (Figure 5.3). Because MCP-1/CCR2 signaling contributes to recruitment of stem cells (Tamura et al., 2011), we tested whether sPDNF-mediated increase in Sca-1 transcript levels occurred in CCR2 ($CCR2^{-/-}$) or CX3CR1 ($CX3CR1^{-/-}$) knockout mice. After multiple doses of IV sPDNF, $CX3CR1^{-/-}$, but not $CCR2^{-/-}$, mice exhibited an increase in Sca-1 transcript levels (Figure 5.3), suggesting sPDNF is promoting the recruitment and/or expansion of Sca-1 expressing cells through a MCP-1/CCR2-signaling-dependent manner. After single IV sPDNF administration, Sca-1 transcript levels are also increased in the heart (Figure 5.4). The increase in Sca-1 in the liver may also reflect an increase in stem cells and contribute to liver regeneration. Furthermore, $Sca\text{-}1^{+}$ cells in hearts are increased after multiple IV sPDNF administrations based on immunofluorescence (Figure 5.5), in agreement with the conclusion that Sca-1 mRNA increase resulting from IV sPDNF administration reflects $Sca\text{-}1^{+}$ cell expansion.

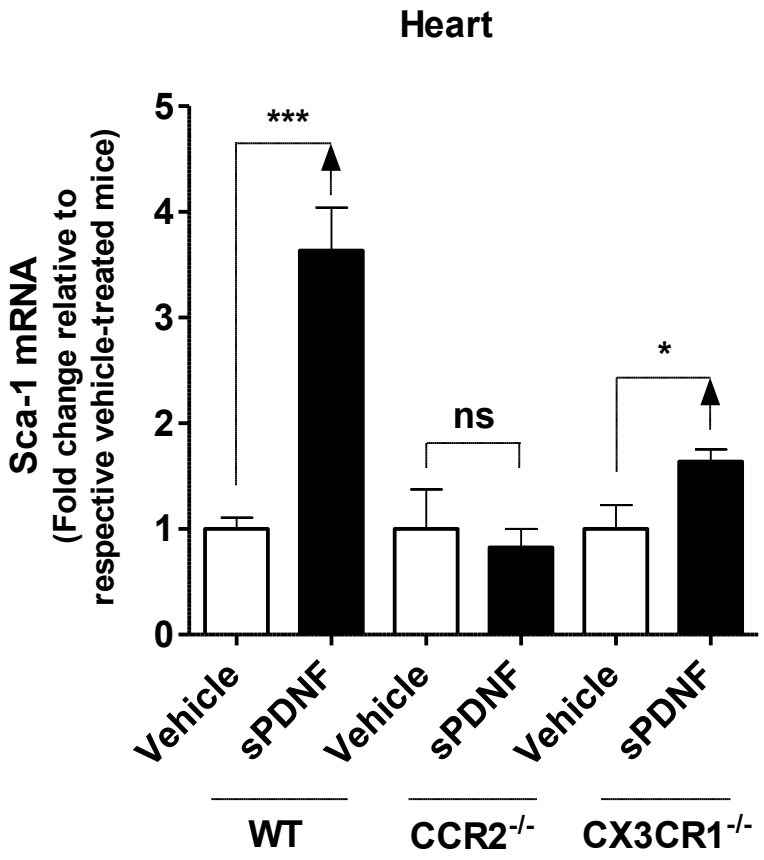

Figure 5.3. Intravenous administration of sPDNF increases transcript of cardiac stem cell marker Sca-1 in the hearts of mice, and depends on the expression of MCP-1 receptor, CCR2.

Wild type (WT) and mice genetically deficient in MCP-1 receptor ($CCR2^{-/-}$) and fractalkine receptor ($CX3CR1^{-/-}$) (all in C56BL/6 background) were injected intravenously with PBS or sPDNF at 0, 3, and 24 h and sacrificed at 48 h, as described in Figure 4.13. Hearts were harvested and processed for qPCR. All genes were normalized to HPRT and related to respective vehicle-treated controls. Bars represent the mean (±SEM) fold change transcript levels of 2-3 mice per group from 2 independent experiments. $^{*}P < 0.05$ and $^{***}P < 0.005$, by one-way ANOVA.

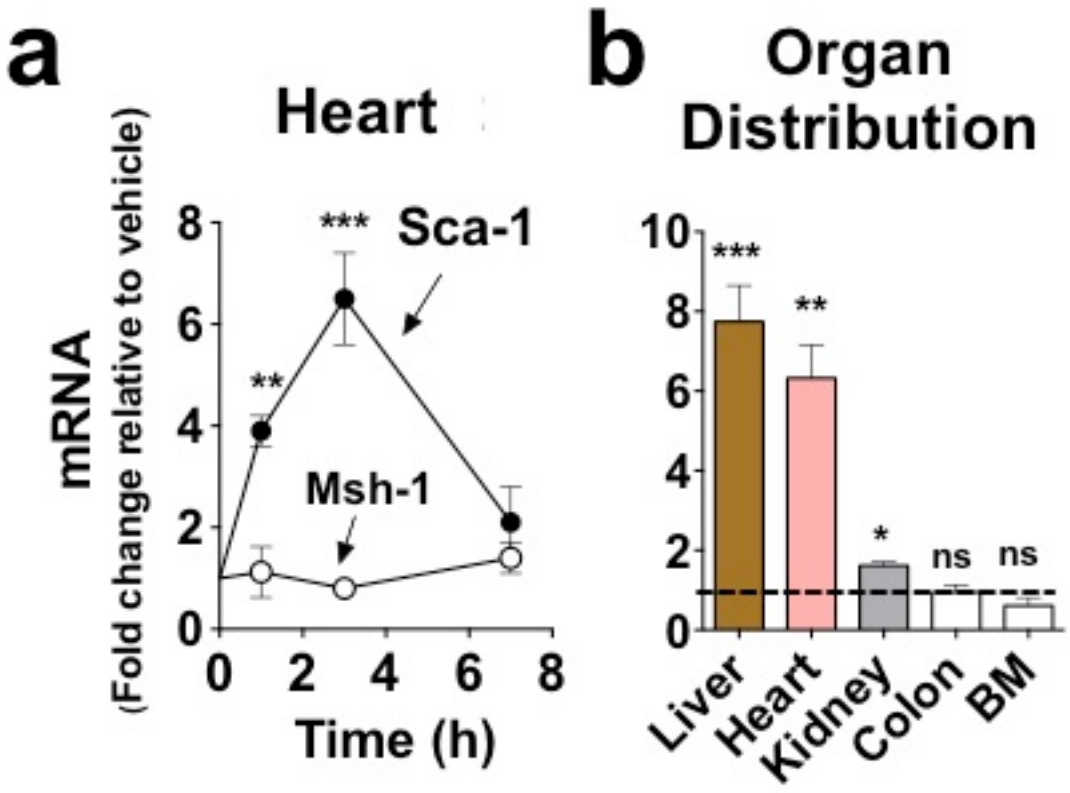

Figure 5.4. IV sPDNF upregulates Sca-1 expression in the heart of naïve mice.

Intravenous (IV) administration of sPDNF into naïve mice ups Sca-1 in the heart and other organs. (**a**) C57BL/6 mice (3 per group) were injected IV with PBS (vehicle) or sPDNF (3 mg/kg body), and sacrificed 0, 1, 3 and 7 h. Stem cell markers Sca-1 and Msh-1 mRNAs in the myocardium were quantified by qPCR; average of three experiments. (**b**) C57BL/6 mice (3 per group) were injected IV with sPDNF (4 mg/kg) or PBS, sacrificed 3-h later, and Sca-1 mRNA quantified by qPCR in various organs (BM, bone marrow); dotted line represents Sca-1 mRNA of vehicle-treated mice set to 1.0, data are representative of 2 experiments.

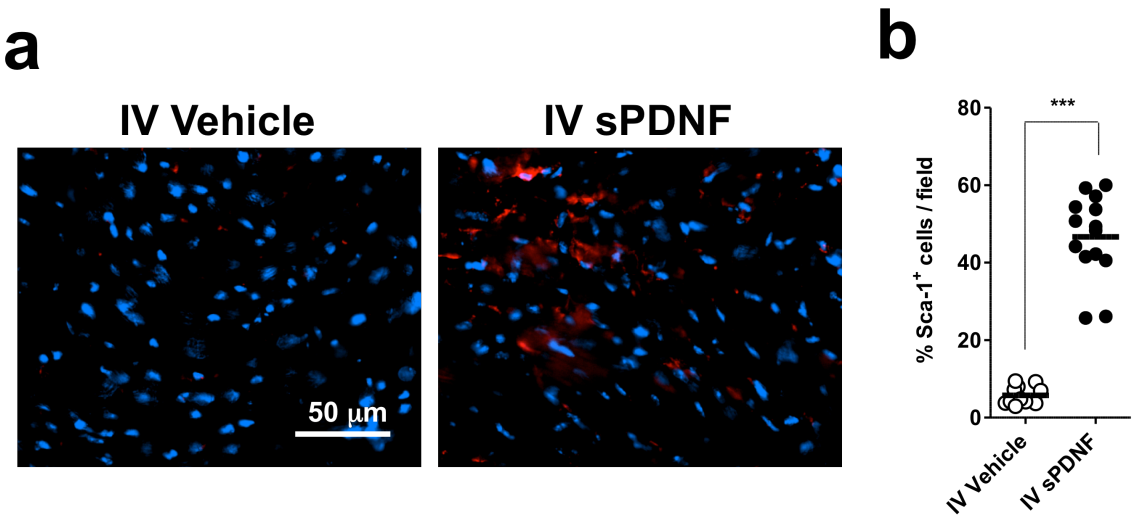

Figure 5.5. IV sPDNF expands Sca-1$^+$ cells in the heart of naïve mice.

C57BL/6 mice were intravenously injected at 0, 3, and 24 h with PBS or 50 μg sPDNF, and sacrificed at 48 h. (**a**) Heart tissues were fixed in paraformaldehyde, embedded in OCT from which frozen sections were made, and tissue sections stained for Sca-1 (red) using specific antibodies and counterstained with DAPI (blue). White bar, 50 μm. (**b**) The percentage of Sca-1$^+$ cells was determined by dividing the number of Sca-1$^+$ cells by the number of total DAPI nuclei signals per field. Bars represent the mean percentage Sca-1$^+$ cells per field. Graph is representative of 3 mice per group from two independent experiments; a total of 12-14 fields (4-5 fields per mouse) per group were analyzed. ***P < 0.001 by student's t-test.

5.3 Isolation and characterization of Sca-1$^+$ cells from the heart

Because Sca-1 transcript and Sca-1$^+$ cells in the heart are increased by *T cruzi* infection and sPDNF administration, and because Sca-1 marks cardiac stem/progenitor cells, we hypothesized this reflected an expansion of Sca-1$^+$ cardiac stem/progenitor cells. To test this hypothesis, we isolated Sca-1$^+$ cardiac cells using an anti-Sca-1 magnetic microbead kit that positively selects for Sca-1$^+$ cells from single cell suspensions (Miltenyi Biotech) (Chen et al., 2003; Matsuura et al., 2004). Preliminary results showed that virtually all cells isolated by the magnetic beads are Sca-1$^+$ as assessed by fluorescence microscopy. Cardiac Sca-1$^+$ cells were then tested for intrinsic characteristic features of stem/progenitor cells: proliferation, clonal expansion, and differentiation (Wiese et al., 2004).

In contrast to primary cultures of non-stem/progenitor cells, such as primary cardiac fibroblasts, which senesce after 5-8 passages, stem/progenitor cells survive in culture for many months, with a doubling time of 45-68 h (Li et al., 2008). We observed that positively selected Sca-1$^+$ cardiac cells continuously grow and expand for months with a doubling time of about 30-50 h; Figure 5.6 displays the continuous growth of cardiac Sca-1$^+$ stem cells for 15 passages (each passage after 3 to 4 days in culture). Similar growth curves have been performed in nine other cardiac Sca-1$^+$ cell isolates. Thus, by this criterion, the cardiac Sca-1$^+$ cells purified by magnetic beads expand similarly to stem/progenitor cells.

Another characteristic feature of stem/progenitor cells is clonogenicity, or the ability of a single cell to grow into a colony. Most terminally differentiated cell types cannot withstand single cell culture (Smits et al., 2009). To determine whether the magnetic bead-purified cardiac Sca-1$^+$ cells are clonogenic, we plated Sca-1$^+$ cells by limiting dilution into 96-well plates (0.5 cells per well) to determine whether single cells would form a colony. After approximately a month in culture, wells containing a single cell grew into colonies; furthermore, colonies preserved Sca-1 expression, as assessed by immunofluorescence (Figure 5.7). Thus, this finding further establishes that the magnetic bead-isolated cardiac Sca-1$^+$ cells are clonogenic.

Yet another criterion is lineage differentiation. Cardiac stem/progenitor cells have been shown to differentiate to cardiomyocytes after brief exposure to 5-azacytidine, or to endothelial cells when cultured with vascular endothelial growth factor (VEGF) (Oh et al., 2003; Ye et al., 2012). To determine whether cardiac Sca-1$^+$ cells differentiated into cardiomyocytes or endothelial cells, we grew them separately in differentiation media containing either 5-azacytidine or VEGF, respectively, or without the differentiating component as control. After two weeks in culture, we observed that Sca-1$^+$ cells differentiated to cardiomyocytes and endothelial cells, based on their expression of myosin heavy chain (MyHC) and von Willebrand factor (vWF), respectively (Figure 5.8). Cells receiving neither 5-azacytidine nor VEGF did not differentiate.

Therefore, based on the characteristics of expansion, clonogenicity, and differentiation, we conclude that the Sca-1^{+} cardiac cells we isolate using the magnetic bead technology are cardiac progenitor cells (CPCs).

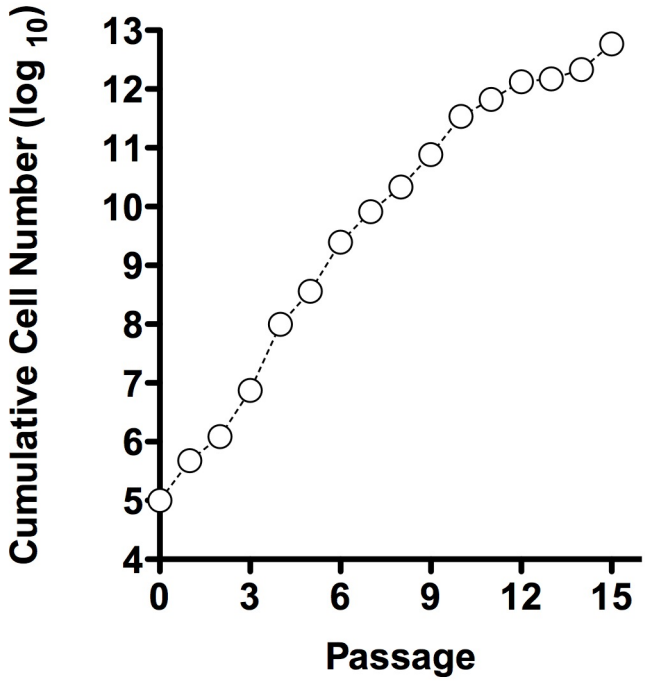

Figure 5.6. Sca-1^{+} cardiac cells expand *in vitro*.

Magnetic bead-isolated Sca-1^{+} cardiac cells were grown in CPC medium and replated every 4-5 days (passage). Points represent the mean ± SD of duplicate wells. Graph is representative of 3 growth curves.

Clonogenicity

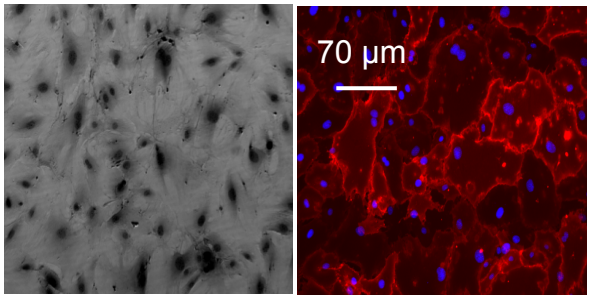

Figure 5.7. Sca-1$^+$ cardiac cells are clonogenic

Magnetic bead-isolated Sca-1$^+$ cardiac cells were cloned into 96-well plates by limiting dilution (0.5 cells per well) and allowed to grow in 10% FCS/DMEM. Microscopic observation confirmed that cells were plated at 0.5 cell per well in approximately 50% of the wells. Media was changed every 3-5 days. Cell colonies were observed after culturing for two weeks. After about one month in culture, colonies were fixed and stained with Diff-Quick and visualized by microscopy (left panel) and with Sca-1 antibodies followed by fluorescence-labeled secondary antibodies (right panel). The figure is representative of many other colonies.

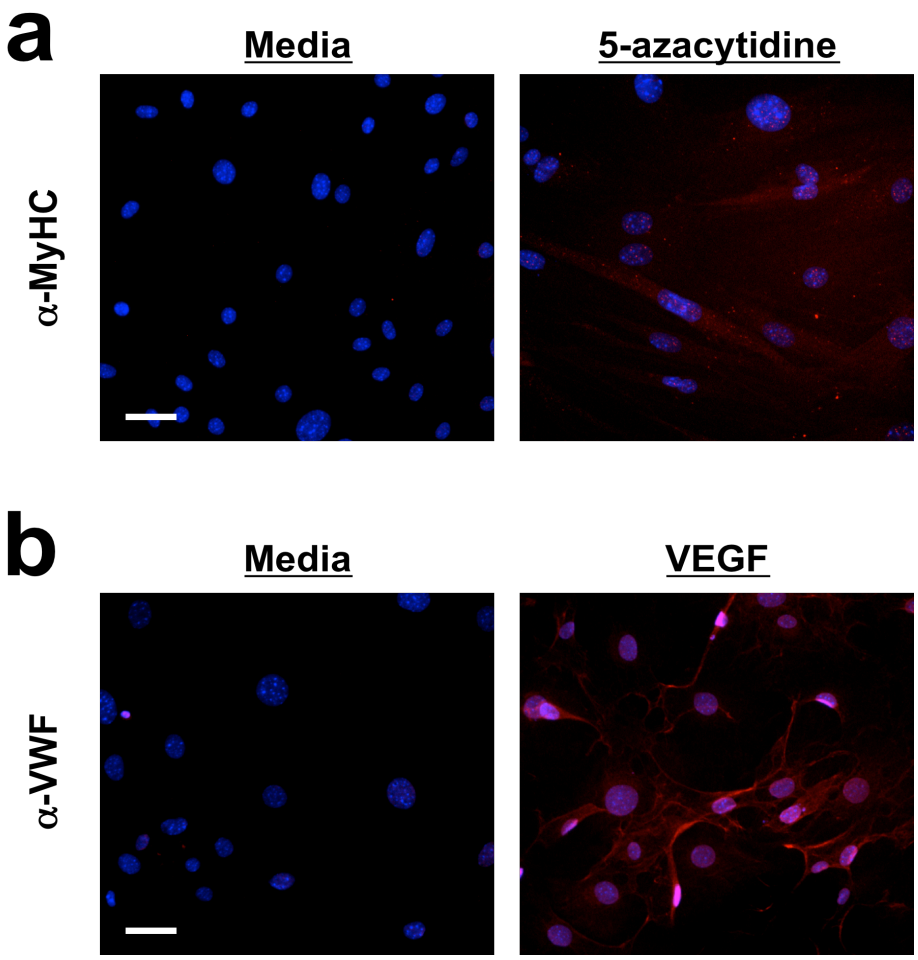

Figure 5.8. Sca-1$^+$ cardiac cells differentiate into cardiomyocytes and endothelial cells.

Sca-1$^+$ cardiac cells were isolated via gentleMACS combined with an anti-Sca-1 positive selection magnetic bead kit (Miltenyi Biotech). (**a**) Cardiomyocyte differentiation. Sca-1$^+$ cardiac cells were plated and left undifferentiated in DMEM/10% FCS (Media) or induced to differentiate into cardiomyocytes (5-azacytidine) (DMEM/10% FCS + 10 mM 5-azacytidine initially for 3 days, then DMEM/10% FCS for 14 days). Cells were fixed and stained with α-MyHC (myosin heavy chain; Millipore) and corresponding Alexa-568 labeled secondary antibody. (**b**) Endothelial cell differentiation. Sca-1$^+$ cardiac cells were plated and left undifferentiated in IMDM/10% FCS (Media) or induced to differentiate into endothelial cells (VEGF) (IMDM/10% FCS + 20 ng/ml VEGF for 14 days). Cells were fixed and stained with α-vWf (von Willebrand factor; Dako) and corresponding Alexa-594 labeled secondary antibody. Both groups were countertained with DAPI (blue). Images were taken using the same exposure times and processed similarly. White bar, 20 μm.

5.4 sPDNF enhances CPC expansion, and survival

It was unknown whether CPCs express Trk receptors. Thus, before assessing the potential effect of *T cruzi* PDNF on CPC growth and survival, we verified whether CPCs express TrkA and TrkC receptors, for this would provide the molecular basis of *T cruzi* PDNF/CPC interaction. Previous studies from our lab showed that TrkA and TrkC are exploited by *T cruzi* PDNF to promote neuronal cell survival and parasite entry (Caradonna and Pereiraperrin, 2009; Chuenkova and PereiraPerrin, 2004; de Melo-Jorge and PereiraPerrin, 2007; Weinkauf et al., 2011), and cardiomyocyte protection against oxidative stress and infection of cardiac cells (Aridgides et al., 2013a, 2013b).

We find that CPCs express TrkA and TrkC, but not TrkB (Figure 5.9), precisely the receptors recognized by *T cruzi*. The expression of TrkA and TrkC is similar to the expression of Trks on other cardiac cell types, as determined by us and others (Aridgides et al., 2013a, 2013b; Meloni et al., 2010).

To test whether PDNF affects expansion of CPCs *ex vivo*, we measured cumulative CPC growth without and with sPDNF for many passages. Our results show that sPDNF enhances CPC growth (Figure 5.10).

To resolve whether sPDNF-enhanced CPC growth is mediated by sPDNF/Trk activation, we inhibited Trk signaling in the CPC cultures with K252b, which inhibits Trk autophosphorylation and blocks Trk signaling (Knüsel et al., 1992; Ross et al., 1995). We found that K252b inhibits sPDNF-mediated enhanced

growth of CPCs (Figure 5.11), consistent with the notion that sPDNF promotes CPC expansion via TrkA and/or TrkC receptors.

To observe whether sPDNF triggers CPC survival, we grew CPCs for many passages in the presence and absence of sPDNF. By passage 18, CPCs grown in medium devoid of sPDNF senesced, a defect blocked by growing the cells in medium containing sPDNF and without changing the medium (Figure 5.12a). This result indicates that sPDNF not only promotes CPC growth, but also CPC survival.

This conclusion is reinforced by a different approach, in which CPCs were grown for up to 17 days without replacing spent media with fresh media containing sPDNF, or not. CPC viability was examined by phase-contrast microscopy and fluorescence microscopy following staining with propidium iodide (PI)/Hoechst dye, which identifies apoptotic cells stained in pink (Aridgides et al., 2013b; Weinkauf and Pereiraperrin, 2009). Strikingly, we found that CPCs grown in spent medium containing sPDNF remained mostly viable up to the 17 days of observation, whereas counterpart cultures of CPCs grown in the absence of sPDNF (Vehicle) displayed significant cell death as early as 6 days (Figure 5.12b, c).

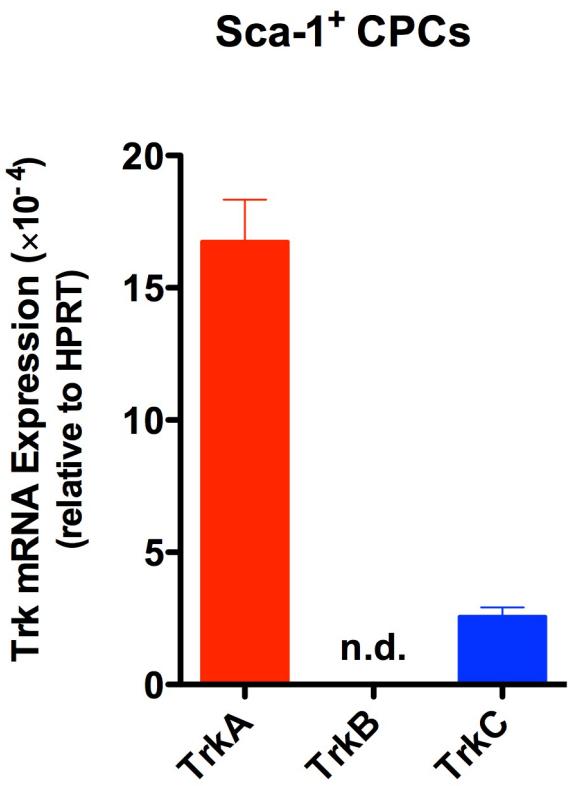

Figure 5.9. Sca-1^{+} CPCs express TrkA, TrkC, but not TrkB.

CPCs were isolated from hearts of C57BL/6 mice and propagated in CPC growing media. Cells were plated at 5×10^{4} cells/well on gelatin-coated 6-well plates. Triplicate samples were collected in Trizol and processed for qPCR. Bars represent the mean ± SD absolute gene expression relative to HPRT. n.d. = not detected. Graph is representative of 3 experiments.

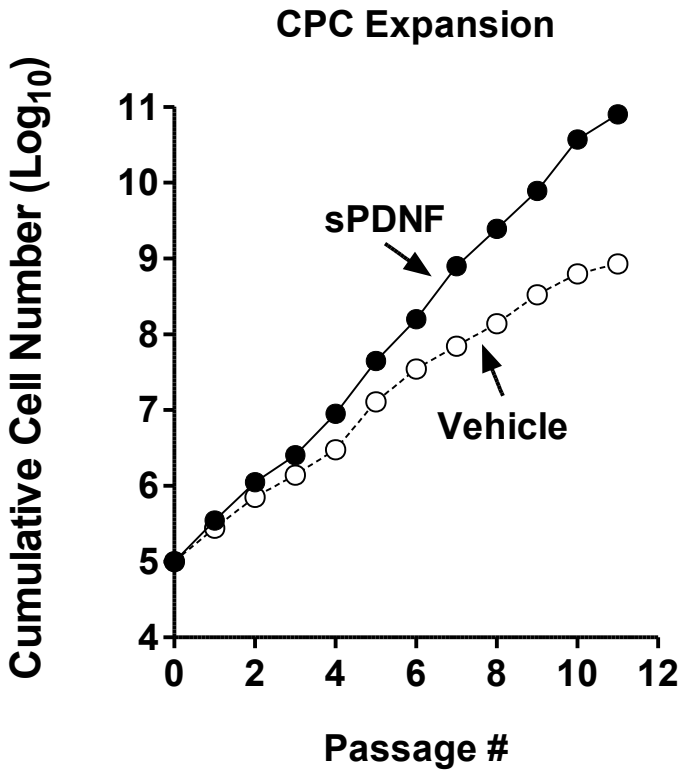

Figure 5.10. sPDNF promotes CPC expansion.

CPCs were isolated from naïve mice and were grown in CPC medium in the presence (sPDNF, 4 μg/ml) or absence (Vehicle) of sPDNF. Points represent the mean of duplicate samples per condition. Graph is representative of 3 growth curves from different CPC isolates.

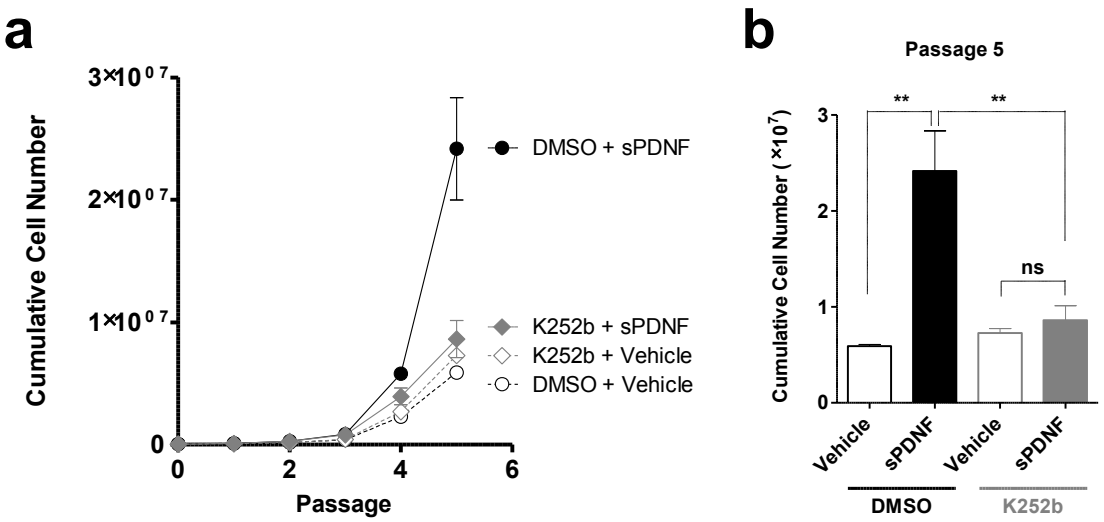

Figure 5.11. sPDNF-enhanced growth of CPCs is inhibited by K252b.

(**a**) CPCs were pretreated with DMSO or K252b in a 1:100 dilution of CPC media for 1 hour. Cells were then plated as in Figure 5.10 into respective wells containing CPC medium ± sPDNF. Points represent the mean ± SD of duplicate wells per condition. Graph is representative of 2 independent experiments. (**b**) Cumulative cell number at passage 5 of (a) is shown.

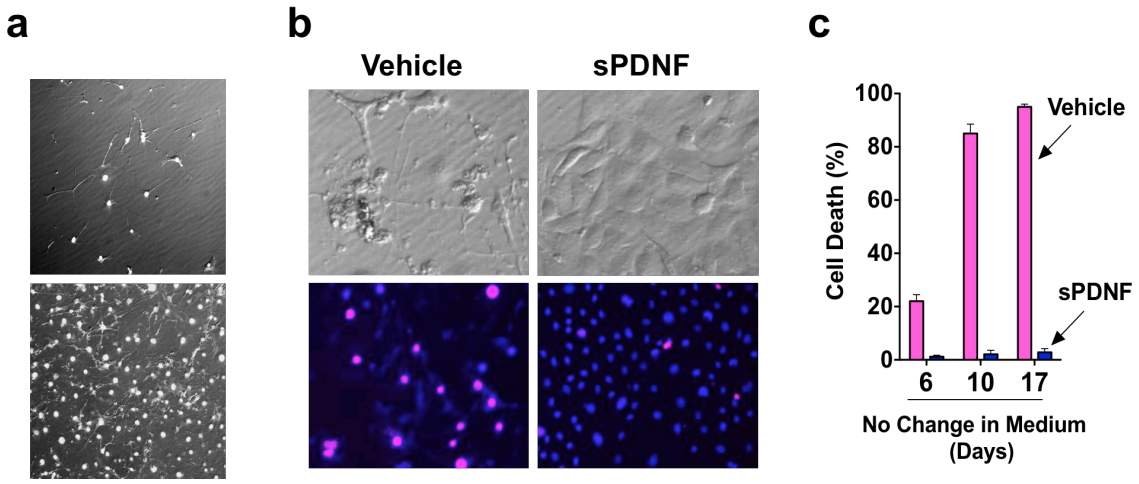

Figure 5.12. sPDNF promotes long-term growth survival of mouse CPCs.

(**a**) CPCs were grown in the absence (upper panel) or presence (lower panel) of sPDNF (1 μg/ml) for 18 passages. Cells are stained with DAPI to highlight cellularity through nuclei density. Of note, while CPCs grown in the absence of sPDNF dramatically slow down growth (senescence), sPDNF counters CPC senescence. (**b**) sPDNF prevents starvation/toxicity-induced CPC death. CPCs (passage 14) were kept for 17 days at 37°C in growth medium (DMEM/Iscove mixture containing 5% FCS plus FGF, EGF, VEGF, insulin, thrombin and cardiotrophin) to which PBS (vehicle) or sPDNF (1 μg/ml) was added. Upper panels represent phase-contrast and lower panels represent propidium iodide/Hoechst stained cells (pink dots = dead cells; blue dots = viable cells) of CPCs kept at 37°C for 17 d without changing the medium. (**c**) Graph depicts mean ± SD % cell death of triplicate wells, representative of two distinct experiments using CPCs at different passages.

5.5 sPDNF stimulates secretion of anti-inflammatory TNF-α-stimulated gene 6 (TSG-6) in CPCs

As pointed out by Singer and Caplan (2011), “although [MSCs] were initially hypothesized to be the panacea for regenerating tissues, MSCs appear to be more important… to regulate the immune response invoked in settings such as tissue injury, transplantation, and autoimmunity.” We therefore reasoned the anti-inflammatory activity of MSCs applies to CPCs. TSG-6 is a most studied stem cell-elicited immunomodulatory factor (Choi et al., 2011; Lee et al., 2009; Nagyeri et al., 2011; Prockop and Youn Oh, 2012). TSG-6 is induced by inflammatory cytokines TNF-α and IL-1β (Mirotsou et al., 2011; Prockop and Youn Oh, 2012; van den Akker et al., 2013). In addition to inflammatory cytokines, TSG-6 can be upregulated in MSCs by growth factors and hormones such as epidermal growth factor (EGF) and gonadotropin (Feng and Liau, 1993; Yoshioka et al., 2000). Therefore, given that sPDNF is a mimic of growth factor NGF and NT-3 and promotes CPC expansion and survival, we surmised that *T cruzi*-elicited expansion and survival of CPCs is accompanied by upregulation of TSG-6.

To find out whether sPDNF upregulates TSG-6 in CPCs, we stimulated the cells with various doses of sPDNF and measured, by ELISA, secreted TSG-6 levels in the CPC-conditioned medium. We found that CPCs secrete TSG-6 in a dose-dependent manner in response to sPDNF stimulation (Figure 5.13).

To determine whether TSG-6 induction is Trk-dependent, we performed lentiviral knockdown of TrkA or TrkC in CPCs and measured their ability to induce TSG-6 secretion in response to sPDNF. Unstimulated CPCs after knockdown with the different lentiviral constructs secrete similar basal levels of TSG-6. Knockdown of TrkA and TrkC inhibited sPDNF-stimulated TSG-6 secretion in CPCs (Figure 5.14), in agreement with the concept that Trk receptor activation by sPDNF is a mechanism responsible for TSG-6 secretion.

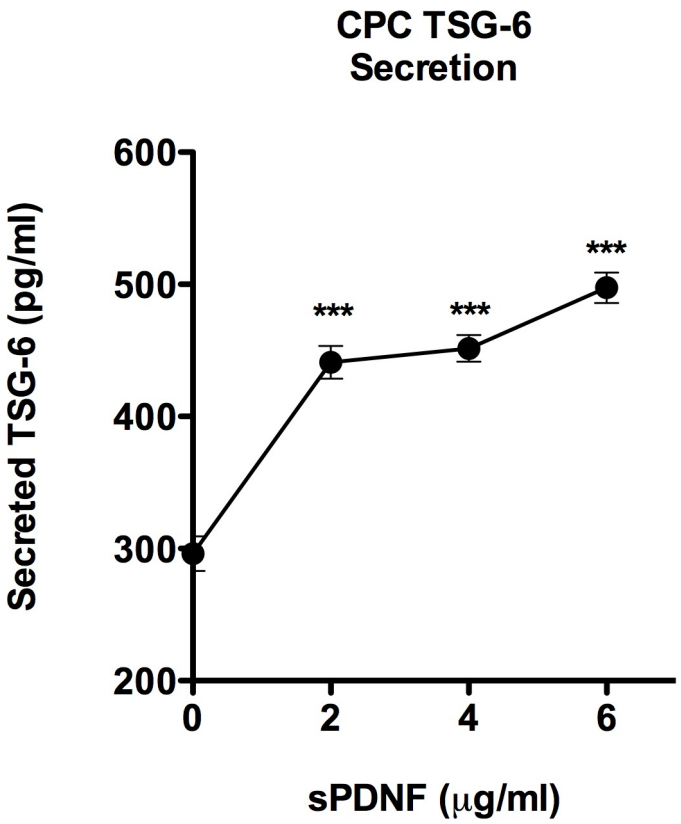

Figure 5.13. sPDNF stimulates CPCs to secrete anti-inflammatory TSG-6 in a dose-dependent manner.

CPCs were plated overnight, serum starved in 0.1% FCS/DMEM for 2 h, then stimulated with 2, 4, or 6 μg/ml sPDNF for 24 h. Supernatants were collected, cleared by centrifugation, and secreted TSG-6 was analyzed by ELISA. Total secreted TSG-6 is shown. Points represent mean ± SEM secreted TSG-6 of 2-3 samples per stimulation ran in duplicate (ELISA); graph is representative of 3 experiments. ***$P < 0.005$ compared to unstimulated, by one-way ANOVA.

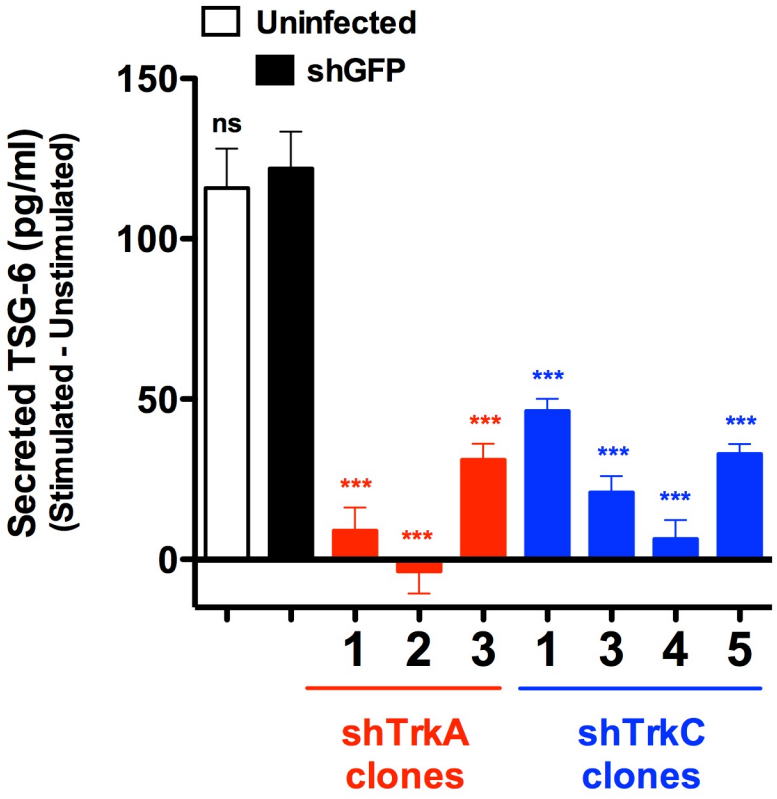

Figure 5.14. TrkA and TrkC knockdown inhibits sPDNF-mediated TSG-6 secretion in CPCs.

CPCs were infected with lentiviral particles harboring shRNAs targeted against GFP (shGFP), TrkA (shTrkA1-4), and TrkC (shTrkC1-5), or left uninfected. Seven days post-lentiviral infection, CPCs were serum starved in 0.1% FCS/DMEM for 2 h, then stimulated with 2 μg/ml sPDNF for 24 h. Supernatants were collected, cleared by centrifugation, and secreted TSG-6 was analyzed by ELISA. Secreted TSG-6 is shown as stimulated cells normalized to unstimulated. Bars represent mean ± SD of duplicate samples ran in duplicate (ELISA); graph representative of 3 independent experiments that showed similar results. ns = not significant and ***$P < 0.005$ compared to shGFP, by one-way ANOVA.

5.6 Summary

We identified and characterized a novel interaction between *T cruzi*, PDNF and the Sca-1$^+$ CPC population. Sca-1$^+$ cells are activated and induced by *T cruzi* infection or IV sPDNF treatment in the heart, which may be partially dependent on MCP-1/CCR2-signaling. *Ex vivo* studies of CPCs revealed that they grow and expand in culture over long periods of time, are clonogenic, and are able to differentiate to cardiomyocytes and endothelial cells. Since CPCs express TrkA and TrkC, they presumably respond to *T cruzi* PDNF. In fact, sPDNF treatment of CPCs, *ex vivo,* enhances growth/expansion in a Trk receptor-dependent manner, and promotes cell survival. CPCs were identified to be a source of anti-inflammatory TSG-6. We found that sPDNF stimulates the secretion of TSG-6 by CPCs, which is dependent on either TrkA and/or TrkC activation. Characterization of CPCs isolated from *T cruzi*-infected mice would provide insight into anti-inflammatory mechanisms in Chagas disease and reveal opportunities for therapeutic intervention.

CHAPTER 6. THERAPEUTIC INTERVENTION IN A MOUSE MODEL OF CHRONIC CHAGASIC CARDIOMYOPATHY (CCC)

6.1 Introduction

Our central hypothesis is that *T cruzi* facilitates mutually beneficial tissue repair in acutely infected hearts through its surface molecule PDNF. Within a reasonable range, robust cardiac parasitism should produce enough PDNF to enhance host physiological repair mechanisms, one of which is expansion and activation of CPCs. PDNF could act both from the surface of parasites infecting cardiac tissue or after it is shed into the extracellular environment (Aridgides et al., 2013a, 2013b). However, this hypothesis cannot be tested in acutely infected hearts because PDNF cannot be knocked-out of the parasite, as there are more than one thousand copies of TS/PDNF in the *T cruzi* genome (Najib M. El-Sayed et al., 2005; N. M. El-Sayed et al., 2005).

However, an alternate hypothesis can be tested *in vivo* in a model of CCC. CCC is the major cause of death in chagasic patients (Davila et al., 2004; Koberle, 1968; Soares et al., 2010). In this condition, tissue-destroying inflammation and fibrosis abounds in the heart, despite parasitism being, paradoxically, extremely rare (Koberle, 1968; Soares et al., 2010). Under conditions of stress, progenitor/stem cells have been shown to play an active role in a negative feedback loop, wherein inflammation triggers them to secrete anti-inflammatory

factors to attenuate the inflammatory cascade before high levels of pro-inflammatory factors accumulate and exert adverse systemic effects (Choi et al., 2011; Lee et al., 2009). Therefore, we wanted to evaluate the properties of CPCs isolated from stressed (mice with CCC) and non-stressed (age-matched, naïve mice) conditions. Furthermore, in accord with our hypothesis, increasing PDNF levels in the heart of mice with CCC should recapitulate the beneficial action of PDNF in acutely infected hearts, where parasite burden is high. We tested this possibility by increasing PDNF levels in cardiac tissues by administering intravenous sPDNF into mice harboring CCC.

6.2 CPCs from CCC mice are growth-defective, produce less anti-inflammatory TSG-6, and are more susceptible to oxidative stress compared to CPCs from naïve mice, and these defects are rescued by sPDNF

Thus far, we have characterized CPCs from naïve mice. We showed that *T cruzi* infection increases the number of Sca-1$^+$ CPCs in the hearts of acutely infected mice (Figures 5.1 & 5.2). This may reflect a compensatory response to quell innate inflammatory immune responses that fight off *T cruzi* infection, and prevent excessive inflammation that could lead to tissue destruction. Following acute infection, parasitemia drops (Figure 6.1a), and for unknown reasons, *T cruzi* is able to persist to the chronic phase of infection, where cardiac parasitism

is focal and barely detectable. Therefore, in the context of CCC mice, *T cruzi* and/or PDNF, due to extremely low abundance, have limited, if any, effects on CPCs. To verify this possibility, we set out to characterize CPCs from CCC mice.

Although certain mouse strains (Balb/c) are more susceptible to *T cruzi* infection than others (C57BL/6), the inoculating dose of parasites may be modified to ensure the survival of mice through the acute phase of infection (Caradonna and Pereiraperrin, 2009). Surviving mice infected with *T cruzi* proceed to the chronic phase of infection, where low levels of *T cruzi*/PDNF in the myocardium may affect CPCs. When we isolated (as in section 5.3) and cultured CPCs from naïve (naïve-CPCs) and CCC (CCC-CPCs) mice, we observed that CCC-CPCs grow less than naïve-CPCs (Figure 6.1b & c). Strikingly, sPDNF rescues defective growth of CCC-CPCs to levels similar to or above that of CPCs from naïve mice (Figure 6.1b & c). In addition, CCC-CPCs secreted lower basal amounts of TSG-6 compared to naïve-CPCs (Figure 6.2), and this deficit was also rescued by sPDNF stimulation (Figure 6.2). Furthermore, when comparing CCC-CPCs isolated from hearts 90- and 146-days post-infection, we find that basal TSG-6 secretion levels are decreased in CPCs isolated from later-stage (146-dpi) CCC hearts, compared to early-stage (90-dpi) (Figure 6.3), suggesting that CPC deficits increase over time with chronic cardiac infection.

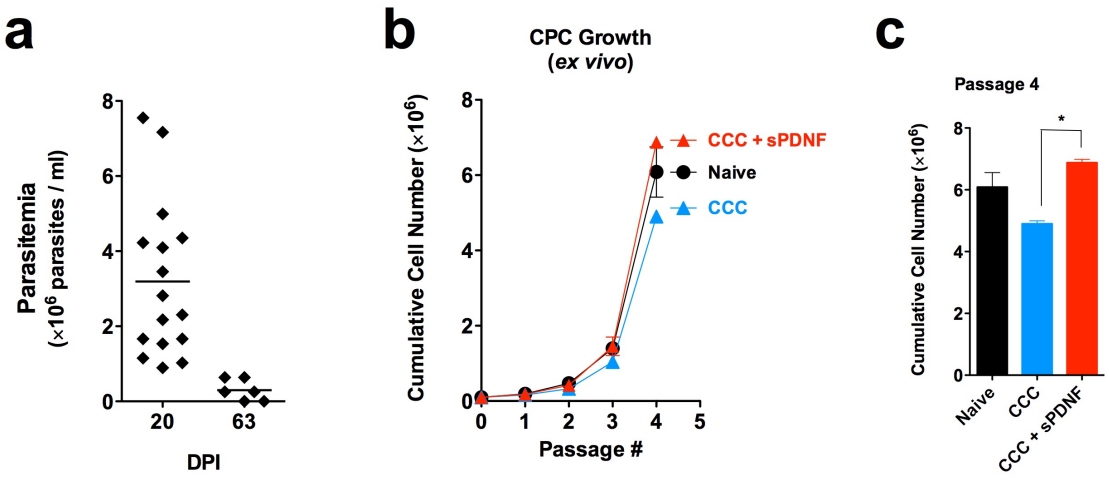

Figure 6.1. sPDNF rescues growth potential of CPCs isolated from CCC mice.

(**a**) Mice were infected and parasitemia monitored for infection progression. CPCs were isolated from naïve or chronically (CCC) infected mice. (**b**) Naïve- and CCC-CPCs were plated as in Figure 5.10, in the absence or presence of sPDNF. Points represent the mean ± SD of duplicate samples per condition. (**c**) Cumulative cell number from passage 4 of (b) is shown. Graph representative of 2 experiments.

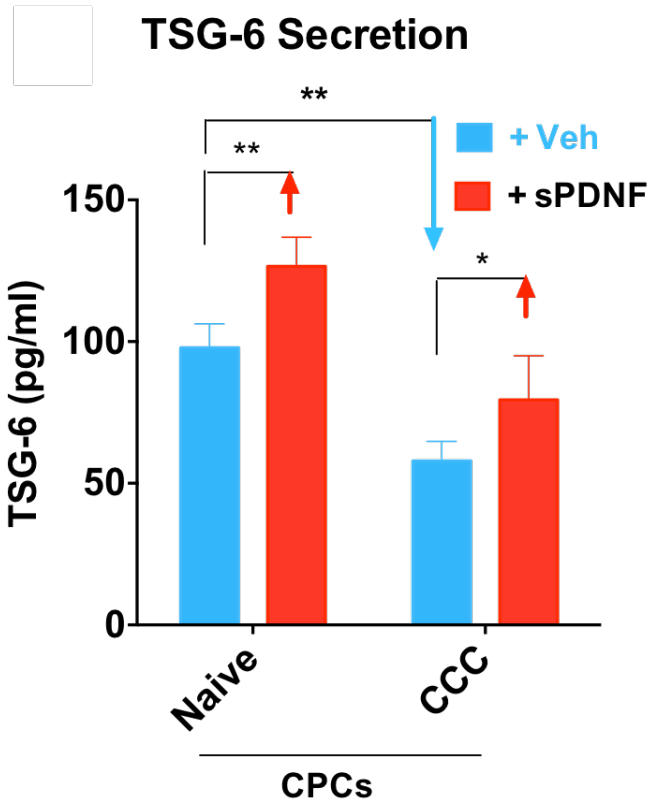

Figure 6.2. sPDNF promotes secretion of anti-inflammatory TSG-6 by CPCs isolated from naïve and CCC mice.

CPCs from naïve or CCC mice were plated overnight, serum starved in DMEM for 2 h, and stimulated with 4 μg/ml sPDNF for 48 h. Cell supernatants were collected, cleared, and tested for secreted TSG-6 by ELISA. Bars represent the mean ± SD of triplicate samples per condition. $*P < 0.05$ and $**P < 0.01$ by one-way ANOVA. Graph is representative of 2 experiments with similar results.

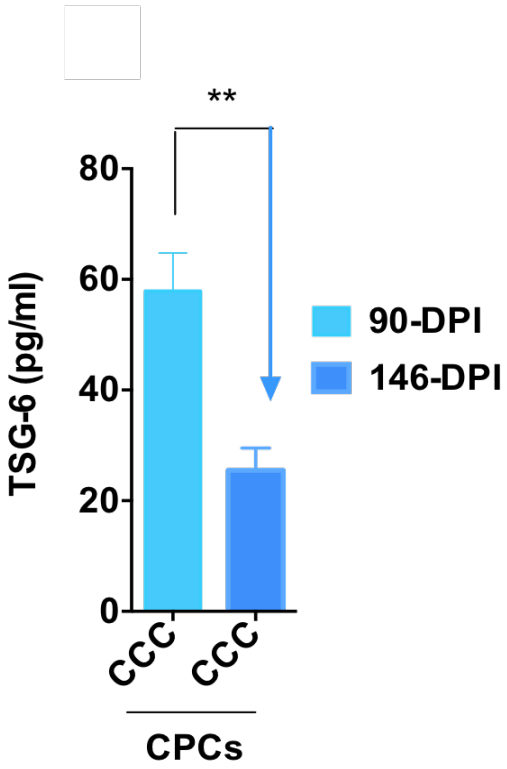

Figure 6.3. Basal TSG-6 secretion is decreased in CPCs isolated from later stage CCC mice.

Cell supernatants were collected from serum starved, unstimulated early passage CPCs isolated from CCC mice at 90- and 146-dpi, and basal TSG-6 levels were measured. Bars represent the mean ± SD of triplicate samples per condition. **P < 0.01 by student's *t*-test.

Oxidative stress contributes to depressed cardiac function and myocardial damage in cardiac tissues bearing excessive inflammation (Ishiyama et al., 1997), raising the possibility that CPCs are damaged by oxidative stress in hearts chronically infected with *T cruzi*. We therefore set out to determine whether CPCs from CCC mice are more susceptible to oxidative stress than CPCs from naïve mice.

CCC-CPCs exposed to H_2O_2 (1.25 mM, 3 h), an oxidative stress stimulant, were more prone to cell death than naïve CPCs subjected to the same oxidative stress (Figure 6.4a). Most important, H_2O_2-mediated cell death of CPCs from both CCC and naïve mouse hearts were rescued by sPDNF (Figure 6.4b, c), a protection consistent with sPDNF-mediated increase in CPC growth (Figure 5.12) and anti-inflammatory secretion (Figure 5.13). Thus, sPDNF rescues the defects in growth/expansion, TSG-6 secretion, and resistance to oxidative stress of CPCs isolated from CCC mice, *ex vivo*.

Thus, these results give strong credence to our central hypothesis that *T cruzi* expresses beneficial factors, such as PDNF, and promotes tissue healing in acutely infected hearts, but cannot do so in chronically infected hearts due to the paucity of PDNF levels, which could be overcome by systemic administration of said factor, sPDNF, in mice with CCC.

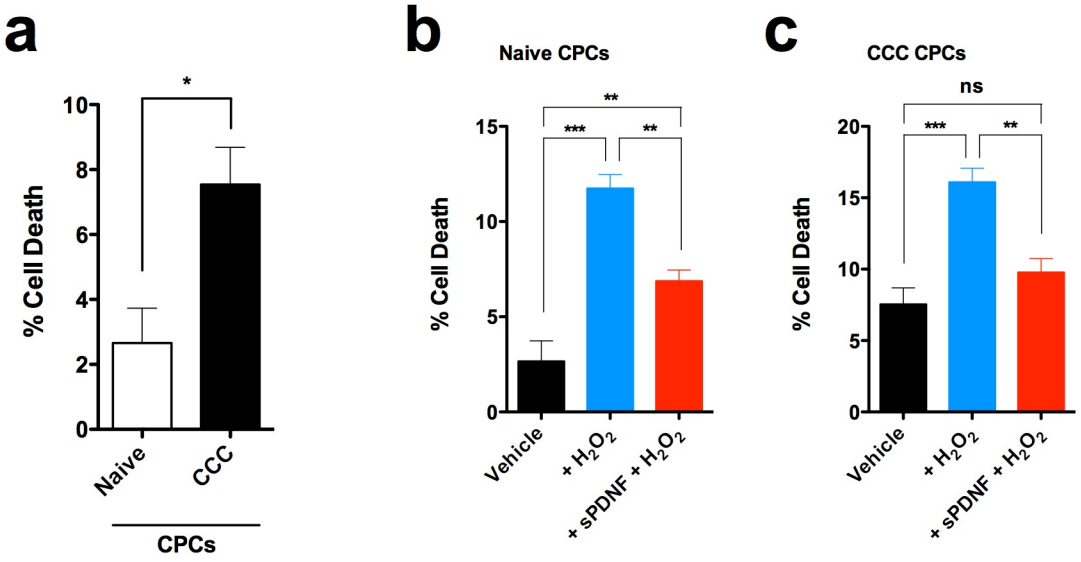

Figure 6.4. sPDNF protects CPCs from H_2O_2-induced cell death.

CPCs (5,000 cells/well) were plated in 96-well plates overnight in CPC medium. Cells were washed with PBS and replaced with 0.1% FCS/DMEM. Cells were pre-treated with 300 ng/ml sPDNF for 30 minutes. 1.25 mM H_2O_2 was added to respective wells for 3 h. PI (5 μg/ml) and Hoechst (10 μg/ml) stain was added per well for 5 minutes, 3 wells at a time. Pictures were taken and dead (pink) and total (pink and blue) cells counted. % Cell Death was calculated as (dead÷total)×100%. Bars represent the mean ± SEM of 3 wells per CPC group of two independent experiments. (**a**) Susceptibility of naïve and CCC CPCs to H_2O_2. Protection of naïve (**b**) and CCC (**c**) CPCs by sPDNF. ns = not significant, *P < 0.05 by student's *t*-test (a) and **P < 0.01, and ***P < 0.005 by one-way ANOVA (b and c).

6.3 IV sPDNF administration rescues defective TSG-6 secretion in CPCs isolated from CCC mice and increases TSG-6 in the sera of mice with CCC

Since *T cruzi* infection can vary depending on the parasite strain/isolate, infection dose, route of infection, and mouse stain infected (Costa, 1999; de Carvalho et al., 2013; Garcia et al., 2005; Zaidenberg et al., 2006), we monitored the progression of *T cruzi* infection in mice by quantifying parasitemia over time. Parasitemia peaks 11 days post-infection during the acute phase, and subsides thereafter to barely detectable levels, subsequently proceeding into the chronic phase of infection. Though the beginning of the indeterminate phase of *T cruzi* infection in mice is approximately 40 days post-infection (Garcia et al., 2005), we waited 3-4 months post-infection, when parasitemia is barely detectable, before we started administering IV sPDNF. IV sPDNF administration consisted of injecting sPDNF IV (1 μg sPDNF per g body weight of mouse) at 0, 3, and 24 h intervals weekly for 3 weeks. Multiple IV sPDNF injections were chosen because we have previously shown that this method increased CCR2, CX3CR1, and Sca-1 transcript and/or cells in the heart (Figures 4.13, 5.3, & 5.5). At 50-60 days after IV sPDNF administration was initiated, mice were sacrificed and organs were harvested for qPCR analysis and tissue histology (Figure 6.5). Other studies that used bone-marrow cell (BMC) therapy to treat CCC in mice have analyzed hearts within a similar timeframe after treatment (Goldenberg et al., 2008; Soares et al., 2011, 2004).

To determine whether IV sPDNF administration had an effect on CPCs, we isolated CPCs from naïve and CCC mice treated with sPDNF (CCC-sPDNF) or PBS (CCC-Placebo) and determined the amount of TSG-6 they secreted. In line with previous findings, CPCs isolated from CCC-Placebo mice secreted less TSG-6 than those isolated from naïve mice (Figure 6.2). Interestingly, CPCs isolated from CCC-sPDNF mice secreted more TSG-6 than those from CCC-Placebo mice (Figure 6.6), suggesting IV sPDNF rescues the potency of CPCs to secrete TSG-6, as observed *ex vivo*. Serum levels of TSG-6 from naïve, CCC-Placebo, and CCC-sPDNF mice revealed that although naïve and CCC-Placebo mice have similar serum levels of TSG-6, CCC-sPDNF mice display elevated levels of TSG-6 (Figure 6.7), suggesting IV sPDNF induces long-lasting secretion of systemic TSG-6.

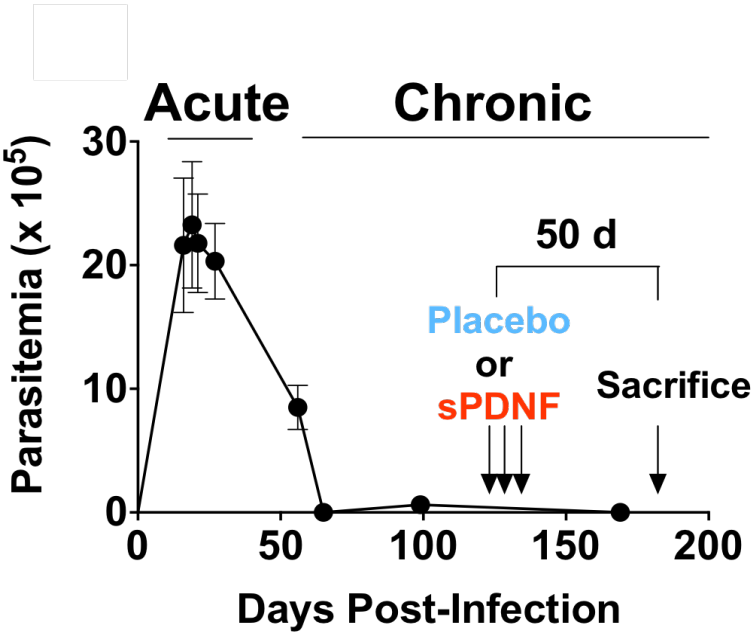

Figure 6.5. Experimental design of IV sPDNF treatment of mice bearing chronic chagasic cardiomyopathy (CCC).

C57BL/6 mice were infected intraperitoneally with *T cruzi* Colombian strain ($8x10^2$ per mouse). Four months later, or 60-d after parasitemia subsides, mice were intravenously injected with Placebo (PBS) or sPDNF (1 μg/g body weight) at 0, 3, and 24 h, weekly for 3 weeks. Mice were sacrificed 50-60 days after IV sPDNF treatment was initiated.

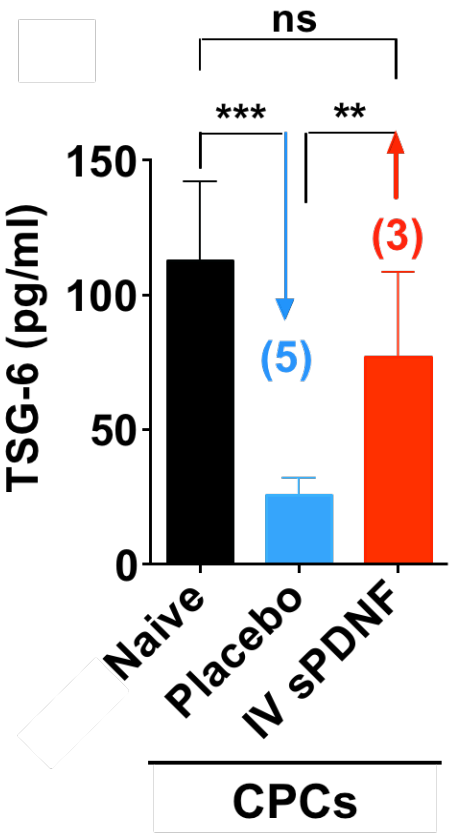

Figure 6.6. IV sPDNF treatment rescues TSG-6 secretion in CPCs isolated from CCC mice.

Experimental protocol is identical to that described in Figure 6.5 except for the use of Balb/c, instead of C57BL/6, mice. Animals were infected by intraperitoneal injection of *80 T cruzi* per mouse and allowed to progress to the chronic stage of infection. At 3 months post-infection, mice were treated with IV Placebo (PBS) or IV sPDNF (25 μg) at 0, 3, and 24 h, weekly for 3 weeks. Mice were sacrificed 56 days after the first IV injection, and CPCs were isolated. Basal TSG-6 secretion levels were determined similar to that described in Figure 6.3. Bars represent the mean ± SD of triplicate samples per condition. ns = not significant, $^{**}P < 0.01$ and $^{***}P < 0.005$ by one-way ANOVA.

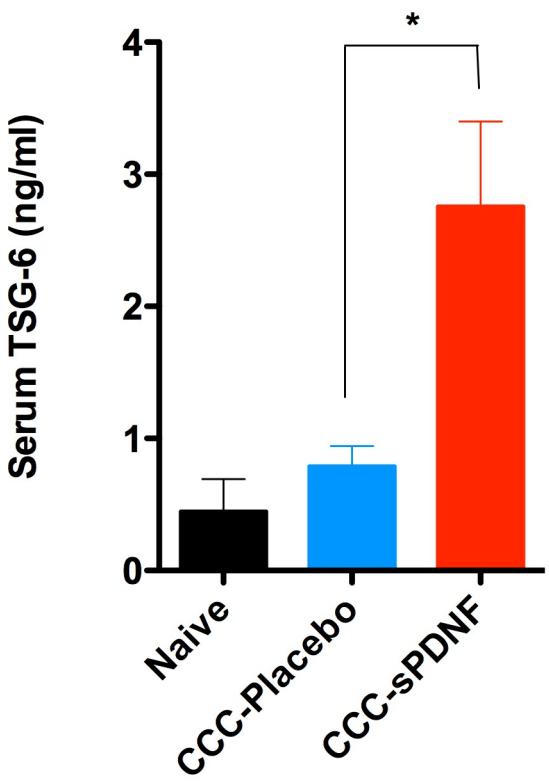

Figure 6.7. IV sPDNF increases anti-inflammatory TSG-6 in the sera of mice with CCC.

C57BL/6 mice were infected with 800 *T cruzi* intraperitoneally and allowed to progress to the chronic stage of infection, when they develop CCC. Mice were treated with IV sPDNF as described in Figure 6.5. Serum was collected 72 d after sPDNF treatment and assayed for TSG-6 by ELISA. Bars represent 4-9 mice per group, combined from 3 independent experiments. *$P < 0.05$ by one-way ANOVA.

6.4 IV sPDNF administration inhibits inflammation in the hearts of CCC mice

Long-lasting anti-inflammatory effects of IV sPDNF administration are perfectly consistent with our central hypothesis that PDNF promotes tissue healing by reducing excessive cardiac inflammation and, at the same time, serves as a promising therapeutic opportunity for CCC. BMC therapy has been shown to decrease inflammation in hearts of C57BL/6 mice chronically infected with *T cruzi* (Goldenberg et al., 2008; Soares et al., 2011, 2004). Thus, we wanted to determine the degree of inflammation in hearts based on histology and qPCR analysis after IV sPDNF administration. Hematoxylin and Eosin (H&E) staining of naïve, CCC-Placebo, and CCC-sPDNF mouse heart sections showed the presence of focal inflammatory foci in CCC-Placebo mice (Figure 6.8), a characteristic of CCC. Remarkably, cardiac sections from CCC-sPDNF mice were devoid of inflammatory foci, and looked similar to age-matched, naïve controls (Figure 6.8). Furthermore, we observed a decrease in the expression of several inflammatory cell markers and pro-inflammatory factors in the heart by qPCR (Figure 6.9), supporting IV sPDNF contributes to long-lasting inhibition of inflammation.

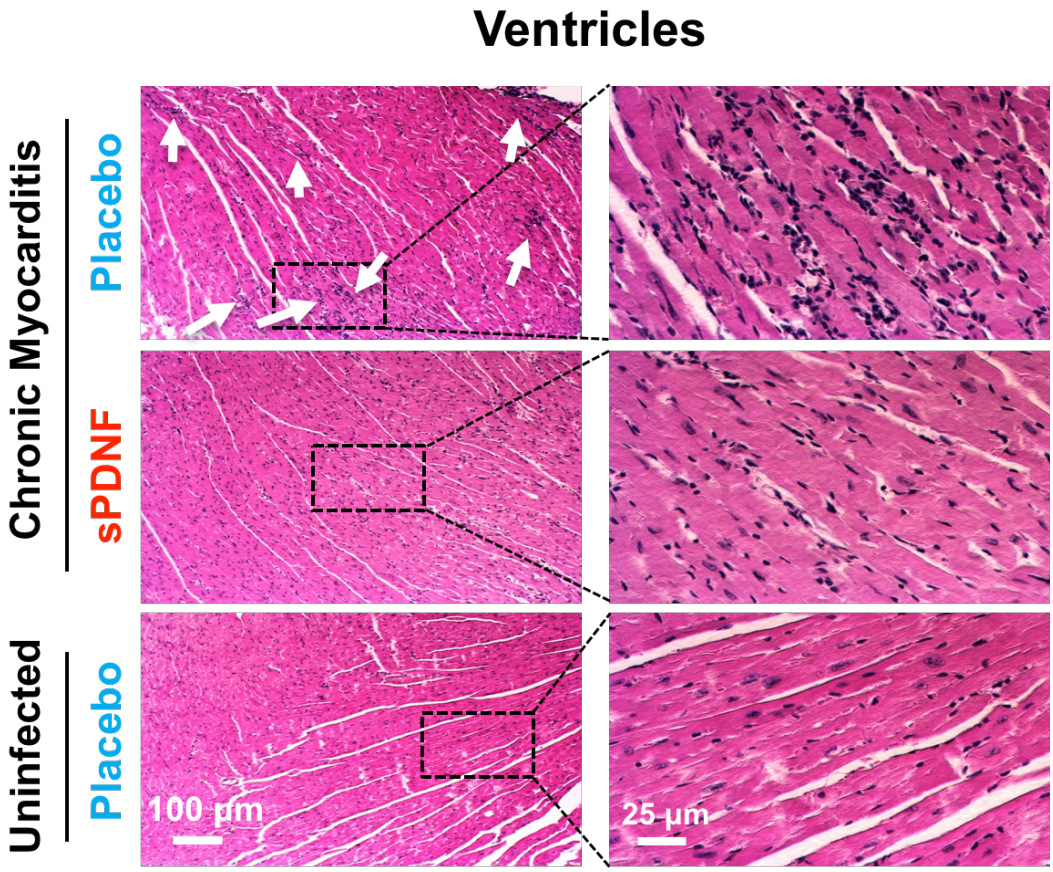

Figure 6.8. IV sPDNF treatment reduces inflammation in the heart of mice with CCC.

Experimental protocol described in Figure 6.5 was performed. Myocardium (ventricles) were paraffin-embedded, sectioned, and stained with H&E. Arrows indicate foci of inflammatory infiltrates, which are abundant in Placebo-treated (IV PBS) CCC mice and rare in IV sPDNF-treated CCC mice. Similar histology was found in 3 other tissue sections in the same set of 3 mice per group from one experiment, and in 4 sections of 5 similarly treated mice per group from a separate experiment.

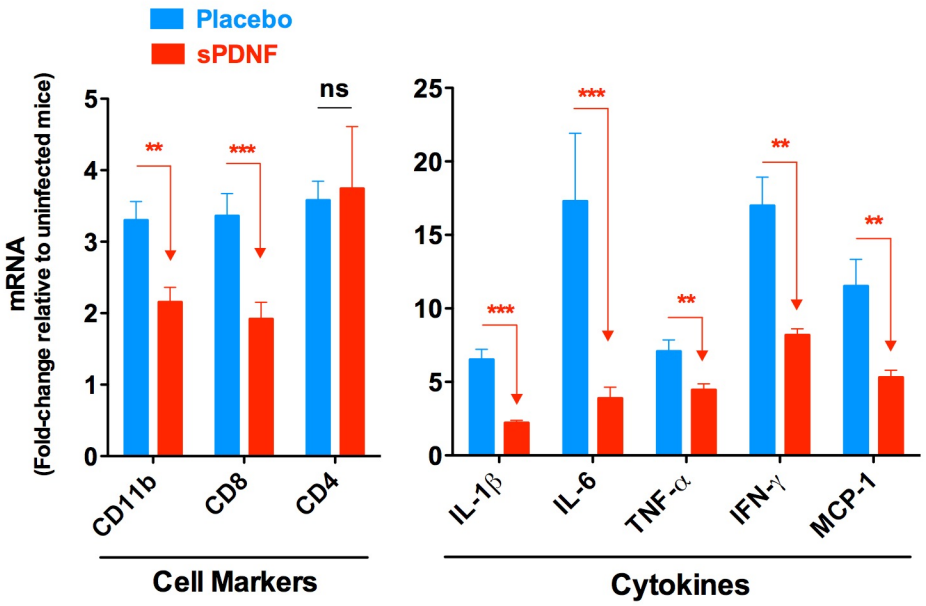

Figure 6.9. IV sPDNF decreases the expression of inflammatory cell markers and cytokines in the heart of CCC mice.

Hearts of CCC mice were assessed by qPCR for the indicated mRNAs normalized to HPRT and made relative to uninfected vehicle-treated mice. $^{**}P < 0.01$ and $^{***}P < 0.001$ by student's *t*-test. Bars representative of 3-5 mice per group; graph representative of 2 independent experiments.

6.5 IV sPDNF administration prevents the progression of cardiac fibrosis in mice with CCC

Cardiac fibrosis, or the deposition of collagen and other extracellular matrix components in heart tissues, is a hallmark of CCC, a deleterious process that can decrease heart function over time (Goldenberg et al., 2008; Soares et al., 2011, 2004; Unnikrishnan and Burleigh, 2004; Wahab et al., 2005; Wang et al., 2010). Therefore, to determine whether IV sPDNF administration affects cardiac fibrosis, we subjected heart tissue sections to Masson's Trichrome staining, which stain muscle red and collagen blue. Digitized images of Trichrome-stained heart sections from CCC-Placebo and CCC-sPDNF mice were analyzed by ImageJ (NIH) to distinguish blue and red pixels, which was then expressed as a percent cardiac fibrosis. We found that IV sPDNF treatment reduced the % cardiac fibrosis in CCC mice, compared to placebo-treated mice (Figure 6.10). Lastly, when we determined the degree of cardiac fibrosis in hearts before and after IV sPDNF treatment and found that IV sPDNF treatment prevents the progression of cardiac fibrosis in the hearts of CCC mice (Figure 6.11).

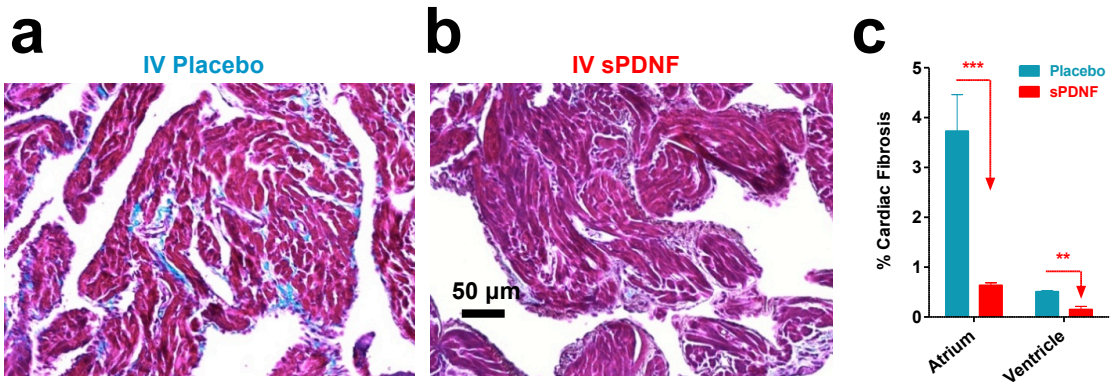

Figure 6.10. IV sPDNF treatment reduces cardiac fibrosis in mice with CCC.

Animals and experimental protocol are described in Figure 6.5. Heart sections were paraffin-embedded, stained with Masson-Trichrome to visualize collagen in fibrotic areas (blue) and viable muscle fibers (red). Panels display sections of atria of mice with CCC administered IV Placebo (**a**) or IV sPDNF (**b**). (**c**) Bar graph shows the quantification of cardiac fibrosis performed with ImageJ software (NIH) in four distinct sections of atria and ventricles and represents the mean ± SEM cardiac fibrosis of three mice per group. % cardiac fibrosis is defined as the ratio of blue pixels to total pixels (blue + red) × 100%; ns = not significant, $^{**}P < 0.01$ and $^{***}P < 0.005$. Data is representative of 2 independent experiments.

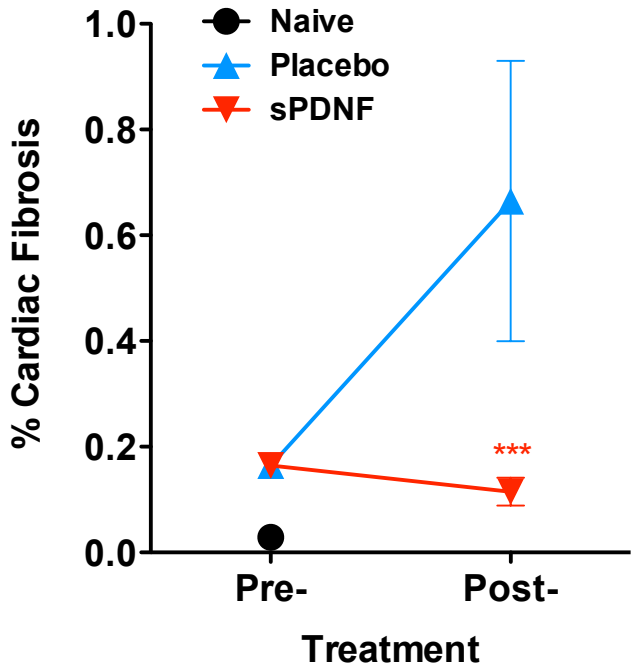

Figure 6.11. IV sPDNF prevents the progression of fibrosis in the heart of CCC mice.

Experimental protocol is identical to that described in Figure 6.5 except for the use of Balb/c (Figure 6.6), instead of C57BL/6, mice. Animals were infected by intraperitoneal injection of *80 T cruzi* per mouse and allowed to progress to the chronic stage of infection. At 3 months post-infection, mice were treated with IV Placebo (PBS) or IV sPDNF (25 μg) at 0, 3, and 24 h, weekly for 3 weeks. Mice were sacrificed before the IV sPDNF treatment was initiated or 56 days after the first IV injection, and hearts were collected for Masson Trichrome staining to visualize fibrosis. Percent fibrosis is calculated as the fibrotic area (blue) ÷ total area (blue+red) ×100%. Points represent 3 mice per group. $^{**}P < 0.01$ and $^{***}P < 0.005$ by student's *t*-test, comparing CCC-Placebo and CCC-sPDNF 56 days after treatment).

6.6 Summary

We show that CPCs isolated from naïve mice are biologically distinct from CPCs purified from CCC mice; specifically, CCC-CPCs grow to a lesser extent, secrete less anti-inflammatory TSG-6, and are more susceptible to oxidative stress than counterpart naïve-CPCs. Most important, defects in CPCs from CCC hearts are rescued by sPDNF stimulation (Figures 6.1 – 6.4), supporting our view that PDNF is critical to tissue healing in acutely infected hearts and, equally important, suggests a potential therapeutic use for sPDNF in CCC, for which there is no cure.

Thus, to increase PDNF levels in the hearts of CCC mice, we administered IV sPDNF treatment in CCC mice, which revealed beneficial anti-inflammatory responses. CPCs from CCC-sPDNF mice secreted higher levels of TSG-6 than those from CCC-Placebo mice (Figure 6.6), which were also supported by elevated TSG-6 serum levels in CCC-sPDNF mice (Figure 6.7). Furthermore, we found that IV sPDNF treatment decreased inflammation in the heart (Figures 6.8 – 6.9) and prevented the progression of cardiac fibrosis (Figures 6.10 – 6.11) in C57BL/6 and Balb/c strains of mice. Whether CPCs from various strains of mice differ remains to be determined. Nevertheless, findings presented thus far suggest IV sPDNF activates tissue resident CPCs in the heart, which may contribute to long-lasting, tissue-repairing, anti-inflammatory responses that subdue inflammation and prevent the progression of cardiac fibrosis, a harmful mechanism in chronic cardiac disorders.

CHAPTER 7. DISCUSSION

7.1 *T cruzi* interaction with host cells

The interaction between *T cruzi*-PDNF with receptors TrkA and TrkC has been shown to trigger parasite invasion in neuronal cells, cardiomyocytes and other cell types and promote pro-survival signals in host cells (Aridgides et al., 2013a, 2013b; Chuenkova and Pereira, 2000; Chuenkova and PereiraPerrin, 2005, 2004; de Melo-Jorge and PereiraPerrin, 2007; Weinkauf et al., 2011). Trks are important receptors for the development and maintenance of the nervous system (Huang and Reichardt, 2003), but the role Trk receptors play in other biological systems, as well as microbial infections, *T cruzi* infection in particular, may be underappreciated. Previous work demonstrated *T cruzi* PDNF as a ligand for NGF and NT-3 receptors, TrkA and TrkC, that leads to parasite entry of host cells and activation of prosurvival and protective events (Aridgides et al., 2013a, 2013b; Chuenkova and PereiraPerrin, 2005, 2004; de Melo-Jorge and PereiraPerrin, 2007; Weinkauf et al., 2011; Weinkauf and Pereiraperrin, 2009). In this thesis, we demonstrate that *T cruzi* PDNF-Trk interaction in the heart promotes tissue repair events, highlighting the therapeutic potential of PDNF to treat CCC, for which there is no effective treatment.

7.2 *T cruzi*/PDNF induction of chemokines

We demonstrated a novel mechanism underlying an innate immune response to *T cruzi*, which, via its outer membrane-bound PDNF, upregulates expression of chemokines MCP-1 and FKN by activating neurotrophic receptors TrkA and TrkC. In this vein, *T cruzi* exploits the pathway used by CTGF/CCN2, an inflammatory/fibrotic matricellular growth factor, which promotes chemokines and inflammatory cytokine expression through the activation of TrkA (Wahab et al., 2005; Wang et al., 2010). Interestingly, other studies identified a relationship between *T cruzi* infection of cultured cells and the expression of CTGF/CCN2 (Unnikrishnan and Burleigh, 2004). However, it remains to be determined whether alteration in CTGF/CCN2 expression by *T cruzi* relates to the results reported here.

Alteration of MCP-1 expression in inflamed, infected tissues is traditionally studied in the context of recruiting pro-inflammatory immune cells for microbicidal purposes, including *T cruzi* infection (Coelho et al., 2002; Machado et al., 2000; Paiva et al., 2009). A first wave of immune cells recruited to infected tissues is composed of Ly-6C^{high} monocytes, a major monocyte subset in the bloodstream that are attracted by MCP-1/CCR2 signaling (Serbina et al., 2008). Ly-6C^{high} monocytes exhibit phagocytic, proteolytic, and inflammatory activities and are thought to control the digestion of damaged tissue (Serbina et al., 2008). It should be noted that recruitment of microbicidal cells by MCP-1 is a mutually beneficial action, as it keeps infection in check, preventing parasite overgrowth,

which would kill the host and subsequently terminate the likelihood of further *T cruzi* transmission (Paiva et al., 2009; Serbina et al., 2008).

However, MCP-1 also attracts anti-inflammatory immune cells and reparative progenitor cells, exemplified by regulatory T cells (Sebastiani et al., 2001) and neural crest-derived cardiac stem/progenitor cells (Tamura et al., 2011). It may be that *T cruzi* PDNF-induced MCP-1 and FKN expression in cardiomyocytes, cardiac fibroblasts, or myocardium reflects an attempt to promote mechanisms of cardioprotection and cardiac repair in acutely infected hearts.

The hypothesis for an anti-inflammatory and repair function of MCP-1 induced in response to PDNF is consistent with other studies that demonstrate cardioprotective effects for MCP-1. Indeed, it has been shown that overexpression of MCP-1 in the heart, under the control of an α-cardiac myosin heavy chain promoter, gives rise to transgenic mice that are significantly protected against cardiac dysfunction and remodeling after myocardial infarction (Morimoto et al., 2006) and severe heart injury caused by ischemia/reperfusion (Morimoto et al., 2008).

Similarly, an anti-inflammatory/repair function of MCP-1 may also apply to the reparative role of FKN, whose expression is also increased by sPDNF. FKN, in contrast to MCP-1, has been rarely studied in the context of *T cruzi* infection. Yet, FKN/CX3CR1 signaling is widely recognized as an important mechanism for tissue repair, especially in the context of wound healing in the myocardium

(Nahrendorf et al., 2007), or in the brains of animal models of Parkinson's and other neurodegenerative disorders (Sheridan and Murphy, 2013). FKN is involved in tissue repair, as it attracts reparative Ly-6C^{low} monocytes through CX3CR1 recognition in the second phase of inflammation, following the initial Ly-6C^{high} monocyte wave (Serbina et al., 2008). Ly-6C^{low} monocytes dampen inflammatory responses to limit tissue damage, and promote angiogenesis through secretion of vascular-endothelial growth factor (VEGF) (Nahrendorf et al., 2007). Thus, increased FKN expression in *ex vivo* cardiomyocytes and cardiac fibroblasts (Figures 4.1 – 4.3), acutely infected hearts (Figure 4.7), or in the myocardium following IV sPDNF (Figure 4.8) may reflect a tissue healing effect as a result of PDNF-Trk receptor activation. The concept that FKN controls tissue repair following myocardial injury is also consistent with the observed sustained expression of FKN, but not of MCP-1, in the absence of overt cardiac parasite burden following the acute phase of infection (Figure 4.7).

The notion that *T cruzi*-PDNF promotes protective chemokine expression in the heart is consistent with recently published work indicating that sPDNF is cardioprotective via paracrine (NGF secretion via TrkC activation) and autocrine (direct TrkA activation) mechanisms (Aridgides et al., 2013a, 2013b). Unlike broad-like kinetics, pulse-like expression of growth factors administered directly into tissues is a sought-after therapeutic property. This is exemplified by intracardiac injection of chemically modified VEGF-A mRNA, which is translated in a pulse-like fashion and, as such, is more effective in directing the fate of CPCs and promoting vascular regeneration after myocardial infarction, than

intracardiac injection of VEGF-A DNA, which generates broad and sustained VEGF-A expression (Zangi et al., 2013). Therefore, like modified VEGF-A mRNA, IV sPDNF induced pulse-like upregulation of cardioprotective growth factors, such as NGF (Aridgides et al., 2013b), MCP-1, and FKN (Figure 4.8), highlighting its use as a therapeutic for injured myocardium, as seen in chronic Chagasic cardiomyopathy, and other tissues where IV sPDNF may trigger repair mechanisms. Furthermore, it is possible that PDNF-mediated modulation of chemokines over the course of *T cruzi* infection may affect other resident cardiac cells, such as stem/progenitor cells, that contribute to promoting reparative and anti-inflammatory responses.

7.3 *T cruzi*/PDNF activation of cardiac progenitor cells (CPCs)

Stem cells are widely studied in great part because of their therapeutic and/or regeneration potential in a wide range of diseases, particularly in the heart (Behfar et al., 2014; Bernstein and Srivastava, 2012; Frangogiannis, 2014; Oh et al., 2003; Pfister et al., 2005; Ptaszek et al., 2012; Tamura et al., 2011; Van Linthout et al., 2011; Ye et al., 2012). One great promise of stem cell therapy is that it may serve as an alternative to whole organ transplant (Behfar et al., 2014; Bernstein and Srivastava, 2012; Van Linthout et al., 2011). Conveniently, bone marrow cell therapy in mouse models of Chagas disease have already been

shown to ameliorate and reverse chronic chagasic cardiomyopathy (Goldenberg et al., 2008; Soares et al., 2011, 2004).

Not surprisingly, stem cells have also been linked to interaction with other microbes. For example, *Mycobacterium tuberculosis* was shown to recruit mesenchymal stem cells to sites of infection to suppress T-cell responses and facilitate persistent infection (Raghuvanshi et al., 2010). Another microbe of the same genus, *Mycobacterium leprae*, was shown to hijack the genomic plasticity of Schwann cells and reprogram them to a stage of progenitor/stem cells (Masaki et al., 2013). Whether *T cruzi* PDNF contributes to the recruitment and/or expansion of stem progenitor cells and their roles in regeneration and/or immunomodulation were discussed in chapters 5 and 6.

We previously showed that Sca-1 transcripts in the heart are increased by multiple IV sPDNF injections, and that this effect is, at least in part, dependent on MCP-1/CCR2 signaling (Figure 5.3). Though not much is known about FKN/CX3CR1 signaling in regards to stem cell recruitment, other studies suggest MCP-1 and FKN chemokines work in concert. Indeed, the contribution of FKN/CX3CR1-signaling is reflected by the lower fold-increase in Sca-1 transcript levels observed in the CX3CR1$^{-/-}$ mice treated with sPDNF, compared to wild-type (Figure 5.3). The increase in Sca-1 transcript levels after either single (Figure 5.4) and multiple IV sPDNF injections (Figure 5.3) differs from the response observed for chemokine receptor transcript levels, where only multiple IV sPDNF injections (Figure 4.13), and not single IV sPDNF injections (Figure

4.12), increased CCR2 or CX3CR1 transcripts in the heart. These data suggest that the increase in Sca-1 transcript reflects the activation and/or expansion of tissue resident cardiac progenitor cells, whereas the increase of chemokine receptor transcripts reflects recruitment of immune cells into the heart after infusion with sPDNF. Cell-fate and flow cytometry analyses of cell populations in the heart at various times after IV sPDNF injections should help to further distinguish cell expansion versus recruitment.

Previous work has shown that TrkA and TrkC are expressed on cardiomyocytes (Cantarella et al., 2002; Caporali et al., 2007; Ieda et al., 2006; Meloni et al., 2010; Zhou et al., 2004) and we were the first to demonstrate expression of TrkA and TrkC on cardiac fibroblasts (Aridgides et al., 2013a, 2013b). In addition, we have shown that *T cruzi*-Trk interaction on cardiac cells promotes survival and invasion (Aridgides et al., 2013a, 2013b). Coupling these findings with advances in stem cell biology, that link activation of Trk receptors to the promotion of stem cell survival (Nguyen et al., 2009), led us to explore the effects of sPDNF on Sca-1^+ cardiac progenitor/stem cells (CPCs).

We show that, similar to cardiomyocytes and cardiac fibroblasts, CPCs express TrkA and TrkC, but not TrkB (Figure 5.9). CPC growth is enhanced when grown in the presence of sPDNF (Figure 5.10), and was inhibited by the Trk inhibitor, K252b (Figure 5.11). These findings are in accordance with studies showing NGF promoting angiogenesis, cardiomyocyte survival, and increasing the number of progenitor cells in a post-MI heart (Meloni et al., 2010). Thus, resident

CPCs may serve as a novel cardiac cell subset target that interacts with *T cruzi* over the course of Chagas disease.

7.4 *T cruzi*/PDNF promotes immunomodulatory mechanisms of CPCs

Initially, stem cell therapy was assumed to contribute to repairing tissues by engrafting and differentiating to replace injured cells (Choi et al., 2011). Repair with functional improvements was observed without evidence of long-term cell engraftment; this was eventually explained by paracrine secretions that had multiple effects, including modulation of inflammatory or immune reactions (Choi et al., 2011). In many experimental models and clinical trials, cells are intravenously infused and yielded surprising functional improvements, despite cells being rapidly trapped in the lung as microemboli (Gao et al., 2001). It was later found that IV infused mesenchymal stromal cells (MSCs) produced functional improvement in mice with MI, at least in part, because the cells trapped as emboli in the lung were activated to express the anti-inflammatory factor TSG-6 (Lee et al., 2009).

TSG-6 has been characterized in many inflammatory models, such as peritonitis (Choi et al., 2011), arthritis (Nagyeri et al., 2011), conjunctivochalasis (Guo et al., 2012), and myocardial infarction (Lee et al., 2009), and is thought to play a role in a negative feedback loop, wherein inflammation triggers MSCs to secrete TSG-6 to attenuate the inflammatory cascade early, before high levels of pro-

inflammatory factors accumulate and begin to exert adverse systemic effects (Choi et al., 2011; Lee et al., 2009). Therefore, TSG-6 should represent an anti-inflammatory biomarker expressed by CPCs. We found that sPDNF stimulated CPCs to secrete TSG-6 in a dose-dependent manner (Figure 5.13), and this stimulation was inhibited by knockdown of TrkA and TrkC (Figure 5.14), suggesting a neurotrophic link between PDNF and CPCs, and subsequent activation of TSG-6 secretion. Thus, *T cruzi* PDNF may harbor similar activities as NGF on CPCs, and actively modulate TSG-6 levels in chronically infected tissue.

7.5 CPCs from CCC mice are deficient in growth, TSG-6 secretion, survival

The stem cell therapy field has shifted from ‘first-generation’ cell-based therapies to ‘next-generation’ stem-cell-based therapies targeting cardiovascular disease, which entails the purification of lineage specific cardiac progenitor cells, as opposed to unfractionated bone-marrow-derived mononuclear stem cells (Behfar et al., 2014).

Patient characteristics affect the number of isolated human cardiac progenitor cells (Itzhaki-Alfia et al., 2009). In humans, it has been observed that patients with aortic stenosis, acute and chronic ischemia, and other cardiomyopathies correlate with increased numbers of cardiac progenitor cells, suggesting local

signals stimulate this response to injury (Itzhaki-Alfia et al., 2009). This idea was tested using “middle aged” mice as cardiac cell donors; it was found that acute myocardial infarction (MI) induced a dramatic increase in the number of cardiac progenitor cells in mice (Ye et al., 2012). This study also demonstrated that cloned Sca-1^{+} cells derived from infarcted “middle aged” hearts gave rise to both myocardial and vascular tissues, and suggests it is a more appropriate source of progenitor cells for autologous cell-therapy post-MI than unfractionated bone-marrow stem cells (Ye et al., 2012). This led us to study differences between CPCs isolated from naïve (naïve-CPCs) and CCC (CCC-CPCs) mice. More CPCs were isolated from CCC hearts than uninfected hearts, in line with studies that reported more progenitor cells in inflammatory settings (Meloni et al., 2010). Upon further characterization, we also found that CCC-CPCs grow less efficiently (Figure 6.1) and secrete less TSG-6 (Figure 6.2) than naïve-CPCs over time (Figure 6.3).

Recently, our lab has shown that *T cruzi* infection and/or sPDNF stimulation confers protection of cardiomyocytes from oxidative stress (Aridgides et al., 2013b). Cardiomyocytes are vulnerable to reactive oxygen species due to their high metabolic rate (Machado et al., 2000). Thus, we tested the susceptibility of CPCs to oxidative stress, and whether this sensitivity can also be rescued by sPDNF. Though cardiomyocytes were susceptible to 150 μM H_2O_2 exposure for 4 hours (Aridgides et al., 2013b), exposing CPCs to these conditions did not kill them. Rather, exposure to 1.25 mM H_2O_2 led to quantifiable levels of CPC death, suggesting CPCs are more resistant to oxidative stress than cardiomyocytes. In

addition, we found that CCC-CPCs were more susceptible to oxidative stress than naïve-CPCs (Figure 6.4).

It may be that *T cruzi* infection elicits an inflammatory response to stimulate CPCs in the myocardium to proliferate and initiate anti-inflammatory responses to counteract inflammation that could otherwise be detrimental to the heart. Anti-inflammatory responses may benefit *T cruzi* by impeding immune responses responsible for clearing the parasites, and contribute to the establishment of focal, chronic infection of the myocardium. Although overall heart parasitism levels in the chronic phase are low, focal infection of the myocardium may represent areas where levels of PDNF are localized and contained. Chronic exposure of CPCs to inflammation, not within the vicinity of *T cruzi* or PDNF, may exhaust their anti-inflammatory capacity and/or ability to secrete TSG-6 over time. Remarkably, *ex vivo* sPDNF stimulation rescued CCC-CPC deficits in cell growth, TSG-6 secretion, and resistance to oxidative stress (Figures 6.1 – 6.4), strongly suggesting potential beneficial anti-inflammatory effects of PDNF on CPCs in inflammatory settings, such as CCC.

7.6 Proof-of-concept: administration of sPDNF in CCC mice ameliorates cardiac inflammation and fibrosis, implying a therapeutic opportunity to treat chronic Chagas heart disease

Parasite burden and, presumably, the amount of PDNF in the hearts of mice chronically infected are low compared to levels in acutely infected hearts. Given that we showed that sPDNF can rescue growth of, TSG-6 secretion by, and promote survival of CPCs, we hypothesized that this novel effect of PDNF on CPCs aids in cardiac repair in *T cruzi* acute infection, when cardiac *T cruzi*/PDNF levels are high. However, it is not practical to demonstrate this hypothesis in acute infection, as it is impossible to generate PDNF knockouts in *T cruzi*, given that there are more than one thousand copies of PDNF in the trypanosome genome (de Souza et al., 2010; Najib M. El-Sayed et al., 2005). However, this hypothesis can be tested in chronically infected mice because parasite load and, consequently, PDNF tissue concentration is very low. Hence, artificially elevating tissue levels of cardioprotective PDNF by systemic administration would be tantamount to the *T cruzi*/PDNF levels in the acute phase of infection, without overt heart parasitism. Indeed, PDNF plays a role in cardiac repair, as exogenous addition of sPDNF to CCC mice ameliorates characteristics of chronic disease, in which IV sPDNF dramatically reduces inflammatory infiltrates, fibrosis and inflammatory markers (chapters 5 & 6). The beneficial effect of intravenous sPDNF in CCC mice may be related to *ex vivo* enhancement by sPDNF on CPC

expansion, survival and secretion of the anti-inflammatory TSG-6 (Figures 6.6 – 6.11).

It remains to be determined whether the histological and biochemical benefit of intravenous sPDNF in CCC mice translates to improved cardiac structure and function, which can be determined by noninvasive procedures such as echocardiography. Furthermore, systemic administration of sPDNF could be beneficial in congestive heart failure akin to, but distinct from, CCC, such as chronic pathologic cardiac remodeling responses caused by a variety of pathologic stimuli, including left ventricle (LV) pressure overload and hypertension, or resultant of inherited valvular or ischaemic diseases (Aukrust et al., 1998; Lefer and Granger, 2000). LV pressure overload is a major cause of cardiomyopathies and gives rise to pathological hallmarks such as excessive inflammation and fibrosis (Braunwald, 2013), in which IV sPDNF may be of preventative therapeutic value.

7.7 Conclusion

"In the moment when I truly understand my enemy, understand him well enough to defeat him, then in that very moment I also love him." *- a quote from* Ender's Game *by Orson Scott Card*

The interaction of *T cruzi* PDNF and Trk receptors in the heart provides insight into the pathogenesis of the parasite. In the acute phase, *T cruzi* disseminates throughout its host, activating innate inflammatory responses that help control infection. Somehow, though, *T cruzi* is able to establish a low, chronic infection in its mammalian host, a majority in which remains asymptomatic for the remainder of their life. This led us to hypothesize that *T cruzi* expresses factors that contribute to wound healing and tissue repair in its host.

If we depict the pathogenesis of Chagas disease as a level of *T cruzi*/PDNF in the heart over time, we can infer beneficial aspects of *T cruzi*/PDNF, as shown in our pathogenesis model depicted in Figure 7.1. In the acute phase, *T cruzi*/PDNF levels are high and activate innate immune responses. PDNF activates TrkA and TrkC on cardiac cells to express chemokines, which recruit immune cells to the heart (blue box, Figure 7.1). Subsequently, chemokines and *T cruzi* PDNF also function to activate anti-inflammatory responses that subdue the initiating inflammatory response, which, if left uncontrolled, could lead to excessive tissue damage and destruction. Promoting anti-inflammatory responses may also

contribute to *T cruzi* evasion of host immune responses, allowing the parasite to persist into the chronic phase of infection.

In the chronic phase, tissue parasitism drops to barely detectable levels. *T cruzi* infection in the heart is low and focal, and is thought to contribute to chronic cardiac inflammation that can eventually lead to cardiac fibrosis. Low *T cruzi*/PDNF levels in the chronic phase of infection would not be sufficient to promote beneficial anti-inflammatory responses, which might explain why CPCs isolated from CCC hearts are defunct in growth/expansion, TSG-6 secretion, and resistance to oxidative stress (red box, Figure 7.1). Reconstituting PDNF levels in the CCC heart by IV sPDNF injections promotes long-lasting beneficial, reparative, and wound healing actions by virtue of rescued CPC TSG-6 secretion, and increased serum levels of TSG-6, which correlated with decreased cardiac inflammation and fibrosis (purple box, Figure 7.1). This highlights the Trk pathway as a novel therapeutic target in CCC, and support *T cruzi* PDNF as a beneficial and potential therapeutic factor.

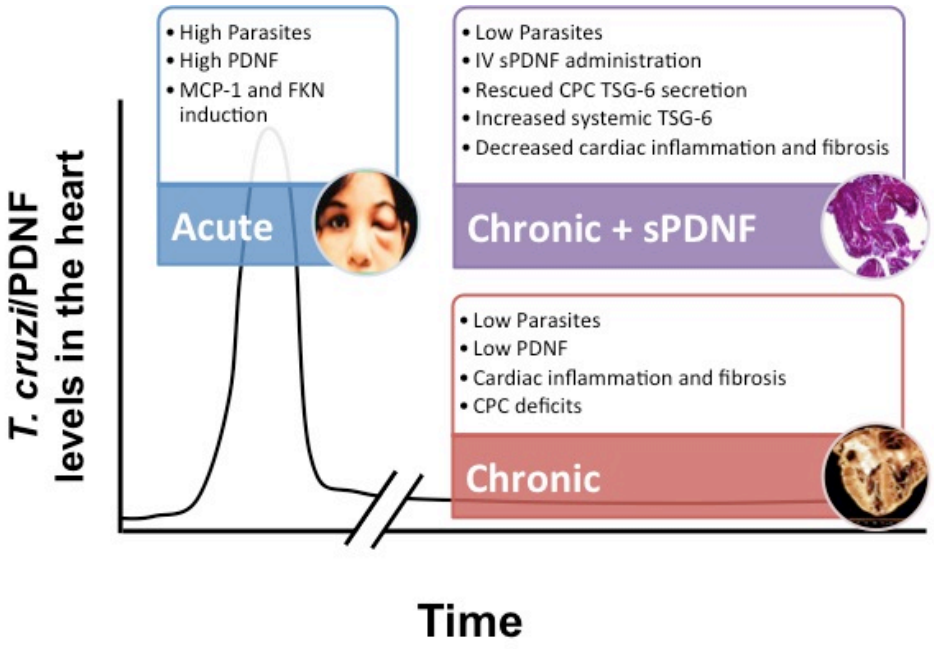

Figure 7.1. A model of the effects of *T cruzi*/PDNF over the course of Chagas disease progression, and the amelioration of CCC with IV sPDNF.

Cardiac tissue parasitism correlates to the level of PDNF present in tissues. High tissue parasitism in the acute phase contributes to the induction of chemokines MCP-1 and FKN (blue box). *T cruzi* infection is controlled, but not eliminated, and progress to the indeterminate chronic phase of the disease. While cardiac inflammation and fibrotic processes occur while tissue parasitism persists at low levels during the chronic phase of the disease, a majority of infected individuals do not present with sequelae (red box). Boosting PDNF levels, by IV sPDNF, in the heart ameliorates cardiac inflammation and fibrosis in CCC mice (purple box), supporting *T cruzi* PDNF as a beneficial factor.

Findings presented in this thesis not only provide insight into the pathogenesis of *T cruzi*, but also highlight a point of intervention in chronic Chagas disease. CCC mice treated with *T cruzi*'s own beneficial factor, PDNF, circumvents the need for cell therapy by directly activating or "jumpstarting" resident cardiac stem/progenitor cells. IV sPDNF bypasses the main hurdles to achieving benefit from stem cell therapy, which include poorly defined cell populations, quality control in cell processing, and limited efficiency in cell delivery (Behfar et al., 2014).

T cruzi/PDNF activates the expression of MCP-1 and FKN chemokines through activation of TrkA and TrkC during the acute phase. *T cruzi*/PDNF and chemokines contribute to the activation of resident CPCs that secrete anti-inflammatory TSG-6, which subdues inflammation (blue box, Figure 7.2). In the chronic phase, the increased amount of CPCs previously activated in the acute phase persist in the heart, but, because of the lack of *T cruzi*/PDNF in the heart during this phase, are less likely to activate anti-inflammatory responses. Defunct CPCs are exemplified by characteristics of decreased cell growth and TSG-6 secretion, and increased susceptibility to oxidative stress (red box, Figure 7.2). Chronic cardiac inflammation and oxidative stress would contribute to hearts becoming fibrotic. Replenishing the heart with IV sPDNF rescues CPC deficits, and activates them to produce TSG-6, which in turn have long-lasting effects on decreasing cardiac inflammation and preventing the progression of cardiac fibrosis (purple box, Figure 7.2). Further physiological and functional studies on

the condition of the CCC heart during IV sPDNF treatment in real-time would provide further insight into tissue repair mechanisms.

Therefore, the results presented in this thesis demonstrate PDNF activation of TrkA and TrkC links novel neurotrophic interactions between *T cruzi* and CPCs, which can be exploited to activate anti-inflammatory responses that contribute to tissue repair mechanisms in chronic Chagas disease. It is not surprising that *T cruzi* harbors such a beneficial factor, which likely contributes to making it a successful pathogen in establishing chronic infection in its host. Indeed, growing evidence of the interplay between neural reflexes with controlling inflammation, and vice versa (Andersson and Tracey, 2012), highlights intriguing links between the nervous and immune systems. The potential therapeutic use of PDNF parallels therapies targeting the neurotrophic Trk pathway to treat neurodegenerative disorders like Alzheimer's and Huntington's disease, but also has the potential to be applied to inflammatory disorders in which a neurotrophic component has not been previously linked or described.

We sometimes forget that the qualities that make pathogens pathogenic are not always negative. By trying to understand the host-pathogen interactions of *T cruzi*, we learned of mutually beneficial effects of the PDNF-Trk interaction during various phases of Chagas disease, enough so, that we were able to implement this knowledge to ameliorate features of disease. Throughout my time here at Tufts, *T cruzi* has found a place in my own heart, metaphorically speaking of course.

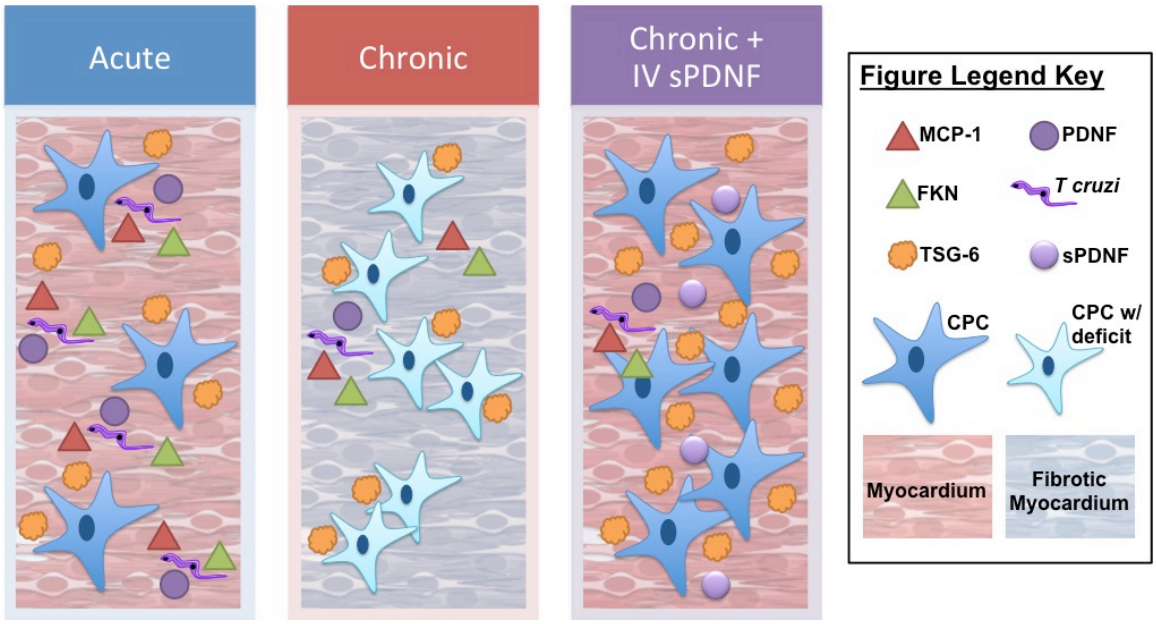

Figure 7.2. A model of *T cruzi*/PDNF interaction with CPCs in the myocardium.

During the acute phase, *T cruzi*/PDNF is readily available and contributes to the induction of chemokines such as MCP-1 and FKN. Chemokine signaling recruits immune cells to the heart and helps control cardiac parasitism. Concomitantly, chemokines as well as PDNF can help to activate tissue resident CPCs that help to subdue inflammatory responses through the secretion of anti-inflammatory TSG-6 (blue box). During the chronic phase, *T cruzi*/PDNF levels are low in the heart and chronic exposure to inflammation likely contributes to subsequent fibrotic processes. CPCs present during the chronic phase of infection are deficient in growth/expansion, TSG-6 secretion, and resistance to oxidative stress (red box). To circumvent these deficits, administration of IV sPDNF would rescue basal TSG-6 secretion of CPCs, and contribute to long-lasting increased systemic TSG-6 serum levels, contributing to decreased cardiac inflammation and fibrosis (purple box).

REFERENCES

Akpan, N., Caradonna, K., Chuenkova, M.V., PereiraPerrin, M., 2008. Chagas' disease parasite-derived neurotrophic factor activates cholinergic gene expression in neuronal PC12 cells. Brain Res 1217, 195–202.

Alves, M.J., Abuin, G., Kuwajima, V.Y., Colli, W., 1986. Partial inhibition of trypomastigote entry into cultured mammalian cells by monoclonal antibodies against a surface glycoprotein of Trypanosoma cruzi. Mol. Biochem. Parasitol. 21, 75–82.

Andersson, U., Tracey, K.J., 2012. Neural reflexes in inflammation and immunity. J. Exp. Med. 209, 1057–1068.

Andrade, A.L.S.S., Martelli, C.M.T., Oliveira, R.M., Silva, S.A., Aires, A.I.S., Soussumi, L.M.T., Covas, D.T., Silva, L.S., Andrade, J.G., Travassos, L.R., Almeida, I.C., 2004. Short Report: Benznidazole Efficacy Among Trypanosoma Cruzi-Infected Adolescents After a Six-Year Follow-Up. Am. J. Trop. Med. Hyg. 71, 594–597.

Andrade, L.O., Andrews, N.W., 2005. The Trypanosoma cruzi-host-cell interplay: location, invasion, retention. Nat Rev Microbiol 3, 819–23.

Araújo, A., Jansen, A.M., Reinhard, K., Ferreira, L.F., 2009. Paleoparasitology of Chagas disease: a review. Mem. Inst. Oswaldo Cruz 104, 9–16.

Aridgides, D., Salvador, R., PereiraPerrin, M., 2013a. Trypanosoma cruzi highjacks TrkC to enter cardiomyocytes and cardiac fibroblasts while exploiting TrkA for cardioprotection against oxidative stress. Cell. Microbiol. 15, 1357–1366.

Aridgides, D., Salvador, R., PereiraPerrin, M., 2013b. Trypanosoma cruzi Coaxes Cardiac Fibroblasts into Preventing Cardiomyocyte Death by Activating Nerve Growth Factor Receptor TrkA. PLoS ONE 8, e57450.

Aukrust, P., Ueland, T., Müller, F., Andreassen, A.K., Nordøy, I., Aas, H., Kjekshus, J., Simonsen, S., Frøland, S.S., Gullestad, L., 1998. Elevated Circulating Levels of C-C Chemokines in Patients With Congestive Heart Failure. Circulation 97, 1136–1143.

Behfar, A., Crespo-Diaz, R., Terzic, A., Gersh, B.J., 2014. Cell therapy for cardiac repair—lessons from clinical trials. Nat. Rev. Cardiol. 11, 232–246.

Bern, C., Kjos, S., Yabsley, M.J., Montgomery, S.P., 2011. Trypanosoma cruzi and Chagas' Disease in the United States. Clin. Microbiol. Rev. 24, 655–681.

Bern, C., Montgomery, S.P., 2009. An Estimate of the Burden of Chagas Disease in the United States. Clin. Infect. Dis. 49, e52–e54.

Bernstein, H.S., Srivastava, D., 2012. Stem cell therapy for cardiac disease. Pediatr. Res. 71, 491–499.

Bestetti, R.B., Couto, L.B., Cardinalli-Neto, A., 2013. When a misperception favors a tragedy: Carlos Chagas and the Nobel Prize of 1921. Int. J. Cardiol. 169, 327–330.

Bestetti, R.B., Martins, C.A., Cardinalli-Neto, A., 2009. Justice where justice is due: A posthumous Nobel Prize to Carlos Chagas (1879–1934), the discoverer of American Trypanosomiasis (Chagas' disease). Int. J. Cardiol. 134, 9–16.

Bevilacqua, M.P., Nelson, R.M., 1993. Selectins. J. Clin. Invest. 91, 379–387.

Borda, E.S., Sterin-Borda, L., 1996. Antiadrenergic and muscarinic receptor antibodies in Chagas' cardiomyopathy. Int. J. Cardiol. 54, 149–156.

Boring, L., Gosling, J., Cleary, M., Charo, I.F., 1998. Decreased lesion formation in CCR2|[minus]|/|[minus]| mice reveals a role for chemokines in the initiation of atherosclerosis. Nature 394, 894–897.

Boscardin, S.B., Torrecilhas, A.C.T., Manarin, R., Revelli, S., Rey, E.G., Tonelli, R.R., Silber, A.M., 2010. Chagas' disease: an update on immune mechanisms and therapeutic strategies. J. Cell. Mol. Med. 14, 1373–1384.

Braunwald, E., 2013. Heart Failure. JACC Heart Fail. 1, 1–20.

Brener, Z., 1973. Biology of Trypanosoma cruzi. Annu Rev Microbiol 27, 347–82.

Buschiazzo, A., Amaya, M.F., Cremona, M.L., Frasch, A.C., Alzari, P.M., 2002. The Crystal Structure and Mode of Action of Trans-Sialidase, a Key Enzyme in Trypanosoma cruzi Pathogenesis. Mol. Cell 10, 757–768.

Cantarella, G., Lempereur, L., Presta, M., Ribatti, D., Lombardo, G., Lazarovici, P., Zappalà, G., Pafumi, C., Bernardini, R., 2002. Nerve growth factor-endothelial cell interaction leads to angiogenesis in vitro and in vivo. FASEB J.

Caporali, A., Emanueli, C., 2009. Cardiovascular Actions of Neurotrophins. Physiol. Rev. 89, 279–308.

Caporali, A., Sala-Newby, G.B., Meloni, M., Graiani, G., Pani, E., Cristofaro, B., Newby, A.C., Madeddu, P., Emanueli, C., 2007. Identification of the prosurvival activity of nerve growth factor on cardiac myocytes. Cell Death Differ. 15, 299–311.

Caradonna, K., Pereiraperrin, M., 2009. Preferential brain homing following intranasal administration of Trypanosoma cruzi. Infect Immun 77, 1349–56.

Chagas, C., 1909a. Neue Trypanosomen: Vorläufige mitteilung. Arch. Für Schiffs- Trop.-Hyg. Leipz. 13, 120–122.

Chagas, C., 1909b. Nova espécie mórbida do homem, produzida por um tripanossoma (trypanosoma Cruzi) (Nota prévia). Braz. Méd. 23, 161.

Chagas, C., 1909c. Nova tripanozomiaze humana: estudos sobre a morfolojia e o ciclo evolutivo do Schizotrypanum cruzi n. gen., n. sp., ajente etiolojico de nova entidade morbida do homem. Mem. Inst. Oswaldo Cruz 1, 159–218.

Chagas, C., 1910. Nova entidade morbida do homem., Rio de Janeiro. Braz.-Medico 24, 423–428, 433–437, 443–447.

Chen, C.-Z., Li, L., Li, M., Lodish, H.F., 2003. The EndoglinPositive Sca-1Positive RhodamineLow Phenotype Defines a Near-Homogeneous Population of Long-Term Repopulating Hematopoietic Stem Cells. Immunity 19, 525–533.

Choi, H., Lee, R.H., Bazhanov, N., Oh, J.Y., Prockop, D.J., 2011. Anti-inflammatory protein TSG-6 secreted by activated MSCs attenuates zymosan-induced mouse peritonitis by decreasing TLR2/NF-κB signaling in resident macrophages. Blood 118, 330–338.

Chong, J.J.H., Chandrakanthan, V., Xaymardan, M., Asli, N.S., Li, J., Ahmed, I., Heffernan, C., Menon, M.K., Scarlett, C.J., Rashidianfar, A., Biben, C., Zoellner, H., Colvin, E.K., Pimanda, J.E., Biankin, A.V., Zhou, B., Pu, W.T., Prall, O.W.J., Harvey, R.P., 2011. Adult Cardiac-Resident MSC-like Stem Cells with a Proepicardial Origin. Cell Stem Cell 9, 527–540.

Chuenkova, M., Pereira, M., Taylor, G., 1999. trans-sialidase of Trypanosoma cruzi: location of galactose-binding site(s). Biochem Biophys Res Commun 262, 549–56.

Chuenkova, M.V., Pereira, M.A., 2000. A trypanosomal protein synergizes with the cytokines ciliary neurotrophic factor and leukemia inhibitory factor to prevent apoptosis of neuronal cells. Mol Biol Cell 11, 1487–98.

Chuenkova, M.V., PereiraPerrin, M., 2004. Chagas' disease parasite promotes neuron survival and differentiation through TrkA nerve growth factor receptor. J Neurochem 91, 385–94.

Chuenkova, M.V., PereiraPerrin, M., 2005. A synthetic peptide modeled on PDNF, Chagas' disease parasite neurotrophic factor, promotes survival and differentiation of neuronal cells through TrkA receptor. Biochemistry (Mosc.) 44, 15685–94.

Chuenkova, M.V., PereiraPerrin, M., 2006. Enhancement of tyrosine hydroxylase expression and activity by Trypanosoma cruzi parasite-derived neurotrophic factor. Brain Res. 1099, 167–175.

Chuenkova, M.V., PereiraPerrin, M., 2009. Trypanosoma cruzi Targets Akt in Host Cells as an Intracellular Antiapoptotic Strategy. Sci. Signal. 2, ra74.

Coelho, P.S., Klein, A., Talvani, A., Coutinho, S.F., Takeuchi, O., Akira, S., Silva, J.S., Canizzaro, H., Gazzinelli, R.T., Teixeira, M.M., 2002. Glycosylphosphatidylinositol-anchored mucin-like glycoproteins isolated from Trypanosoma cruzi trypomastigotes induce in vivo leukocyte recruitment dependent on MCP-1 production by IFN-gamma-primed-macrophages. J Leukoc Biol 71, 837–44.

Cohen, S., Levi-Montalcini, R., Hamburger, V., 1954. A NERVE GROWTH-STIMULATING FACTOR ISOLATED FROM SARCOM AS 37 AND 180*. Proc. Natl. Acad. Sci. U. S. A. 40, 1014–1018.

Colli, W., 1993. Trans-sialidase: a unique enzyme activity discovered in the protozoan Trypanosoma cruzi. FASEB J. Off. Publ. Fed. Am. Soc. Exp. Biol. 7, 1257–1264.

Copley, R.R., Russell, R.B., Ponting, C.P., 2001. Sialidase-like Asp-boxes: Sequence-similar structures within different protein folds. Protein Sci. 10, 285–292.

Coppola, V., Barrick, C.A., Southon, E.A., Celeste, A., Wang, K., Chen, B., Haddad, E.-B., Yin, J., Nussenzweig, A., Subramaniam, A., Tessarollo, L., 2004. Ablation of TrkA function in the immune system causes B cell abnormalities. Development 131, 5185–5195.

Costa, S.C.G. da, 1999. Mouse as a model for Chagas disease: does mouse represent a good model for Chagas disease? Mem. Inst. Oswaldo Cruz 94, 269–272.

Costantini, C., Scrable, H., Puglielli, L., 2006. An aging pathway controls the TrkA to p75NTR receptor switch and amyloid β-peptide generation. EMBO J. 25, 1997–2006.

Coura, J.R., 2009. Present situation and new strategies for Chagas disease chemotherapy: a proposal. Mem. Inst. Oswaldo Cruz 104, 549–554.

Coura, J.R., Borges-Pereira, J., 2011. Chronic phase of Chagas disease: why should it be treated? A comprehensive review. Mem. Inst. Oswaldo Cruz 106, 641–645.

Coura, J.R., Borges-Pereira, J., 2012. Chagas disease: What is known and what should be improved: a systemic review. Rev. Soc. Bras. Med. Trop. 45, 286–296.

Coura, J.R., Castro, S.L. de, 2002. A Critical Review on Chagas Disease Chemotherapy. Mem. Inst. Oswaldo Cruz 97, 3–24.

Coura, J.R., Dias, J.C.P., 2009. Epidemiology, control and surveillance of Chagas disease: 100 years after its discovery. Mem. Inst. Oswaldo Cruz 104, 31–40.

Crowell, R.L., 1986. Virus attachment and entry into cells: proceedings of an ASM conference held in Philadelphia, Pennsylvania, 10-13 April 1985. American Society for Microbiology.

Cummings, K.L., Tarleton, R.L., 2003. Rapid quantitation of Trypanosoma cruzi in host tissue by real-time PCR. Mol Biochem Parasitol 129, 53–9.

Davila, D.F., Donis, J.H., Torres, A., Ferrer, J.A., 2004. A modified and unifying neurogenic hypothesis can explain the natural history of chronic Chagas heart disease. Int J Cardiol 96, 191–5.

De Carvalho, K.A.T., Abdelwahid, E., Ferreira, R.J., Irioda, A.C., Guarita-Souza, L.C., 2013. Preclinical stem cell therapy in Chagas Disease: Perspectives for future research. World J. Transplant. 3, 119–126.

De Melo-Jorge, M., PereiraPerrin, M., 2007. The Chagas' disease parasite Trypanosoma cruzi exploits nerve growth factor receptor TrkA to infect mammalian hosts. Cell Host Microbe 1, 251–61.

De Souza, W., de Carvalho, T.M.U., Barrias, E.S., 2010. Review on *Trypanosoma cruzi*: Host Cell Interaction. Int. J. Cell Biol. 2010, e295394.

Dias, J.C.P., Silveira, A.C., Schofield, C.J., 2002. The impact of Chagas disease control in Latin America: a review. Mem. Inst. Oswaldo Cruz 97, 603–612.

Donovan, M.J., Hahn, R., Tessarollo, L., Hempstead, B.L., 1996. Identification of an essential nonneuronal function of neurotrophin 3 in mammalian cardiac development. Nat. Genet. 14, 210–213.

El-Sayed, N.M., Myler, P.J., Bartholomeu, D.C., Nilsson, D., Aggarwal, G., Tran, A.-N., Ghedin, E., Worthey, E.A., Delcher, A.L., Blandin, G., Westenberger, S.J., Caler, E., Cerqueira, G.C., Branche, C., Haas, B., Anupama, A., Arner, E., Åslund, L., Attipoe, P., Bontempi, E., Bringaud, F., Burton, P., Cadag, E., Campbell, D.A., Carrington, M., Crabtree, J., Darban, H., Silveira, J.F. da, Jong, P. de, Edwards, K., Englund, P.T., Fazelina, G., Feldblyum, T., Ferella, M., Frasch, A.C., Gull, K., Horn, D., Hou, L., Huang, Y., Kindlund, E., Klingbeil, M., Kluge, S., Koo, H., Lacerda, D., Levin, M.J., Lorenzi, H., Louie, T., Machado, C.R., McCulloch, R., McKenna, A., Mizuno, Y., Mottram, J.C., Nelson, S., Ochaya, S., Osoegawa, K., Pai, G., Parsons, M., Pentony, M., Pettersson, U., Pop, M., Ramirez, J.L., Rinta, J., Robertson, L., Salzberg, S.L., Sanchez, D.O., Seyler, A., Sharma, R., Shetty, J., Simpson, A.J., Sisk, E., Tammi, M.T., Tarleton, R., Teixeira, S., Aken, S.V., Vogt, C., Ward, P.N., Wickstead, B., Wortman, J., White, O., Fraser, C.M., Stuart, K.D., Andersson, B., 2005. The Genome Sequence of Trypanosoma cruzi, Etiologic Agent of Chagas Disease. Science 309, 409–415.

El-Sayed, N.M., Myler, P.J., Blandin, G., Berriman, M., Crabtree, J., Aggarwal, G., Caler, E., Renauld, H., Worthey, E.A., Hertz-Fowler, C., Ghedin, E., Peacock, C., Bartholomeu, D.C., Haas, B.J., Tran, A.N., Wortman, J.R., Alsmark, U.C., Angiuoli, S., Anupama, A., Badger, J., Bringaud, F., Cadag, E., Carlton, J.M., Cerqueira, G.C., Creasy, T., Delcher, A.L., Djikeng, A., Embley, T.M., Hauser, C., Ivens, A.C., Kummerfeld, S.K., Pereira-Leal, J.B., Nilsson, D., Peterson, J., Salzberg, S.L., Shallom, J., Silva, J.C., Sundaram, J., Westenberger, S., White, O., Melville, S.E., Donelson, J.E., Andersson, B., Stuart, K.D., Hall, N., 2005. Comparative genomics of trypanosomatid parasitic protozoa. Science 309, 404–9.

Estani, S.S., Segura, E.L., Ruiz, A.M., Velazquez, E., Porcel, B.M., Yampotis, C., 1998. Efficacy of chemotherapy with benznidazole in children in the indeterminate phase of Chagas' disease. Am. J. Trop. Med. Hyg. 59, 526–529.

Faillard, H., 1989. The early history of sialic acids. Trends Biochem. Sci. 14, 237–241.

Feizi, T., 1991. Carbohydrate differentiation antigens: probable ligands for cell adhesion molecules. Trends Biochem. Sci. 16, 84–86.

Fenderson, B.A., Eddy, E.M., Hakomori, S.-I., 1990. Glycoconjugate expression during embryogenesis and its biological significance. BioEssays 12, 173–179.

Feng, P., Liau, G., 1993. Identification of a novel serum and growth factor-inducible gene in vascular smooth muscle cells. J. Biol. Chem. 268, 9387–9392.

Fortress, A.M., Buhusi, M., Helke, K.L., Granholm, A.-C.E., 2011. Cholinergic Degeneration and Alterations in the TrkA and p75NTR Balance as a Result of Pro-NGF Injection into Aged Rats. J. Aging Res. 2011, e460543.

Frangogiannis, N.G., 2014. The inflammatory response in myocardial injury, repair, and remodelling. Nat. Rev. Cardiol. 11, 255–265.

Fujiyoshi, M., Ozaki, M., 2011. Molecular mechanisms of liver regeneration and protection for treatment of liver dysfunction and diseases. J. Hepato-Biliary-Pancreat. Sci. 18, 13–22.

Fukuda, M., 1991. Cell Surface Carbohydrates and Cell Development. CRC Press.

Fuse, K., Kodama, M., Hanawa, H., Okura, Y., Ito, M., Shiono, T., Maruyama, S., Hirono, S., Kato, K., Watanabe, K., Aizawa, Y., 2001. Enhanced expression and production of monocyte chemoattractant protein-1 in myocarditis. Clin. Exp. Immunol. 124, 346–352.

Gao, J., Dennis, J.E., Muzic, R.F., Lundberg, M., Caplan, A.I., 2001. The dynamic in vivo distribution of bone marrow-derived mesenchymal stem cells after infusion. Cells Tissues Organs 169, 12–20.

Gao, W., Wortis, H.H., Pereira, M.A., 2002. The Trypanosoma cruzi trans-sialidase is a T cell-independent B cell mitogen and an inducer of non-specific Ig secretion. Int. Immunol. 14, 299–308.

Garcia, S., Ramos, C.O., Senra, J.F.V., Vilas-Boas, F., Rodrigues, M.M., Campos-de-Carvalho, A.C., Ribeiro-dos-Santos, R., Soares, M.B.P., 2005. Treatment with Benznidazole during the Chronic Phase of Experimental Chagas' Disease Decreases Cardiac Alterations. Antimicrob. Agents Chemother. 49, 1521–1528.

Giordano, R., Fouts, D.L., Tewari, D., Colli, W., Manning, J.E., Alves, M.J.M., 1999. Cloning of a Surface Membrane Glycoprotein Specific for the Infective Form of Trypanosoma cruzi Having Adhesive Properties to Laminin. J. Biol. Chem. 274, 3461–3468.

Glant, T.T., Kamath, R.V., Bárdos, T., Gál, I., Szántó, S., Murad, Y.M., Sandy, J.D., Mort, J.S., Roughley, P.J., Mikecz, K., 2002. Cartilage-specific constitutive expression of TSG-6 protein (product of tumor necrosis factor α–stimulated gene 6) provides a chondroprotective, but not antiinflammatory, effect in antigen-induced arthritis. Arthritis Rheum. 46, 2207–2218.

Goldenberg, R.C.S., Jelicks, L.A., Fortes, F.S.A., Weiss, L.M., Rocha, L.L., Zhao, D., Carvalho, A.C. de, Spray, D.C., Tanowitz, H.B., 2008. Bone Marrow Cell Therapy Ameliorates and Reverses Chagasic Cardiomyopathy in a Mouse Model. J. Infect. Dis. 197, 544–547.

Gottlieb, R.A., 2011. Cell Death Pathways in Acute I/R Injury. J. Cardiovasc. Pharmacol. Ther. 16, 233–238.

Green, S.R., Han, K.H., Chen, Y., Almazan, F., Charo, I.F., Miller, Y.I., Quehenberger, O., 2006. The CC chemokine MCP-1 stimulates surface expression of CX3CR1 and enhances the adhesion of monocytes to fractalkine/CX3CL1 via p38 MAPK. J Immunol 176, 7412–20.

Guo, P., Zhang, S.-Z., He, H., Zhu, Y.-T., Tseng, S.C.G., 2012. TSG-6 Controls Transcription and Activation of Matrix Metalloproteinase 1 in Conjunctivochalasis. Invest. Ophthalmol. Vis. Sci. 53, 1372–1380.

Gupta, S., Wen, J.-J., Garg, N.J., 2009. Oxidative Stress in Chagas Disease. Interdiscip. Perspect. Infect. Dis. 2009, e190354.

Hamilton, P.B., Teixeira, M.M.G., Stevens, J.R., 2012. The evolution of Trypanosoma cruzi: the “bat seeding” hypothesis. Trends Parasitol. 28, 136–141.

Hardison, J.L., Kuziel, W.A., Manning, J.E., Lane, T.E., 2006. Chemokine CC receptor 2 is important for acute control of cardiac parasitism but does not contribute to cardiac inflammation after infection with Trypanosoma cruzi. J Infect Dis 193, 1584–8.

Hempstead, B.L., Martin-Zanca, D., Kaplan, D.R., Parada, L.F., Chao, M.V., 1991. High-affinity NGF binding requires coexpression of the trk proto-oncogene and the low-affinity NGF receptor. Nature 350, 678–683.

Hempstead, B.L., Schleifer, L.S., Chao, M.V., 1989. Expression of functional nerve growth factor receptors after gene transfer. Science 243, 373–375.

Hertz, L., Peng, L., Lai, J.C., 1998. Functional studies in cultured astrocytes. Methods San Diego Calif 16, 293–310.

Higuchi, M. de L., 1999. Human chronic chagasic cardiopathy: participation of parasite antigens, subsets of lymphocytes, cytokines and microvascular abnormalities. Mem. Inst. Oswaldo Cruz 94, 263–267.

Higuchi, M. de L., Benvenuti, L.A., Reis, M.M., Metzger, M., 2003. Pathophysiology of the heart in Chagas' disease: current status and new developments. Cardiovasc. Res. 60, 96–107.

Hoff, R., Teixeira, R.S., Carvalho, J.S., Mott, K.E., 1978. Trypanosoma cruzi in the cerebrospinal fluid during the acute stage of Chagas' disease. N Engl J Med 298, 604–6.

Hotez, P.J., Dumonteil, E., Woc-Colburn, L., Serpa, J.A., Bezek, S., Edwards, M.S., Hallmark, C.J., Musselwhite, L.W., Flink, B.J., Bottazzi, M.E., 2012. Chagas Disease: "The New HIV/AIDS of the Americas." PLoS Negl Trop Dis 6, e1498.

Huang, C., Gu, H., Yu, Q., Manukyan, M.C., Poynter, J.A., Wang, M., 2011. Sca-1+ Cardiac Stem Cells Mediate Acute Cardioprotection via Paracrine Factor SDF-1 following Myocardial Ischemia/Reperfusion. PLoS ONE 6, e29246.

Huang, E.J., Reichardt, L.F., 2003. Trk receptors: roles in neuronal signal transduction. Annu Rev Biochem 72, 609–42.

Ieda, M., Kanazawa, H., Ieda, Y., Kimura, K., Matsumura, K., Tomita, Y., Yagi, T., Onizuka, T., Shimoji, K., Ogawa, S., Makino, S., Sano, M., Fukuda, K., 2006. Nerve Growth Factor Is Critical for Cardiac Sensory Innervation and Rescues Neuropathy in Diabetic Hearts. Circulation 114, 2351–2363.

Indo, Y., 2001. Molecular basis of congenital insensitivity to pain with anhidrosis (CIPA): Mutations and polymorphisms in TRKA (NTRK1) gene encoding the receptor tyrosine kinase for nerve growth factor. Hum. Mutat. 18, 462–471.

Ishiyama, S., Hiroe, M., Nishikawa, T., Abe, S., Shimojo, T., Ito, H., Ozasa, S., Yamakawa, K., Matsuzaki, M., Mohammed, M.U., Nakazawa, H., Kasajima, T., Marumo, F., 1997. Nitric Oxide Contributes to the Progression of Myocardial Damage in Experimental Autoimmune Myocarditis in Rats. Circulation 95, 489–496.

Itzhaki-Alfia, A., Leor, J., Raanani, E., Sternik, L., Spiegelstein, D., Netser, S., Holbova, R., Pevsner-Fischer, M., Lavee, J., Barbash, I.M., 2009. Patient Characteristics and Cell Source Determine the Number of Isolated Human Cardiac Progenitor Cells. Circulation 120, 2559–2566.

Jacoby, J.J., Kalinowski, A., Liu, M.-G., Zhang, S.S.-M., Gao, Q., Chai, G.-X., Ji, L., Iwamoto, Y., Li, E., Schneider, M., Russell, K.S., Fu, X.-Y., 2003. Cardiomyocyte-restricted knockout of STAT3 results in higher sensitivity to inflammation, cardiac fibrosis, and heart failure with advanced age. Proc. Natl. Acad. Sci. 100, 12929–12934.

Jelicks, L.A., Koba, W., Tanowitz, H.B., Mendez-Otero, R., Campos de Carvalho, A.C., Spray, D.C., 2012. Mesenchymal Bone Marrow Cell Therapy in a Mouse Model of Chagas Disease. Where Do the Cells Go? PLoS Negl Trop Dis 6, e1971.

Kawaguchi-Manabe, H., Ieda, M., Kimura, K., Manabe, T., Miyatake, S., Kanazawa, H., Kawakami, T., Ogawa, S., Suematsu, M., Fukuda, K., 2007. A novel cardiac hypertrophic factor, neurotrophin-3, is paradoxically downregulated in cardiac hypertrophy. Life Sci. 81, 385–392.

Kawai, T., Akira, S., 2007. TLR signaling. Semin. Immunol., TLR-mediated Innate Immune Recognition 19, 24–32.

Klein, R., Parada, L.F., Coulier, F., Barbacid, M., 1989. trkB, a novel tyrosine protein kinase receptor expressed during mouse neural development. EMBO J. 8, 3701–3709.

Knüsel, B., Kaplan, D.R., Winslow, J.W., Rosenthal, A., Burton, L.E., Beck, K.D., Rabin, S., Nikolics, K., Hefti, F., 1992. K-252b Selectively Potentiates Cellular Actions and trk Tyrosine Phosphorylation Mediated by Neurotrophin-3. J. Neurochem. 59, 715–722.

Koberle, F., 1968. Chagas' disease and Chagas' syndromes: the pathology of American trypanosomiasis. Adv Parasitol 6, 63–116.

Krause, D.S., 2002. Plasticity of marrow-derived stem cells. Publ. Online 16 May 2002 Doi101038sjgt3301760 9.

Kroll-Palhares, K., Silverio, J.C., da Silva, A.A., Michailowsky, V., Marino, A.P., Silva, N.M., Carvalho, C.M., Pinto, L.M., Gazzinelli, R.T., Lannes-Vieira, J., 2008. TNF/TNFR1 signaling up-regulates CCR5 expression by CD8+ T lymphocytes and promotes heart tissue damage during Trypanosoma cruzi infection: beneficial effects of TNF-alpha blockade. Mem Inst Oswaldo Cruz 103, 375–85.

Kropf, S.P., Sá, M.R., 2009. The discovery of Trypanosoma cruzi and Chagas disease (1908-1909): tropical medicine in Brazil. História Ciênc. Saúde-Manguinhos 16, 13–34.

Labovsky, V., Smulski, C.R., Gómez, K., Levy, G., Levin, M.J., 2007. Anti-β1-adrenergic receptor autoantibodies in patients with chronic Chagas heart disease. Clin. Exp. Immunol. 148, 440–449.

Lamballe, F., Klein, R., Barbacid, M., 1991. trkC, a new member of the trk family of tyrosine protein kinases, is a receptor for neurotrophin-3. Cell 66, 967–979.

Lee, R.H., Pulin, A.A., Seo, M.J., Kota, D.J., Ylostalo, J., Larson, B.L., Semprun-Prieto, L., Delafontaine, P., Prockop, D.J., 2009. Intravenous hMSCs Improve Myocardial Infarction in Mice because Cells Embolized in Lung Are Activated to Secrete the Anti-inflammatory Protein TSG-6. Cell Stem Cell 5, 54–63.

Lefer, D.J., Granger, D.N., 2000. Oxidative stress and cardiac disease. Am. J. Med. 109, 315–323.

Lehmann, M.H., Kühnert, H., Müller, S., Sigusch, H.H., 1998. MONOCYTE CHEMOATTRACTANT PROTEIN 1 (MCP-1) GENE EXPRESSION IN DILATED CARDIOMYOPATHY. Cytokine 10, 739–746.

Leri, A., 2009. Human Cardiac Stem Cells The Heart of a Truth. Circulation 120, 2515–2518.

Lesley, J., Gál, I., Mahoney, D.J., Cordell, M.R., Rugg, M.S., Hyman, R., Day, A.J., Mikecz, K., 2004. TSG-6 Modulates the Interaction between Hyaluronan and Cell Surface CD44. J. Biol. Chem. 279, 25745–25754.

Levi-Montalcini, R., 1952. Effects of Mouse Tumor Transplantation on the Nervous System. Ann. N. Y. Acad. Sci. 55, 330–344.

Levi-Montalcini, R., 1987. The nerve growth factor: thirty-five years later. EMBO J. 6, 1145–1154.

Levi-Montalcini, R., Hamburger, V., 1951. Selective growth stimulating effects of mouse sarcoma on the sensory and sympathetic nervous system of the chick embryo. J. Exp. Zool. 116, 321–361.

Levi-Montalcini, R., Meyer, H., Hamburger, V., 1954. In Vitro Experiments on the Effects of Mouse Sarcomas 180 and 37 on the Spinal and Sympathetic Ganglia of the Chick Embryo. Cancer Res. 14, 49–57.

Lin, M.I., Das, I., Schwartz, G.M., Tsoulfas, P., Mikawa, T., Hempstead, B.L., 2000. Trk C Receptor Signaling Regulates Cardiac Myocyte Proliferation during Early Heart Development in Vivo. Dev. Biol. 226, 180–191.

Livak, K.J., Schmittgen, T.D., 2001. Analysis of Relative Gene Expression Data Using Real-Time Quantitative PCR and the 2−ΔΔCT Method. Methods 25, 402–408.

Li, Y., Zhang, C., Xiong, F., Yu, M., Peng, F., Shang, Y., Zhao, C., Xu, Y., Liu, Z., Zhou, C., Wu, J., 2008. Comparative study of mesenchymal stem cells from C57BL/10 and mdx mice. BMC Cell Biol. 9, 24.

Lu, B., Petrola, Z., Luquetti, A.O., PereiraPerrin, M., 2008. Auto-antibodies to Receptor Tyrosine Kinases TrkA, TrkB and TrkC in Patients with Chronic Chagas' Disease. Scand. J. Immunol. 67, 603–609.

Machado, F.S., Martins, G.A., Aliberti, J.C.S., Mestriner, F.L.A.C., Cunha, F.Q., Silva, J.S., 2000. Trypanosoma cruzi–Infected Cardiomyocytes Produce Chemokines and Cytokines That Trigger Potent Nitric Oxide–Dependent Trypanocidal Activity. Circulation 102, 3003–3008.

Magdesian, M.H., Tonelli, R.R., Fessel, M.R., Silveira, M.S., Schumacher, R.I., Linden, R., Colli, W., Alves, M.J., 2007. A conserved domain of the gp85/trans-sialidase family activates host cell extracellular signal-regulated kinase and facilitates Trypanosoma cruzi infection. Exp Cell Res 313, 210–8.

Marino, A.P.M.P., Silva, A. da, Santos, P. dos, Pinto, L.M. de O., Gazzinelli, R.T., Teixeira, M.M., Lannes-Vieira, J., 2004. Regulated on Activation, Normal T Cell Expressed and Secreted (RANTES) Antagonist (Met-RANTES) Controls the Early Phase of Trypanosoma cruzi–Elicited Myocarditis. Circulation 110, 1443–1449.

Martire, A., Fernandez, B., Buehler, A., Strohm, C., Schaper, J., Zimmermann, R., Kolattukudy, P.E., Schaper, W., 2003. Cardiac overexpression of monocyte chemoattractant protein-1 in transgenic mice mimics ischemic preconditioning through SAPK/JNK1/2 activation. Cardiovasc. Res. 57, 523–534.

Masaki, T., Qu, J., Cholewa-Waclaw, J., Burr, K., Raaum, R., Rambukkana, A., 2013. Reprogramming Adult Schwann Cells to Stem Cell-like Cells by Leprosy Bacilli Promotes Dissemination of Infection. Cell 152, 51–67.

Matsumori, A., Furukawa, Y., Hashimoto, T., Yoshida, A., Ono, K., Shioi, T., Okada, M., Iwasaki, A., Nishio, R., Matsushima, K., Sasayama, S., 1997. Plasma Levels of the Monocyte Chemotactic and Activating

Factor/Monocyte Chemoattractant Protein-1 are Elevated in Patients with Acute Myocardial Infarction. J. Mol. Cell. Cardiol. 29, 419–423.

Matsuura, K., Nagai, T., Nishigaki, N., Oyama, T., Nishi, J., Wada, H., Sano, M., Toko, H., Akazawa, H., Sato, T., Nakaya, H., Kasanuki, H., Komuro, I., 2004. Adult Cardiac Sca-1-positive Cells Differentiate into Beating Cardiomyocytes. J. Biol. Chem. 279, 11384–11391.

Meloni, M., Caporali, A., Graiani, G., Lagrasta, C., Katare, R., Linthout, S.V., Spillmann, F., Campesi, I., Madeddu, P., Quaini, F., Emanueli, C., 2010. Nerve Growth Factor Promotes Cardiac Repair following Myocardial Infarction. Circ. Res. 106, 1275–1284.

Meloni, M., Descamps, B., Caporali, A., Zentilin, L., Floris, I., Giacca, M., Emanueli, C., 2012. Nerve Growth Factor Gene Therapy Using Adeno-Associated Viral Vectors Prevents Cardiomyopathy in Type 1 Diabetic Mice. Diabetes 61, 229–240.

Michailowsky, V., Silva, N.M., Rocha, C.D., Vieira, L.Q., Lannes-Vieira, J., Gazzinelli, R.T., 2001. Pivotal role of interleukin-12 and interferon-gamma axis in controlling tissue parasitism and inflammation in the heart and central nervous system during Trypanosoma cruzi infection. Am J Pathol 159, 1723–33.

Milner, C.M., Day, A.J., 2003. TSG-6: a multifunctional protein associated with inflammation. J. Cell Sci. 116, 1863–1873.

Mirotsou, M., Jayawardena, T.M., Schmeckpeper, J., Gnecchi, M., Dzau, V.J., 2011. Paracrine mechanisms of stem cell reparative and regenerative actions in the heart. J. Mol. Cell. Cardiol., Special Issue: Cardiovascular Stem Cells Revisited 50, 280–289.

Montgomery, S.P., Starr, M.C., Cantey, P.T., Edwards, M.S., Meymandi, S.K., 2014. Neglected Parasitic Infections in the United States: Chagas Disease. Am. J. Trop. Med. Hyg. 90, 814–818.

Morimoto, H., Hirose, M., Takahashi, M., Kawaguchi, M., Ise, H., Kolattukudy, P.E., Yamada, M., Ikeda, U., 2008. MCP-1 induces cardioprotection against ischaemia/reperfusion injury: role of reactive oxygen species. Cardiovasc Res 78, 554–62.

Morimoto, H., Takahashi, M., Izawa, A., Ise, H., Hongo, M., Kolattukudy, P.E., Ikeda, U., 2006. Cardiac Overexpression of Monocyte Chemoattractant Protein-1 in Transgenic Mice Prevents Cardiac Dysfunction and Remodeling After Myocardial Infarction. Circ. Res. 99, 891–899.

Nagyeri, G., Radacs, M., Ghassemi-Nejad, S., Tryniszewska, B., Olasz, K., Hutas, G., Gyorfy, Z., Hascall, V.C., Glant, T.T., Mikecz, K., 2011. TSG-6 Protein, a Negative Regulator of Inflammatory Arthritis, Forms a Ternary Complex with Murine Mast Cell Tryptases and Heparin. J. Biol. Chem. 286, 23559–23569.

Nahrendorf, M., Swirski, F.K., Aikawa, E., Stangenberg, L., Wurdinger, T., Figueiredo, J.-L., Libby, P., Weissleder, R., Pittet, M.J., 2007. The healing myocardium sequentially mobilizes two monocyte subsets with divergent and complementary functions. J. Exp. Med. 204, 3037–3047.

Nguyen, N., Lee, S.B., Lee, Y.S., Lee, K.-H., Ahn, J.-Y., 2009. Neuroprotection by NGF and BDNF Against Neurotoxin-Exerted Apoptotic Death in Neural Stem Cells Are Mediated Through Trk Receptors, Activating PI3-Kinase and MAPK Pathways. Neurochem. Res. 34, 942–951.

Niu, J., Kolattukudy, P.E., 2009. Role of MCP-1 in cardiovascular disease: molecular mechanisms and clinical implications. Clin. Sci. 117, 95–109.

Nogueira, N., 1983. Host and parasite factors affecting the invasion of mononuclear phagocytes by Trypanosoma cruzi. Ciba Found. Symp. 99, 52–73.

Oh, H., Bradfute, S.B., Gallardo, T.D., Nakamura, T., Gaussin, V., Mishina, Y., Pocius, J., Michael, L.H., Behringer, R.R., Garry, D.J., Entman, M.L., Schneider, M.D., 2003. Cardiac progenitor cells from adult myocardium: Homing, differentiation, and fusion after infarction. Proc. Natl. Acad. Sci. 100, 12313–12318.

Ouaissi, M.A., Cornette, J., Afchain, D., Capron, A., Gras-Masse, H., Tartar, A., 1986. Trypanosoma cruzi infection inhibited by peptides modeled from a fibronectin cell attachment domain. Science 234, 603–607.

Paiva, C.N., Figueiredo, R.T., Kroll-Palhares, K., Silva, A.A., Silverio, J.C., Gibaldi, D., Pyrrho Ados, S., Benjamim, C.F., Lannes-Vieira, J., Bozza, M.T., 2009. CCL2/MCP-1 controls parasite burden, cell infiltration, and mononuclear activation during acute Trypanosoma cruzi infection. J Leukoc Biol 86, 1239–46.

Parikh, V., Howe, W.M., Welchko, R.M., Naughton, S.X., D'Amore, D.E., Han, D.H., Deo, M., Turner, D.L., Sarter, M., 2013. Diminished trkA receptor signaling reveals cholinergic-attentional vulnerability of aging. Eur. J. Neurosci. 37, 278–293.

Pereira-Chioccola, V.L., Acosta-Serrano, A., Almeida, I.C. de, Ferguson, M.A., Souto-Padron, T., Rodrigues, M.M., Travassos, L.R., Schenkman, S.,

2000. Mucin-like molecules form a negatively charged coat that protects Trypanosoma cruzi trypomastigotes from killing by human anti-alpha-galactosyl antibodies. J. Cell Sci. 113, 1299–1307.

Pereira, M.E., 1983. A developmentally regulated neuraminidase activity in Trypanosoma cruzi. Science 219, 1444–1446.

Pereira, M.E., Zhang, K., Gong, Y., Herrera, E.M., Ming, M., 1996. Invasive phenotype of Trypanosoma cruzi restricted to a population expressing trans-sialidase. Infect. Immun. 64, 3884–3892.

Pereira, P.C.M., Navarro, E.C., 2013. Challenges and perspectives of Chagas disease: a review. J. Venom. Anim. Toxins Trop. Dis. 19, 34.

Pfister, O., Mouquet, F., Jain, M., Summer, R., Helmes, M., Fine, A., Colucci, W.S., Liao, R., 2005. CD31- but Not CD31+ cardiac side population cells exhibit functional cardiomyogenic differentiation. Circ Res 97, 52–61.

Prata, A., 2001. Clinical and epidemiological aspects of Chagas disease. Lancet Infect. Dis. 1, 92–100.

Previato, J.O., Andrade, A.F., Pessolani, M.C., Mendonça-Previato, L., 1985. Incorporation of sialic acid into Trypanosoma cruzi macromolecules. A proposal for a new metabolic route. Mol. Biochem. Parasitol. 16, 85–96.

Prockop, D.J., Youn Oh, J., 2012. Mesenchymal Stem/Stromal Cells (MSCs): Role as Guardians of Inflammation. Mol. Ther. 20, 14–20.

Ptaszek, L.M., Mansour, M., Ruskin, J.N., Chien, K.R., 2012. Towards regenerative therapy for cardiac disease. The Lancet 379, 933–942.

Raghuvanshi, S., Sharma, P., Singh, S., Kaer, L.V., Das, G., 2010. Mycobacterium tuberculosis evades host immunity by recruiting mesenchymal stem cells. Proc. Natl. Acad. Sci. 107, 21653–21658.

Rassi Jr, A., Rassi, A., Marin-Neto, J.A., 2010. Chagas disease. The Lancet 375, 1388–1402.

Reichardt, L.F., 2006. Neurotrophin-regulated signalling pathways. Philos. Trans. R. Soc. B Biol. Sci. 361, 1545–1564.

Reid, R.R., Prodeus, A.P., Khan, W., Hsu, T., Rosen, F.S., Carroll, M.C., 1997. Endotoxin shock in antibody-deficient mice: unraveling the role of natural antibody and complement in the clearance of lipopolysaccharide. J. Immunol. 159, 970–975.

Rosenbaum, M.B., 1964. CHAGASIC MYOCARDIOPATHY. Prog. Cardiovasc. Dis. 7, 199–225.

Ross, A.H., 1991. Identification of tyrosine kinase Trk as a nerve growth factor receptor. Cell Regul. 2, 685–690.

Ross, A.H., McKinnon, C.A., Daou, M.-C., Ratliff, K., Wolf, D.E., 1995. Differential Biological Effects of K252 Kinase Inhibitors Are Related to Membrane Solubility but Not to Permeability. J. Neurochem. 65, 2748–2756.

Salvador, R., Aridgides, D., PereiraPerrin, M., 2014. Parasite-Derived Neurotrophic Factor/trans-Sialidase of Trypanosoma cruzi Links Neurotrophic Signaling to Cardiac Innate Immune Response. Infect. Immun. 82, 3687–3696.

Santos-Buch, C.A., Teixeira, A.R.L., 1974. The Immunology of Experimental Chagas' Disease Iii. Rejection of Allogeneic Heart Cells in Vitro. J. Exp. Med. 140, 38–53.

Santos, R.R. dos, Rassi, S., Feitosa, G., Grecco, O.T., Rassi, A., Cunha, A.B. da, Carvalho, V.B. de, Guarita-Souza, L.C., Oliveira, W. de, Tura, B.R., Soares, M.B.P., Carvalho, A.C.C. de, 2012. Cell Therapy in Chagas Cardiomyopathy (Chagas Arm of the Multicenter Randomized Trial of Cell Therapy in Cardiopathies Study) A Multicenter Randomized Trial. Circulation 125, 2454–2461.

Saravanakumar, M., Devaraj, H., 2013. Distribution and homing pattern of c-kit+ Sca-1+ CXCR4+ resident cardiac stem cells in neonatal, postnatal, and adult mouse heart. Cardiovasc. Pathol. 22, 257–263.

Schenkman, S., Eichinger, D., Pereira, M.E., Nussenzweig, V., 1994. Structural and functional properties of Trypanosoma trans-sialidase. Annu Rev Microbiol 48, 499–523.

Schenkman, S., Jiang, M.-S., Hart, G.W., Nussenzweig, V., 1991. A novel cell surface trans-sialidase of trypanosoma cruzi generates a stage-specific epitope required for invasion of mammalian cells. Cell 65, 1117–1125.

Sebastiani, S., Allavena, P., Albanesi, C., Nasorri, F., Bianchi, G., Traidl, C., Sozzani, S., Girolomoni, G., Cavani, A., 2001. Chemokine Receptor Expression and Function in CD4+ T Lymphocytes with Regulatory Activity. J. Immunol. 166, 996–1002.

Serbina, N.V., Jia, T., Hohl, T.M., Pamer, E.G., 2008. Monocyte-Mediated Defense Against Microbial Pathogens. Annu. Rev. Immunol. 26, 421–452.

Sgambatti de Andrade, A.L.S., Zicker, F., de Oliveira, R.M., Almeida e Silva, S., Luquetti, A., Travassos, L.R., Almeida, I.C., de Andrade, S.S., Guimarães de Andrade, J., Martelli, C.M., 1996. Randomised trial of efficacy of benznidazole in treatment of early Trypanosoma cruzi infection. The Lancet 348, 1407–1413.

Sheridan, G.K., Murphy, K.J., 2013. Neuron–glia crosstalk in health and disease: fractalkine and CX3CR1 take centre stage. Open Biol. 3, 130181.

Singer, N.G., Caplan, A.I., 2011. Mesenchymal stem cells: mechanisms of inflammation. Annu. Rev. Pathol. 6, 457–478.

Smits, A.M., van Vliet, P., Metz, C.H., Korfage, T., Sluijter, J.P., Doevendans, P.A., Goumans, M.-J., 2009. Human cardiomyocyte progenitor cells differentiate into functional mature cardiomyocytes: an in vitro model for studying human cardiac physiology and pathophysiology. Nat. Protoc. 4, 232–243.

Soares, M.B.P., Lima, R.S. de, Rocha, L.L., Vasconcelos, J.F., Rogatto, S.R., Santos, R.R. dos, Iacobas, S., Goldenberg, R.C., Iacobas, D.A., Tanowitz, H.B., Carvalho, A.C.C. de, Spray, D.C., 2010. Gene Expression Changes Associated with Myocarditis and Fibrosis in Hearts of Mice with Chronic Chagasic Cardiomyopathy. J. Infect. Dis. 202, 416–426.

Soares, M.B.P., Lima, R.S., Rocha, L.L., Takyia, C.M., Pontes-de-Carvalho, L., Campos de Carvalho, A.C., Ribeiro-dos-Santos, R., 2004. Transplanted Bone Marrow Cells Repair Heart Tissue and Reduce Myocarditis in Chronic Chagasic Mice. Am. J. Pathol. 164, 441–447.

Soares, M.B.P., Lima, R.S., Souza, B.S.F., Vasconcelos, J.F., Rocha, L.L., Santos, R.R. dos, Iacobas, S., Goldenberg, R.C., Lisanti, M.P., Iacobas, D.A., Tanowitz, H.B., Spray, D.C., Carvalho, A.C.C. de, 2011. Reversion of gene expression alterations in hearts of mice with chronic chagasic cardiomyopathy after transplantation of bone marrow cells. Cell Cycle 10, 1448–1455.

Sreejit, P., Kumar, S., Verma, R.S., 2008. An improved protocol for primary culture of cardiomyocyte from neonatal mice. Vitro Cell Dev Biol Anim 44, 45–50.

Stevens, J.R., Noyes, H.A., Dover, G.A., Gibson, W.C., 1999. The ancient and divergent origins of the human pathogenic trypanosomes, Trypanosoma brucei and T. cruzi. Parasitology 118 (Pt 1), 107–116.

Streiger, M.L., del Barco, M.L., Fabbro, D.L., Arias, E.D., Amicone, N.A., 2004. [Longitudinal study and specific chemotherapy in children with chronic

Chagas' disease, residing in a low endemicity area of Argentina]. Rev. Soc. Bras. Med. Trop. 37, 365–375.

Tamura, Y., Matsumura, K., Sano, M., Tabata, H., Kimura, K., Ieda, M., Arai, T., Ohno, Y., Kanazawa, H., Yuasa, S., Kaneda, R., Makino, S., Nakajima, K., Okano, H., Fukuda, K., 2011. Neural Crest–Derived Stem Cells Migrate and Differentiate Into Cardiomyocytes After Myocardial Infarction. Arterioscler. Thromb. Vasc. Biol. 31, 582–589.

Tarleton, R.L., 2003. Chagas disease: a role for autoimmunity? Trends Parasitol. 19, 447–451.

Tarleton, R.L., Zhang, L., 1999. Chagas disease etiology: autoimmunity or parasite persistence? Parasitol Today 15, 94–9.

Teixeira, A.R.L., Nitz, N., Guimaro, M.C., Gomes, C., 2006. Chagas disease. Postgrad. Med. J. 82, 788–798.

Teixeira, A.R., Nascimento, R.J., Sturm, N.R., 2006. Evolution and pathology in Chagas disease: a review. Mem. Inst. Oswaldo Cruz 101, 463–491.

Teixeira, A.R., Teixeira, M.L., Santos-Buch, C.A., 1975. The immunology of experimental Chagas' disease. IV. Production of lesions in rabbits similar to those of chronic Chagas' disease in man. Am. J. Pathol. 80, 163–180.

Teixeira, M.M., Gazzinelli, R.T., Silva, J.S., 2002. Chemokines, inflammation and Trypanosoma cruzi infection. Trends Parasitol. 18, 262–265.

Tessarollo, L., Tsoulfas, P., Donovan, M.J., Palko, M.E., Blair-Flynn, J., Hempstead, B.L., Parada, L.F., 1997. Targeted deletion of all isoforms of the trkC gene suggests the use of alternate receptors by its ligand neurotrophin-3 in neuronal development and implicates trkC in normal cardiogenesis. Proc. Natl. Acad. Sci. 94, 14776–14781.

Tomita, Y., Matsumura, K., Wakamatsu, Y., Matsuzaki, Y., Shibuya, I., Kawaguchi, H., Ieda, M., Kanakubo, S., Shimazaki, T., Ogawa, S., Osumi, N., Okano, H., Fukuda, K., 2005. Cardiac neural crest cells contribute to the dormant multipotent stem cell in the mammalian heart. J. Cell Biol. 170, 1135–1146.

Tompkins, S., 2014. Bugs' "kiss" a major threat to dogs [WWW Document]. Houst. Chron. URL http://www.chron.com/sports/outdoors/article/Bugs-kiss-a-major-threat-to-dogs-5461828.php#src=fb (accessed 8.4.14).

Troy, F.A., 1992. Polysialylation: from bacteria to brains. Glycobiology 2, 5–23.

Unnikrishnan, M., Burleigh, B.A., 2004. Inhibition of host connective tissue growth factor expression: a novel Trypanosoma cruzi-mediated response. FASEB J. 18, 1625–1635.

Urbanek, K., Quaini, F., Tasca, G., Torella, D., Castaldo, C., Nadal-Ginard, B., Leri, A., Kajstura, J., Quaini, E., Anversa, P., 2003. Intense myocyte formation from cardiac stem cells in human cardiac hypertrophy. Proc. Natl. Acad. Sci. 100, 10440–10445.

Van den Akker, F., Deddens, J.C., Doevendans, P.A., Sluijter, J.P.G., 2013. Cardiac stem cell therapy to modulate inflammation upon myocardial infarction. Biochim. Biophys. Acta BBA - Gen. Subj., Biochemistry of Stem Cells 1830, 2449–2458.

Van Linthout, S., Stamm, C., Schultheiss, H.-P., Tsch&#246, Pe, C., 2011. Mesenchymal Stem Cells and Inflammatory Cardiomyopathy: Cardiac Homing and Beyond. Cardiol. Res. Pract. 2011, e757154.

Ventura-Garcia, L., Roura, M., Pell, C., Posada, E., Gascón, J., Aldasoro, E., Muñoz, J., Pool, R., 2013. Socio-Cultural Aspects of Chagas Disease: A Systematic Review of Qualitative Research. PLoS Negl Trop Dis 7, e2410.

Vianna, G., 1911. Contribuição para o estudo da anatomia patolojica da “Molestia de Carlos Chagas”: (Esquizotripanoze humana ou tireoidite parazitaria). Mem. Inst. Oswaldo Cruz 3, 276–294.

Wahab, N.A., Weston, B.S., Mason, R.M., 2005. Connective Tissue Growth Factor CCN2 Interacts with and Activates the Tyrosine Kinase Receptor TrkA. J. Am. Soc. Nephrol. 16, 340–351.

Wang, N., Shao, Y., Mei, Y., Zhang, L., Li, Q., Li, D., Shi, S., Hong, Q., Lin, H., Chen, X., 2012. Novel mechanism for mesenchymal stem cells in attenuating peritoneal adhesion: accumulating in the lung and secreting tumor necrosis factor α-stimulating gene-6. Stem Cell Res. Ther. 3, 51.

Wang, X., McLennan, S.V., Allen, T.J., Twigg, S.M., 2010. Regulation of pro-inflammatory and pro-fibrotic factors by CCN2/CTGF in H9c2 cardiomyocytes. J. Cell Commun. Signal. 4, 15–23.

Wang, Y., Hagel, C., Hamel, W., Müller, S., Kluwe, L., Westphal, M., 1998. Trk A, B, and C are commonly expressed in human astrocytes and astrocytic gliomas but not by human oligodendrocytes and oligodendroglioma. Acta Neuropathol. (Berl.) 96, 357–364.

Wegner, D.H., Rohwedder, R.W., 1972. The effect of nifurtimox in acute Chagas’ infection. Arzneimittelforschung. 22, 1624–1635.

Weinkauf, C., Pereiraperrin, M., 2009. Trypanosoma cruzi promotes neuronal and glial cell survival through the neurotrophic receptor TrkC. Infect Immun 77, 1368–75.

Weinkauf, C., Salvador, R., PereiraPerrin, M., 2011. Neurotrophin Receptor TrkC Is an Entry Receptor for Trypanosoma cruzi in Neural, Glial, and Epithelial Cells. Infect. Immun. 79, 4081–4087.

Wiese, C., Rolletschek, A., Kania, G., Blyszczuk, P., Tarasov, K.V., Tarasova, Y., Wersto, R.P., Boheler, K.R., Wobus, A.M., 2004. Nestin expression – a property of multi-lineage progenitor cells? Cell. Mol. Life Sci. CMLS 61, 2510–2522.

Wisniewski, H.-G., Burgess, W.H., Oppenheim, J.D., Vilcek, J., 1994. TSG-6, an Arthritis-Associated Hyaluronan Binding Protein, Forms a Stable Complex with the Serum Protein Inter-.alpha.-inhibitor. Biochemistry (Mosc.) 33, 7423–7429.

Ye, J., Boyle, A., Shih, H., Sievers, R.E., Zhang, Y., Prasad, M., Su, H., Zhou, Y., Grossman, W., Bernstein, H.S., Yeghiazarians, Y., 2012. Sca-1+ Cardiosphere-Derived Cells Are Enriched for Isl1-Expressing Cardiac Precursors and Improve Cardiac Function after Myocardial Injury. PLoS ONE 7, e30329.

Yeo, G.S.H., Connie Hung, C.-C., Rochford, J., Keogh, J., Gray, J., Sivaramakrishnan, S., O'Rahilly, S., Farooqi, I.S., 2004. A de novo mutation affecting human TrkB associated with severe obesity and developmental delay. Nat. Neurosci. 7, 1187–1189.

Yoshioka, S., Ochsner, S., Russell, D.L., Ujioka, T., Fujii, S., Richards, J.S., Espey, L.L., 2000. Expression of tumor necrosis factor-stimulated gene-6 in the rat ovary in response to an ovulatory dose of gonadotropin. Endocrinology 141, 4114–4119.

Zaidenberg, A., Luong, T., Lirussi, D., Bleiz, J., Buono, M.B.D., Quijano, G., Drut, R., Kozubsky, L., Marron, A., Buschiazzo, H., 2006. Treatment of Experimental Chronic Chagas Disease with Trifluralin. Basic Clin. Pharmacol. Toxicol. 98, 351–356.

Zangi, L., Lui, K.O., von Gise, A., Ma, Q., Ebina, W., Ptaszek, L.M., Später, D., Xu, H., Tabebordbar, M., Gorbatov, R., Sena, B., Nahrendorf, M., Briscoe, D.M., Li, R.A., Wagers, A.J., Rossi, D.J., Pu, W.T., Chien, K.R., 2013. Modified mRNA directs the fate of heart progenitor cells and induces vascular regeneration after myocardial infarction. Nat. Biotechnol. 31, 898–907.

Zhou, S., Chen, L.S., Miyauchi, Y., Miyauchi, M., Kar, S., Kangavari, S., Fishbein, M.C., Sharifi, B., Chen, P.-S., 2004. Mechanisms of Cardiac Nerve Sprouting After Myocardial Infarction in Dogs. Circ. Res. 95, 76–83.

Zingales, B., Andrade, S.G., Briones, M.R.S., Campbell, D.A., Chiari, E., Fernandes, O., Guhl, F., Lages-Silva, E., Macedo, A.M., Machado, C.R., Miles, M.A., Romanha, A.J., Sturm, N.R., Tibayrenc, M., Schijman, A.G., 2009. A new consensus for Trypanosoma cruzi intraspecific nomenclature: second revision meeting recommends TcI to TcVI. Mem. Inst. Oswaldo Cruz 104, 1051–1054.